TAYLOR DISPERSION STUDIES OF DIFFUSION IN ELECTROLYTE SOLUTIONS

by
Ruanhui Lu

Department of Chemistry

Submitted in partial fulfilment
of the requirements for the degree of
Master of Science

Faculty of Graduate Studies
The University of Western Ontario
London, Ontario
December 1997

ABSTRACT

Binary mutual diffusion coefficients of aqueous solutions of LiF, NaF and KF have been measured by the Taylor dispersion (peak-broadening) technique at 25 °C. The measured diffusion coefficients are used to evaluate resistance coefficients for the mutual diffusion of aqueous fluoride salts. The results help to complete the database for aqueous alkali halides, the simplest of all aqueous electrolytes.

Binary diffusion coefficients have also been measured for aqueous solutions of ethylamine, diethylamine and triethylamine at concentrations from 0.2 to 100 mmol dm^{-3}, and for aqueous solutions of the isomers of aminobenzoic acid at concentrations from 0.05 to 10.0 mmol dm^{-3}. In dilute solutions the diffusion coefficient of these weak bases and acids changes very rapidly with concentration because of ionic dissociation or hydrolysis reactions. In this region the measured diffusion coefficients are interpolated or extrapolated to zero initial concentration difference to determine the true differential diffusion coefficient at each carrier-stream composition. These results show that Taylor dispersion can be used to measure diffusion in difficult cases where the diffusion coefficient changes rapidly with concentration along the diffusion path. Analysis of the results provides the mobilities of the ionic and molecular forms of the solutes. The results illustrate that the diffusion coefficient of a weak electrolyte is not the simple concentration-weighted average of the diffusion coefficients of the molecular and ionized forms of the total electrolyte.

A new dispersion experiment is developed by connecting the outlet of a short dispersion tube to the pump inlet to form a closed-circuit flow path. At the start of each run,

one half of the circuit is filled initially with solution at concentration $C + (\Delta C/2)$ and the other half is filled with solution at concentration $C - (\Delta C/2)$. Pumping the solutions around the circuit generates exponentially-damped concentration oscillations in a refractometer detector. Fourier analysis of the detector signal gives the diffusion coefficients. The modified dispersion experiment allows diffusion measurements to be made on a few milliliters of solution instead of hundreds of milliliters required for conventional dispersion measurements. The closed-circuit is used to measure the binary diffusion coefficient of aqueous $LaCl_3$ at concentrations from 0.015 to 2.784 mol dm^{-3} at 25 °C. Resistance coefficients of $LaCl_3$ are then evaluated.

ACKNOWLEDGEMENTS

I wish to express my deepest appreciation to Dr. D.G. Leaist, my supervisor, for his constant guidance, encouragement and assistance throughout my graduate studies.

I also thank Dr. R.K. Chan and Dr. W.J. Meath for their helpful suggestions in the writing of this thesis.

Special thanks to Nicolette Curtis, Robert Donkers and Ling Hao for their technical assistance and friendship.

I must thank my parents, Denan Lu and Huafang Chen, and my sister Wei Lu, for their understanding and encouragement.

TABLE OF CONTENTS

LIST OF FIGURES

LIST OF TABLES

CHAPTER 1

INTRODUCTION

Diffusion is a fundamental mixing process in which concentration differences are smoothed out by the random thermal motions of molecules. Because diffusion is slow, it limits the rates of important chemical, biological, geological and industrial mass transfer processes. In addition, diffusion measurements can provide valuable information about intermolecular forces, the structure of solutions, and the sizes and shapes of ions and molecules.

The work reported in this thesis is a study of diffusion in a number of binary aqueous electrolyte solutions. Diffusion in these systems is described by Fick's diffusion equation

$$J = -D\nabla C$$

where ∇C is the gradient in the electrolyte concentration, J is the electrolyte flux and D is the binary coefficient. The physical interpretation of electrolyte diffusion coefficients (and the closely related mobility and resistance coefficients) is summarized briefly in Chapter 2.

Electrolyte diffusion coefficients can be measured by a variety of optical,[1-4] conductimetric,[5-8] and diaphragm-cell techniques.[9-10] These methods are well-established and reliable, but the experimental procedures are laborious and time-consuming. Recently, a much more convenient diffusion experiment based on Taylor dispersion has been developed.[11-16] In a Taylor experiment, a narrow band of solution is injected into a laminar carrier solution which is pumped through a long (~3000 cm) capillary tube. The injected solute spreads out into a nearly Gaussian profile as it flows along the tube. Diffusion

coefficients are evaluated from the shape of the eluted solute peak which is monitored by a suitable detector, such as a flow-through refractometer. This technique is rapid, accurate (~1%), and free of errors from convection. All of the diffusion coefficients reported in this thesis were measured by the Taylor dispersion. The theory and procedure of this technique are briefly described in Chapter 3.

Over the years a large body of diffusion data has been reported for aqueous solutions of alkali halides (LiCl, NaCl, KCl, NaBr, *etc.*), the simplest of all aqueous electrolytes. Yet, surprisingly, reliable diffusion coefficients are still not available for aqueous fluorides, perhaps because these solutions can etch conventional glass diffusion cells, especially under acidic conditions. In Chapter 4, binary diffusion coefficients are reported for aqueous solutions of LiF, NaF and KF. These results together with previously reported activity and density data are used to evaluate resistance coefficients for the aqueous fluoride salts. The results will help to complete the database for aqueous alkali halides. Moreover, fluoride salts are especially interesting because the aqueous F^- ion, the first member of the halide series, has unusual properties, such as strong hydration, which are not suggested by extrapolation of the properties of Cl^-, Br^- and I^- ions.

Chapters 5 and 6 of this thesis deal with the diffusion behavior of weak electrolytes. Since weak electrolytes diffuse in solution as molecular species together with ions produced by dissociation (*e.g.*, $AB \rightleftharpoons A^- + B^-$), their diffusional properties are more complex than those for either strong electrolytes or non-electrolytes.[8,17,18] Dissociation influences the rate of the diffusion of a weak electrolyte in two ways. First, by increasing the number of free solute particles, dissociation increases the free-energy (chemical-potential) gradient that drives the solute through the solvent. Secondly, dissociation tends to reduce the overall mobility of

the weak electrolyte because the movement of two separate ions experiences more frictional resistance than transport of a single molecular species. This means that diffusion measurements can provide information about the mobilities and thermodynamic activities of species in solution.

Binary diffusion coefficients are reported in Chapters 5 and 6 for aqueous solutions of the following weak electrolytes: ethylamine, diethylamine, triethylamine, and the isomers of aminobenzoic acid. The diffusion coefficient of a solution of a weak base or a weak acid changes very rapidly at low concentrations where dissociation becomes extensive. This causes the measured diffusion coefficients to vary with the initial concentration difference, yielding an ill-defined apparent diffusion coefficient corresponding to some concentration intermediate between that of the injected solution and the carrier solution. The work reported here shows that this difficulty can be overcome by interpolating or extrapolating measured diffusion coefficients to zero initial concentration difference in order to determine an accurate value for the diffusion coefficient at each carrier-solution composition. It turns out, counterintuitively, that the diffusion coefficient of a weak electrolyte is not the concentration-weighted average of the diffusion coefficients of the molecular and ionized forms of the total electrolyte.

Chapter 7 of this thesis deals with a modification of the conventional Taylor experiment: dispersion in a ring. Closed-circuit flow is achieved by connecting the outlet of a short dispersion tube to the pump inlet. At the start of each run, one half of the circuit is filled with solution at concentration $C + (\Delta C/2)$, the other half is filled with solution at concentration $C - (\Delta C/2)$. Because the average concentration of the diffusing solute (C) around the circuit is constant, larger concentration differences and less sensitive detectors can

be used in the measurements Moreover, recirculation drastically reduces the required volume of solution relative to that used in traditional once-through Taylor dispersion measurements, from liters to milliliters. To illustrate these advantages, closed-circuit Taylor dispersion is used to measure binary diffusion coefficients for concentrated aqueous solutions of $LaCl_3$. This work was undertaken to investigate the diffusion behavior of a higher-valent salt. Purified $LaCl_3$ is relatively expensive, so it is important in practice to be able to make reliable diffusion measurements on small volumes of solution of this salt. The problem of dispersion in a closed-circuit is shown to bear a striking resemblance to the problem of heat flow in a ring-shaped thermal conductor — the first application of Fourier analysis.

References

1 L. G. Longsworth, *J. Am. Chem. Soc.*, 1947, **69**, 2510.

2 J. A. Rard and D. G. Miller, *J. Solution Chem.*, 1979, **8**, 701.

3 J. A. Rard and D. G. Miller, *J. Solution Chem.*, 1979, **8**, 755.

4 J. A. Rard and D. G. Miller, *J. Chem. Eng. Data*, 1980, **25**, 211.

5 H. S. Harned and D. M. French, *Ann. N. Y. Acad. Sci.*, 1945, **44**, 267.

6 H. S. Harned and R. L. Nuttall, *J. Am. Chem. Soc.*, 1947, **69**, 736.

7 E. L. Holt and P. A. Lyons, *J. Phys. Chem.*, 1965, **69**, 2341.

8 D. G. Leaist and P. A. Lyons, *J. Solution Chem.*, 1984, **13**, 77.

9 R. H. Stocks, *J. Am. Chem. Soc.*, 1950, **72**, 763.

10 D. G. Leaist, *J. Chem. Soc., Faraday Trans. 1*, 1987, **83**, 829.

11 G. I. Taylor, *Proc. R. Soc. London Ser. A*, 1953, **219**, 186.

12 G. I. Taylor, *Proc. Phys. Soc.*, 1954, **B67**, 857.

13 R. Aris, *Proc. R. Soc. London Ser. A*, 1956, **235**, 67.

14 W. E. Price, *J. Chem. Soc., Faraday Trans. 1*, 1988, **84**, 2431.

15 D. G. Leaist, *J. Phys. Chem.*, 1990, **94**, 5180.

16 D. G. Leaist, *J. Chem. Soc., Faraday Trans.*, 1992, **88**, 2897.

17 D. G. Leaist, *J. Chem. Soc., Faraday Trans. 1*, 1984, **80**, 3041.

18 R. A. Noulty and D. G. Leaist, *J. Chem. Eng. Data*, 1987, **32**, 418.

CHAPTER 2

DIFFUSION EQUATIONS FOR BINARY SOLUTIONS

2.1. Fick's Laws

Graham [1] (1850) appears to be the first to understand that the rate of diffusion of a substance is proportional to its concentration gradient. Later, in the 1880's, Fick established the empirical equations for diffusion.[1] For a two-component system, he obtained the expression

$$J = -D\nabla C \tag{2.1.1}$$

where J is the solute flux in moles per unit area per unit time. D is the binary diffusion coefficient and ∇C is the gradient in the solute concentration. Eqn. (2.1.1) is often called Fick's first law of diffusion.

During unsteady diffusion processes, concentrations change with time along the diffusion path. Eqn. (2.1.1) and the continuity equation

$$\frac{\partial C}{\partial t} = -\nabla J \tag{2.1.2}$$

lead to the expression

$$\frac{\partial C}{\partial t} = \nabla(D\nabla C) \tag{2.1.3}$$

for the rate of change of concentration. Eqn. (2.1.3) is called Fick's second law of diffusion.

2.2. Onsager Equation and Mobility

Fick's equations provide a convenient empirical description of diffusion in terms of measurable concentration gradients. On a more fundamental level, Onsager[2] recognized that the correct driving force for the diffusion of a solute is the gradient in its chemical potential

$$J = -L\nabla\mu \qquad (2.2.1)$$

L is called the Onsager transport coefficient and $\nabla\mu$ is the gradient in the solute chemical potential. Onsager coefficients and diffusion coefficients are related as follows

$$D = L\frac{d\mu}{dC} \qquad (2.2.2)$$

Another useful quantity, the solute mobility U, is defined as the ratio of the diffusion velocity to the driving force.[3]

$$U = -\frac{v}{\nabla\mu} = \frac{L}{C} \qquad (2.2.3)$$

Qualitatively, the mobility of a solute is inversely proportional to the effective diameter of the solute molecules and the viscosity of the solvent.

It is tempting to think of the diffusion coefficient as a purely kinetic quantity. Combining eqns. (2.2.2) and (2.2.3) shows, however, that the diffusion coefficient is the product of both a mobility and an equilibrium thermodynamic factor.

$$D = U\frac{d\mu}{d\ln C} \qquad (2.2.4)$$

The thermodynamic factor is often overlooked in diffusion studies.

2.3. Electrolyte Diffusion

In a solution containing a single electrolyte (such as HCl dissolved in water), the diffusion of two ionic species (*e.g.*, H^+ and Cl^-) is strongly coupled by the electric field which is generated to slow down the more mobile ion and speed up the slower one so that charge separation is prevented. Because the two ions diffuse at the same rate, only one solute flux is independent and hence the binary diffusion equations apply.

In dilute electrolyte solutions, the diffusion velocity of ion i can be expressed approximately as the product of its mobility (u_i) and the driving force ($-\nabla\tilde{\mu}_i$) acting on the ion.

$$v_i = -u_i\nabla\tilde{\mu}_i \tag{2.3.1}$$

Here $\tilde{\mu}_i$ is the electrochemical potential of ion i, the sum of its chemical potential μ and its electric potential energy $z_iF\phi$.

$$\tilde{\mu}_i = \mu_i + z_iF\phi \tag{2.3.2}$$

z_i is the valence of ion i, F the Faraday constant, and ϕ the electric potential. The chemical potential is given by

$$\mu_i = \mu_i^0 + RT\ln\gamma_i c_i \tag{2.3.3}$$

R is the gas constant, T the temperature, μ_i^0 the standard chemical potential of ion i, and γ_i the ionic activity coefficient (a measure of the departure from ideal-solution behavior). The driving force acting on each ion is therefore

$$-\nabla\tilde{\mu}_i = -(RT\nabla\ln\gamma_i c_i + z_iF\nabla\phi) \tag{2.3.4}$$

Defining the electric field, $E = -\nabla\phi$, gives

$$-\nabla\tilde{\mu}_i = -RT\nabla\ln\gamma_i c_i + z_iFE \tag{2.3.5}$$

In very dilute solutions, γ_i is unity, and eqn. (2.3.5) simplifies to

$$-\nabla\tilde{\mu}_i = -RT\nabla\ln c_i - z_iFE \tag{2.3.6}$$

The flux of ion i is the product of its concentration and diffusion speed

$$j_i = c_i v_i \tag{2.3.7}$$

and hence

$$j_i = -c_i u_i[RT\nabla\ln c_i - z_iFE] = -RTu_i\nabla c_i + c_i u_i z_iFE \tag{2.3.8}$$

Identifying RTu_i as the diffusion coefficient of ion i gives

$$j_i = -D_i\nabla c_i + (F/RT)c_i z_i D_i E \tag{2.3.9}$$

This important result is the Nernst-Planck equation.[4] The first term on the right side of eqn (2.3.9) is the flux of ion i contributed by pure diffusion of the ion down its concentration gradient. The second term is the ionic flux driven by the electric field.

2.4. Strong Electrolyte Diffusion

Consider salt M_pX_q, one mole of which dissociates into p moles of cations of valence z_+ and q moles of anions of valence z_-. The cations M^{z+} and anions X^{z-} must diffuse at the same velocity to keep the solution electrically neutral.

$$v = v_+ = v_- = -u_+(\nabla\mu_+ - z_+FE) = -u_-(\nabla\mu_- - z_-FE) \tag{2.4.1}$$

Solving for the electric-field term FE gives

$$FE = \frac{1}{z_+}\left(\frac{v}{u_+} + \nabla\mu_+\right) = \frac{1}{z_-}\left(\frac{v}{u_-} + \nabla\mu_-\right) \tag{2.4.2}$$

Using the electroneutrality condition

$$pz_{-} + qz_{+} = 0 \tag{2.4.3}$$

and the fact that the chemical potential of the electrolyte is the sum of the electrochemical potentials of its constituent ions

$$\mu = p\mu_{-} + q\mu_{+} \tag{2.4.4}$$

yields

$$v = -\frac{u_{+}u_{-}}{pu_{-} + qu_{+}}(p\nabla\mu_{-} + q\nabla\mu_{+}) = -\frac{u_{+}u_{-}}{pu_{-} + qu_{+}}\nabla\mu \tag{2.4.5}$$

Then flux of the electrolyte is therefore

$$J = Cv = -\frac{u_{+}u_{-}}{pu_{-} + qu_{+}}\frac{d\mu}{d\ell nC}\nabla C \tag{2.4.6}$$

Comparing eqns. (2.4.6) and (2.1.1) shows that the binary diffusion coefficient of the electrolyte is given by

$$D = \frac{u_{+}u_{-}}{pu_{-} + qu_{+}}\frac{d\mu}{d\ell nC} \tag{2.4.7}$$

In addition, eqns. (2.4.7) and (2.2.4) show that the mobility of the electrolyte is

$$U = \frac{u_{+}u_{-}}{pu_{-} + qu_{+}} \tag{2.4.8}$$

The quantity RTL/C is often called the "mobility factor" of an electrolyte

$$\frac{RTL}{C} = RTU = \frac{RTu_+u_-}{pu_+ + qu_-} \tag{2.4.9}$$

To evaluate the thermodynamic contribution to the diffusion coefficient, we start by expressing the chemical potential of the electrolyte M_pX_q as the sum of the electrochemical potentials of the constituent ions

$$\mu = p\tilde{\mu}_+ + q\tilde{\mu}_- = p(\tilde{\mu}_+^0 + RT\ln\gamma_+c_+ + z_+F\phi) + q(\tilde{\mu}_-^0 + RT\ln\gamma_-c_- + z_-F\phi) \tag{2.4.10}$$

Note that $c_+ = pC$, $c_- = qC$ and $pz_+F\phi + qz_-F\phi = 0$. By defining the mean ionic activity coefficient $\gamma_\pm$

$$\gamma_+^p\gamma_-^q = \gamma_\pm^{p+q} \tag{2.4.11}$$

eqn. (2.4.10) simplifies to

$$\mu = \mu^0 + RT\ln\left[\gamma_\pm^{p+q}(pC)^p(qC)^q\right] \tag{2.4.12}$$

Differentiation gives

$$\frac{C}{RT}\frac{d\mu}{dC} = (p+q)\left(1 + \frac{d\ln\gamma_\pm}{d\ln C}\right) \tag{2.4.13}$$

for the thermodynamic factor $(C/RT)d\mu/dC$ of the electrolyte.

Substituting eqn. (2.4.13) and the expression for the limiting equivalent conductivity

$$\lambda_i^0 = |z_i| F^2 u_i \qquad (2.4.14)$$

into eqn. (2.4.7) yields

$$D = \frac{RT(p+q)\lambda_+^0\lambda_-^0}{F^2 pz_+(\lambda_+^0+\lambda_-^0)}\left(1 - \frac{d\ln\gamma_\pm}{d\ln C}\right) \qquad (2.4.15)$$

For an infinitely dilute solution, the activity-coefficient term $d\ln\gamma_\pm / d\ln C$ is zero and the limiting expressions

$$\lim_{C\to 0} \frac{RTL^0}{C} = \frac{RT\lambda_+^0\lambda_-^0}{F^2 pz_+(\lambda_+^0+\lambda_-^0)} \qquad (2.4.16)$$

$$\lim_{C\to 0} \frac{C}{RT}\frac{d\mu}{dC} = p + q \qquad (2.4.17)$$

$$D^0 = \frac{RT(p+q)\lambda_+^0\lambda_-^0}{F^2 pz_+(\lambda_+^0+\lambda_-^0)} \qquad (2.4.18)$$

are obtained for the mobility, thermodynamic factor, and diffusion coefficient of electrolyte M_pX_q.

The limiting diffusion coefficients of the ions are related to their mobilities and equivalent conductivities by

$$D_i^0 = RTu_i^0 \qquad (2.4.19)$$

and

$$D_i^0 = \frac{RT\lambda_i^0}{F^2|z_i|} \tag{2.4.20}$$

Substituting eqn. (2.4.20) into eqn. (2.4.18) gives the expression

$$D^0 = \frac{(p+q)D_+^0 D_-^0}{qD_+^0 + pD_-^0} \tag{2.4.21}$$

for the limiting diffusion coefficient of the electrolyte in terms of the limiting diffusion coefficients of its constituent ions.

Eqns. (2.4.18) and (2.4.21) provide an accurate estimate of D only in the limit of infinite dilution. At higher concentrations, D values can be estimated by applying correction factors to D^0 to allow for nonideal thermodynamic behavior and the increase in the solution viscosity.

$$D = D^0\left(1 + \frac{d\ln\gamma_\pm}{d\ln C}\right)\frac{\eta^0}{\eta} \tag{2.4.22}$$

η^0 and η are the viscosities of the pure solvent and the solution respectively.

2.5. Weak Electrolyte Diffusion

A weak electrolyte, such as aqueous acetic acid, is not completely dissociated into its constituent ions. Diffusion of these electrolytes is complicated because the molecular form of the electrolyte diffuses in local equilibrium with its ionic forms.

In an aqueous solution of weak acid HA, for example, the following equilibrium exists:

$$HA \rightleftharpoons H^+ + A^-$$

In this case there are fluxes of three solute species, which may be numbered: 0. molecular HA; 1. H^+; 2. A^-. However, there are also two constraints on the fluxes of the species: electroneutrality and local equilibrium of the dissociation reaction. Hence there is still only one independent solute flux, and eqns. (2.1.1) and (2.2.1) for binary diffusion still apply.

The flux of the "total" electrolyte is the sum of fluxes of the molecular HA and dissociated A^- species.

$$J = j_0 + j_2 \tag{2.5.1}$$

Thus

$$-L\nabla\tilde{\mu}_0 = -l_0\nabla\tilde{\mu}_0 - l_2\nabla\tilde{\mu}_2 \tag{2.5.2}$$

where L is the Onsager transport coefficient of the total weak electrolyte component and l_i the Onsager transport coefficient of species i. The diffusion coefficient, Onsager coefficient, and mobility of species i are related as follows

$$u_i = \frac{l_i}{c_i} = \frac{D_i}{RT} \tag{2.5.3}$$

Because of the electroneutrality requirement

$$-l_1\nabla\tilde{\mu}_1 = -l_2\nabla\tilde{\mu}_2 \tag{2.5.4}$$

and the equilibrium condition

$$\nabla\tilde{\mu}_0 = \nabla\tilde{\mu}_1 + \nabla\tilde{\mu}_2 \tag{2.5.5}$$

it follows that

$$\nabla\tilde{\mu}_2 = \frac{l_1}{l_1 + l_2}\nabla\tilde{\mu}_0 \tag{2.5.6}$$

Substituting eqn. (2.5.6) into eqn. (2.5.2) gives the expression

$$L = l_0 + \frac{l_1 l_2}{l_1 + l_2} \tag{2.5.7}$$

for the Onsager coefficient of the total weak electrolyte component in terms of the Onsager coefficients of the constituent species (HA, H^+, A^-).

Since $l_i = c_i D_i / RT$, one obtains

$$L = \frac{C}{RT}\left[(1 - \alpha)D_0 + \frac{\alpha}{2}D_=\right] \tag{2.5.8}$$

Here α is the degree of hydrolysis which is calculated from the ionization constant of the molecular acid:

$$K_a = \frac{a_{H^+} a_{A^-}}{a_{HA}} = \frac{\alpha^2 C}{1 - \alpha}\frac{\gamma_=^2}{\gamma_m} \tag{2.5.9}$$

γ_m is the activity coefficient of the molecular solute and a_i is the activity of species i. $D_=$ is the limiting diffusion coefficient of fully ionized HA:

$$D_= = \frac{2D_1 D_2}{D_1 + D_2} \tag{2.5.10}$$

Differentiation of eqn. (2.5.9) and

$$\mu = \mu^0 + RT\ln a_{HA} = \mu^0 + RT\ln[(1 - \alpha)C\gamma_m] \tag{2.5.11}$$

gives

$$\frac{d\mu}{dC} = \frac{RT}{C}\left[1 + \frac{\alpha}{(2 - \alpha)}\left(1 + \frac{d\ln(\gamma_{\pm}^2/\gamma_m)}{d\ln C}\right) + \frac{d\ln\gamma_m}{d\ln C}\right] \qquad (2.5.12)$$

For a very dilute solution, $\gamma_{\pm}$ and γ_m are unity. Combining eqns. (2.5.8) and (2.5.12) and omitting the activity-coefficient terms yields

$$D = \left[(1 - \alpha)D_0 + \frac{\alpha}{2}D_{\pm}\right]\frac{2}{(2 - \alpha)} \qquad (2.5.13)$$

This result is interesting and perhaps unexpected. It shows that the diffusion coefficient of a weak electrolyte is not a simple concentration-weighted average of the diffusion coefficients of the species, *i.e.*,

$$D \neq (1 - \alpha)D_0 + \alpha D_{\pm} \qquad (2.5.14)$$

For a weak electrolyte, the thermodynamic factor is

$$\frac{C}{RT}\frac{d\mu}{dC} = \frac{2}{2 - \alpha} \qquad (2.5.15)$$

It ranges from 1 for a completely associated electrolyte (HA, $\alpha = 0$), to 2 for a completely dissociated electrolyte ($H^+ + A^-$, $\alpha = 1$). The mobility factor is

$$\frac{RTL}{C} = (1 - \alpha)D_0 + \frac{\alpha}{2}D_{\pm} \qquad (2.5.16)$$

2.6. References

1 E. L. Cussler, *Diffusion: Mass Transfer in Fluids Systems*, Chapter 2 and 6-8, Cambridge University Press, London, 1984.

2 L. Onsager, *Phys. Rev.*, 1931, **37**, 405; 1931, **38**, 2265.

3 D G. Leaist, *Encyclopaedia of Applied Physics*, Vol. 5, ed. G. L. Trigg, VCH Publishers, Inc., 1992, p. 61.

4 A. J. Bard and L. R. Faulkner, *Electrochemical Methods: Fundamentals and applications*, Wiley, New York, 1980.

CHAPTER 3

TAYLOR DISPERSION MEASUREMENTS

The diffusion coefficients reported in this thesis were measured by the Taylor dispersion (peak-broadening) method. In this chapter the equipment and procedure used in Taylor dispersion measurements are briefly described. Other techniques could be used to measure diffusion. Among these methods, diaphragm-cell and conductimetric techniques are reliable and well established,[1-5] but they are also very time-consuming (several *days* are required for a *single* diffusion measurement) and rarely used anymore. Though highly accurate (0.2% error in D), Gouy and Rayleigh optical interferometric techniques [6-8] are elaborate and prone to gravitational instabilities and convection. Moreover, they are laborious. At most, only one or two diffusion measurements can be made per day.

Sir Geoffrey Taylor published the first dispersion paper in 1953.[9] Since then the technique has been used to measure diffusion coefficients for hundreds of different systems.[10-16] At the start of a dispersion run, a small volume of solution is injected into a laminar carrier stream at the entrance to a long capillary tube. The injected sample spreads out into a nearly Gaussian distribution as it flows along the tube. Diffusion coefficients are calculated from the shape of the eluted peak which is measured by a suitable detector, such as a flow-through spectrophotometer or refractometer.

The Taylor dispersion technique has a number of important advantages. Rapid diffusion measurements are possible because a solute dispersion can be achieved in 1-2 hours. Errors from unwanted convection are completely avoided because the solutions are confined

within fine-bore tubing. Standard liquid chromatography pumps, valves, detectors available in many laboratories can be employed. Equally important, the experimental procedure is readily automated.

3.1. Theory of Taylor Dispersion for Binary System

Suppose a small volume ΔV of solution containing solute at concentration $C_0 + \Delta C$ is injected at time $t = 0$ into a laminar carrier solution of slightly different concentration C_0 flowing at mean velocity u in a capillary tube of inner radius r. At the tube outlet, a distance l downstream from the injection point, the radially-averaged concentration of the dispersed solute is given by the expression [9,17]

$$C(t) = C_0 + \frac{\Delta C \Delta V}{\pi r^3 u}\left(\frac{12D}{\pi t}\right)^{\frac{1}{2}} \exp\left[-\frac{12D(t - t_R)^2}{r^2 t}\right] \qquad (3.1)$$

where t_R is the retention time

$$t_R = l/u \qquad (3.2)$$

Eqn. (3.1) is valid if the flow is laminar and if longitudinal diffusion is negligible [18] (an accurate assumption for liquids, but not gases)

$$l/u >> 0.8r^2/D \qquad (3.3)$$

A liquid-chromatography detector at the tube outlet monitors the eluted peak. The detector signal $V(t)$, relative to the baseline signal $V_0 + V_1 t$, is proportional to the changes in the concentration of the solute

$$V(t) = V_0 - V_1 t + s[C(t) - C_0] \qquad (3.4)$$

where s is the detector sensitivity. The term $V_1 t$ is included to allow for small linear drifts in the baseline signal, usually a voltage.

Combining eqns. (3.1) and (3.4) yields

$$V(t) = V_0 - V_1 t + V_{max}(t_R/t)^{1/2}\exp\left[\frac{-12D(t - t_R)^2}{r^2 t}\right] \qquad (3.5)$$

Since $12D(t - t_R)^2/r^2 t \approx 12D(t - t_R)^2/r^2 t_R$, eqn. (3.5) shows that the eluted sample peak resembles a Gaussian distribution of variance $r^2 t_R/24D$. Here V_{max} is the peak height relative to the baseline $V_0 + V_1 t$. The parameters V_0, V_1, V_{max}, t_R and D can be determined by using least squares to fit eqn. (3.5) to the measured detector signal.

3.2. Experimental

Teflon dispersion tubes were used in this work. The inner radius of each tube was determined by weighing the tube when empty and when filled with water of known density. Each tube was coiled in the form of a 75-cm diameter helix and held at 25.0 °C in a thermostat. A metering pump (Gilson model MiniPlus 2) was used to pump a carrier solution though each tube at a typical flow rate of about 0.2 cm^3 min^{-1}. Solution samples were injected into the carrier solution by using an injection valve fitted with a 20 μL sample loop. The dispersed sample was monitored at the tube outlet by a liquid-chromatography differential refractometer detector (Waters model 410 or Gilson model 131). The refractometer output voltages were displayed on a chart recorder (ABB Goerz model SE

Fig. 3.1 Dispersion profile for a carrier stream containing 100 mmol L^{-1} aqueous KF solution; ΔC° = -25 mmol L^{-1}.

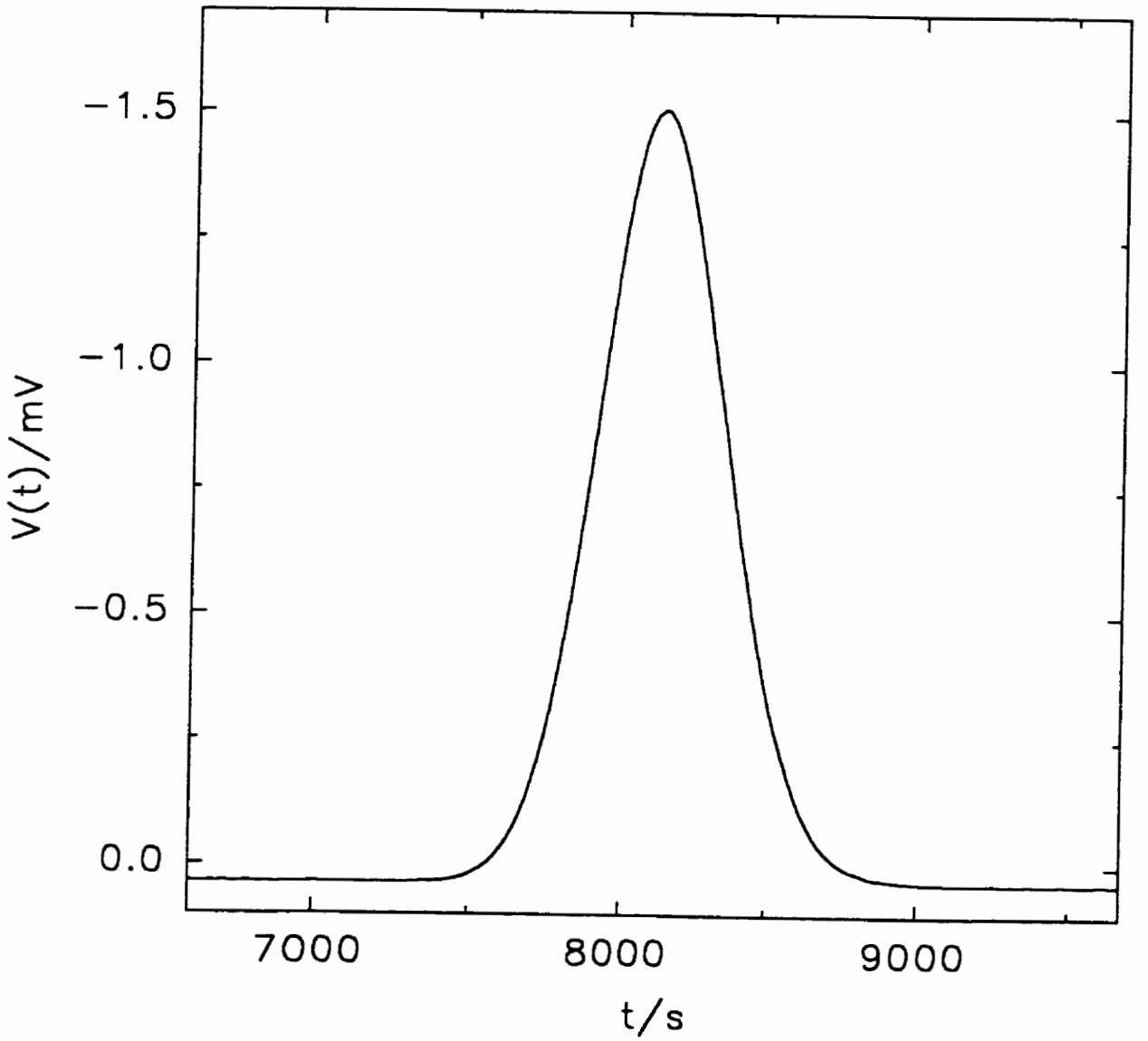
−1.5
−1.0
−0.5
0.0
V(t)/mV
7000
8000
9000
t/s

Fig. 3.2 Schematic diagram of the Taylor dispersion apparatus.

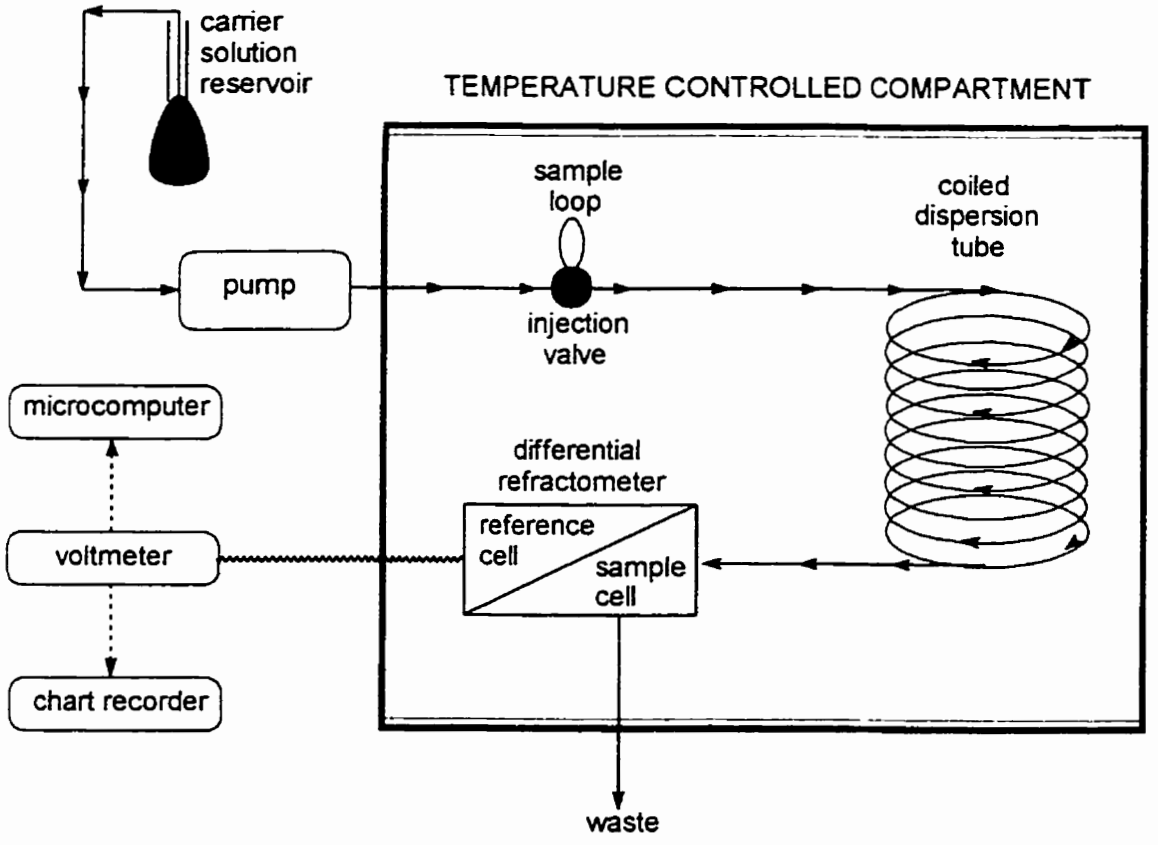
carrier
solution
reservoir
TEMPERATURE CONTROLLED COMPARTMENT
sample
loop
coiled
dispersion
tube
pump
injection
valve
microcomputer
differential
refractometer
reference
cell
sample
cell
voltmeter
chart recorder
waste

120) and measured by a digital voltmeter (Hewlett-Packard model 34401A) at accurately-timed intervals (Fig. 3.1). The voltage readings were stored in a microcomputer for later analysis. Fig. 3.2 shows a schematic diagram of the Taylor dispersion equipment.

All the chemicals used in this work were reagent-grade (>99% purity). Solutions were prepared with distilled, deionized water in calibrated volumetric flasks. Before each set of measurements, each dispersion tube and detector were flushed with 100-200 mL of carrier solution to establish a stable refractometer baseline signal. Samples of solution were injected into the carrier stream at intervals of 60-90 minutes to avoid overlapping the dispersion peaks

3.3. References

1 R. H. Stokes, *J. Am. Chem. Soc.*, 1950, **72**, 763.

2 D. G. Leaist, *J. Chem. Soc., Faraday Trans. 1*, 1987, **83**, 829.

3 H. S. Harned and D. M. French, *Ann. N. Y. Acad. Sci.*, 1945, **44**, 267.

4 H. S. Harned and R. L. Nuttall, *J. Am. Chem. Soc.*, 1947, **69**, 736.

5 E. L. Holt and P. A. Lyons, *J. Phys. Chem.*, 1965, **69**, 2341.

6 L. G. Longsworth, *J. Am. Chem. Soc.*, 1947, **69**, 2510.

7 J. A. Rard and D. G. Miller, *J. Solution Chem.*, 1979, **8**, 701.

8 J. A. Rard and D. G. Miller, *J. Chem. Eng. Data*, 1980, **25**, 211.

9 G. I. Taylor, *Proc. R. Soc. London Ser. A*, 1953, **219**, 186.

10 D. F. Evans, T. Tominaga and H. T. Davis, *J. Chem. Phys.*, 1981, **74**, 1298.

11 S. H. Chen, H. T. Davis and D. F. Evans, *J. Chem. Phys.*, 1982, **77**, 2540.

12 M. A. Matthews and A. Akgerman, *AICHE J.*, 1987, **33**, 881.

13 J. B. Rodden, C. Erkey and A. Akgerman, *J. Chem. Eng. Data*, 1988, **33**, 450.

14 D. G. Leaist, *Electrochimica Acta*, 1988, **33**, 795.

15 D. G. Leaist, *J. Chem. Soc., Faraday Trans.*, 1991, **87**, 597.

16 D. G. Leaist, *Ber. Bunsenges. Phys. Chem.*, 1991, **95**, 117.

17 R. Aris, *Proc. R. Soc. London Ser. A*, 1956, **235**, 67.

18 W. N. Gill and R. Sankarasubramanian, *Proc. R. Soc. London Ser. A*, 1970, **316**, 341.

CHAPTER 4

MUTUAL DIFFUSION IN SOLUTIONS OF ALKALI METAL HALIDES. AQUEOUS LiF, NaF AND KF AT 25 °C

4.1. Introduction

Studies of diffusion in electrolyte solutions [1-3] provide basic information about mass transport and its relation to the structure of solutions and the mobility, activity and solvation of ions. Diffusion coefficients for these systems are also used in studies of electrochemical reactions, ion exchange, membrane separations, the growth and dissolution of crystals, the transmission of nerve impulses and many other important processes.[4] Although accurate diffusion data are relatively abundant for aqueous solutions of alkali halides,[5-14] no reliable diffusion coefficients appear to be available for the fluorides except for the results of a conductimetric study[15] of diffusion in dilute HF and KF solutions (< 0.1 mol dm^{-3}). A possible explanation for the scarcity of diffusion data for aqueous fluoride solutions is their ability to attack glass, especially under acidic conditions. Etching would introduce solution impurities and damage the glass cells commonly employed in capillary-tube, NMR, porous-diaphragm and optical interferometric diffusion experiments.[1,2]

In this study mutual diffusion coefficients (interdiffusion coefficients) are reported for binary aqueous solutions of LiF and NaF. In addition, diffusion measurements for aqueous KF solutions are extended from 0.1 to 8.0 mol dm^{-3}. The results will help to complete the database for aqueous alkali halides, the simplest of all aqueous electrolytes. It many cases the first member in a chemical series has properties which differ in interesting ways from the

properties suggested by extrapolation from higher in the series. Indeed, the mobility of the aqueous F^- ion is a surprising 40% smaller than the mobilities of Cl^-, Br^- and I^- ions.[1] It is therefore of interest to compare the diffusion of aqueous fluoride salts with the diffusion of the corresponding chlorides, bromides and iodides. Moreover, diffusion data for aqueous fluoride solutions can be used in studies of fluoride recovery from phosphate rock,[16] silicate dissolution,[17] and the fluoridation of teeth.[18]

4.2. Experimental

The mutual diffusion coefficients reported in this chapter were measured by the Taylor dispersion (peak-broadening) method.[2,19,20] At the start of each run a 6-port Teflon injection valve was used to introduce 20 mm^3 of solution into a laminar carrier stream of slightly different composition at the entrance to a Teflon dispersion tube (length 3448 cm, inner radius $r = 0.0443_6$ cm). Flow rates were controlled by a metering pump (Gilson model MiniPuls 4, size 13 Viton tubing) to give retention times of about 8 ks.

Dispersion of the injected samples was monitored by a conductivity detector (Waters model 430, 7 mm^3 Teflon flow cell with stainless-steel electrodes) or a differential refractometer (Waters model 401, twin 10 mm^3 quartz flow cells) at the outlet of the dispersion tube. Detector voltages $V(t)$ were measured at accurately-timed 5-s intervals with a digital voltmeter (Hewlett-Packard model 34401A). A 0.2 MPa backpressure regulator in the outlet line of each detector was used to prevent bubble formation and to maintain a steady flow of carrier solution.

Binary mutual diffusion coefficients (D) were evaluated by fitting the dispersion equation

$$V(t) = V_0 + V_1 t + V_{max}(t_R/t)^{1/2}\exp[-12D(t - t_R)^2/r^2 t] \quad (4.1)$$

to the detector voltages. The additional fitting parameters were the mean sample retention time t_R, peak height V_{max}, baseline voltage V_0, and baseline slope V_1 (to allow for small linear drifts in the detector signal).

The concentrations of the injected solutions and the carrier solutions differed by ±0.002 mol dm^{-3} for the most dilute carrier solutions up to ±0.100 mol dm^{-3} for the most concentrated solutions. At least two solutions of different composition were injected into each carrier solution to confirm that the measured diffusion coefficients were independent of the initial concentration difference and therefore represented the differential value of the D at the carrier-stream composition.

Solutions were prepared in calibrated polypropylene volumetric flasks using distilled, deionized water and reagent-grade LiF, NaF and KF (Caledon Laboratories). The purity of each salt (> 99%) was determined by conversion to HF in column of cation exchange beads followed by titration against standardized NaOH solutions[21]. The accuracy of the reported salt concentrations is ±0.5%.

4.3. Results and Discussion

Table 4.1 gives the average diffusion coefficient determined from six to eight injections into each carrier solution. Values of D from replicate injections were usually reproducible to within ±0.5%. The diffusion measurements for the LiF and NaF solutions were restricted to relatively low concentrations by the limited solubilities of these salts (0.051 and 0.98 mol dm^{-3}, respectively, at 25 °C).[22]

Table 4.1 includes accurate limiting D^0 values for infinitely dilute solutions of LiF,

Table 4.1 Binary mutual diffusion coefficients, thermodynamic factors and resistance coefficients of aqueous LiF, NaF and KF solutions at 25 °C

C mol dm^{-3}	D 10^{-9} m^2 s^{-1}	$1 + (d\ln\gamma/d\ln m_1)$	$(\varphi/2RT)/10^9$ s m^{-2}
	LiF		
0.000	1.213[a]	-	-
0.002	1.18_0[b]	-	-
0.005	1.17_6[b]	-	-
0.010	1.14_6[b]	-	-
0.025	1.10_8[b]	-	-
0.050	1.09_7[b]	-	-
	NaF		
0.000	1.401[a]	1.000	0.714
0.002	1.38_0[b]	0.976	0.707
0.005	1.35_7[b]	0.965	0.711
0.010	1.34_8[b]	0.953	0.707
0.025	1.33_9[b]	0.934	0.698
0.035	1.32_0[b]	0.926	0.702
0.050	1.31_3[b]	0.918	0.699
0.100	1.28_4[b]	0.902	0.702
0.100	1.29_7[b]	0.902	0.695

Table 4.1 (cont.)

0.150	1.27_6^b	0.892	0.699
0.200	1.25_1^b	0.886	0.708
0.300	1.25_6^b	0.877	0.698
0.300	1.25_1^b	0.877	0.701
0.400	1.23_1^b	0.869	0.706
0.500	1.21_0^c	0.863	0.713
0.600	1.19_7^c	0.858	0.717
0.800	1.17_5^c	0.854	0.727
0.900	1.17_8^c	0.854	0.724

KF

0.000	1.682^a	1.000	0.594
0.002	1.63_4^b	0.979	0.599
0.005	1.62_7^b	0.969	0.596
0.010	1.61_7^b	0.957	0.592
0.015	1.60_0^b	0.949	0.593
0.025	1.58_8^b	0.938	0.591
0.050	1.57_0^b	0.920	0.586
0.100	1.55_2^b	0.903	0.581
0.200	1.54_3^b	0.892	0.578
0.200	1.55_0^b	0.892	0.575

Table 4.1 (cont.)

0.300	1.53_4[b]	0.892	0.581
0.300	1.53_9[b]	0.892	0.580
0.310	1.52_9[c]	0.892	0.583
0.500	1.54_7[b]	0.907	0.586
0.500	1.54_8[c]	0.907	0.586
0.800	1.55_3[c]	0.943	0.607
1.00	1.55_1[c]	0.970	0.625
1.50	1.57_6[c]	1.045	0.663
2.00	1.58_9[c]	1.124	0.707
2.50	1.60_4[c]	1.204	0.751
3.00	1.62_9[c]	1.286	0.789
4.00	1.64_2[c]	1.457	0.887
5.00	1.66_3[c]	1.641	0.987
6.00	1.67_5[c]	1.844	1.101
6.50	1.67_5[c]	1.953	1.166
6.75	1.65_9[c]	2.010	1.212
7.00	1.64_0[c]	2.068	1.261
8.00	1.60_2[c]	2.318	1.447

[a]Calculated from limiting ionic conductivities.

[b]Conductivity detector.

[c]Differential refractometer detector.

NaF and KF obtained independently from Nernst's equation $D^0(MF) = 2D^0(M^+)D^0(F^-)/[D^0(M^+) + D^0(F^-)]$ and the limiting ionic diffusion coefficients $D^0(F^-) = 1.482 \times 10^{-9}$, $D^0(Li^+) = 1.030 \times 10^{-9}$, $D^0(Na^+) = 1.334 \times 10^{-9}$ and $D^0(K^+) = 1.957 \times 10^{-9}$ m^2 s^{-1}. The latter were calculated from the respective limiting ionic conductivities [1,23] (λ^0) 0.005567, 0.003868, 0.005010 and 0.007350 S m^2 mol^{-1} by using the relation $D^0 = RT\lambda^0/F^2$. R is the gas constant, T the temperature, and F the Faraday constant.

The conductivity detector was well suited to fluoride diffusion measurements because of its corrosion resistance. Unfortunately, this detector could not be used at salt concentration above about 0.5 mol dm^{-3} owing to the high background conductivity of the carrier solutions. In this region dispersion was followed by the refractometer detector. Despite concern that its quartz flow cells would be attacked, repeated check diffusion measurements with 0.300 mol dm^{-3} aqueous NaCl solutions ($D = 1.473 \times 10^{-9}$ m^2 s^{-1}, from Rayleigh interferometry) [8] gave no indication of loss of sensitivity or increased noise in the refractometer signal. The pH of the fluoride solutions used in this study (7.0 to 7.5) was evidently high enough to prevent significant etching. The NaCl runs served the additional purpose of indicating an accuracy of ±1% for the reported D values of the fluoride solutions.

Fig. 4.1 shows that the diffusion coefficients of the LiF and NaF solutions decrease smoothly with increasing salt concentration. For the KF solutions there is a shallow minimum in D near 0.4 mol dm^{-3} followed by a weak maximum near 6 mol dm^{-3}. The diffusion coefficients of dilute KF solutions determined previously by a modified Harned conductimetric technique are also plotted in Fig. 4.1. Agreement with the present results is within the combined accuracies of the conductimetric (±0.5) and dispersion (±1%) measurements.

Fig. 4.1 Binary mutual diffusion coefficients of aqueous solutions of alkali metal halides at 25 °C. ■, limiting diffusion coefficients of LiF, NaF and KF calculated from ionic conductivities. ○, D values for LiF, NaF and KF measured by Taylor dispersion with the conductivity detector. ●, D values for NaF and KF measured by Taylor dispersion with the refractometer detector. □, D values for KF measured by Harned's restricted-diffusion method.[15]

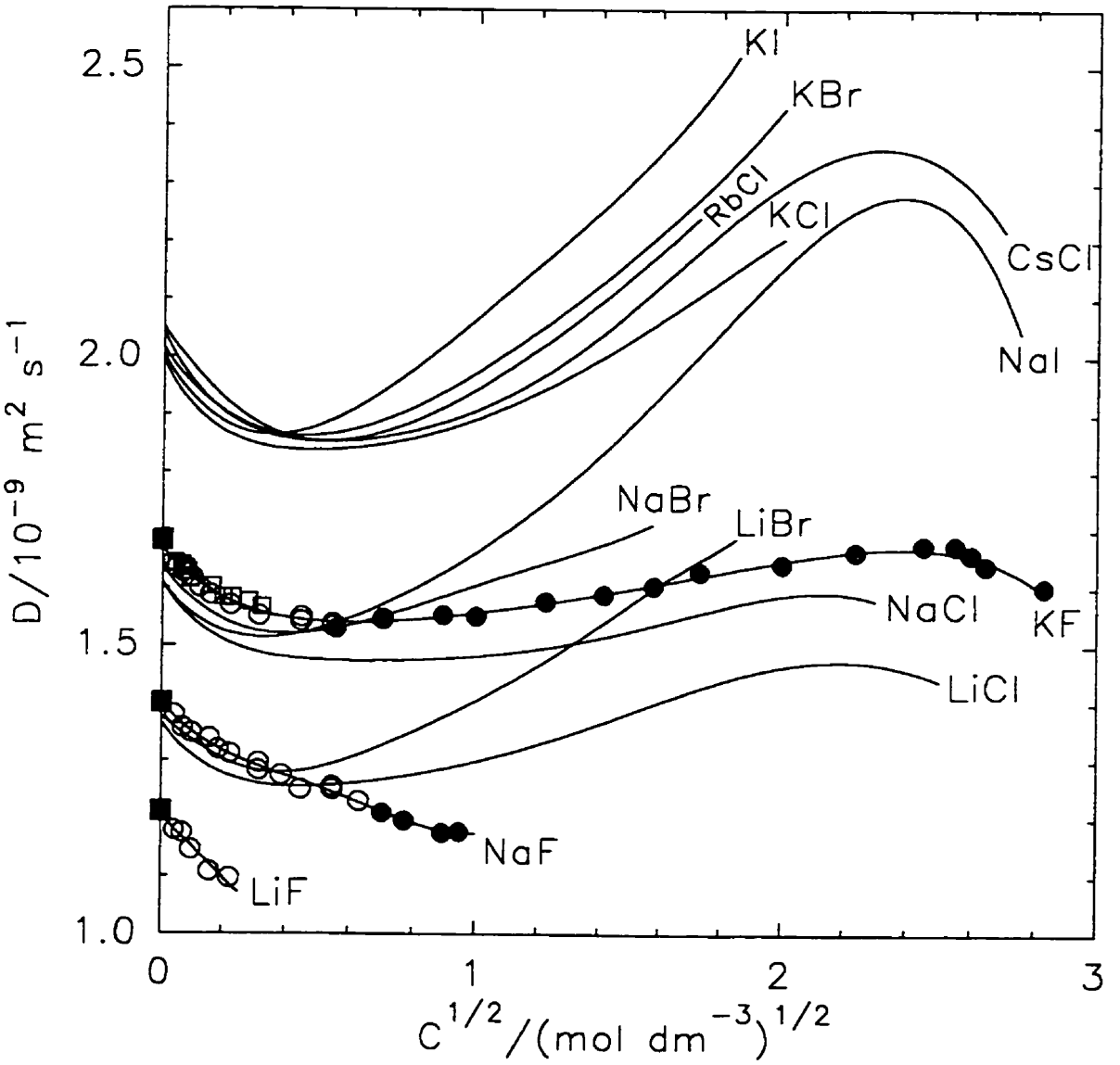
KI
KBr
RbCl
KCl
CsCl
NaI
NaBr
LiBr
NaCl
KF
LiCl
NaF
LiF
2.5
2.0
1.5
1.0
0
1
2
3
D/10^-9 m^2 s^-1
C^1/2/(mol dm^-3)^1/2

Over the years conductimetric, optical, and diaphragm-cell techniques have been used to measure accurate binary mutual diffusion coefficients for 10 other aqueous alkali halides: LiCl,[5-7] LiBr,[12] NaCl,[5,8] NaBr,[12] NaI,[7] KCl,[9,10] KBr,[12] KI,[13] RbCl[14] and CsCl.[11] There are far too many overlapping data points to crowd onto a single plot. Instead, the polynomials in $C^{1/2}$ shown in Fig. 4.1 were fitted to the reported D values for comparison with the present fluoride results. In cases where two or more data sets were available for the same salt over the same concentration range, only the most accurate diffusion coefficients from optical interferometry[7,8,10,11] were used in the fitting procedure.

The collection of data in Fig. 4.1 reveals a curious result: aqueous alkali halides can be classified into three main groups depending on their diffusion coefficients in dilute solutions (< 0.1 mol dm^{-3}). In this region differences in the D values are governed primarily by differences in the ionic diffusion coefficients for each salt. At 25 °C the limiting diffusion coefficients[1] of K^+, Rb^+, Cs^+, Cl^-, Br^-, and I^- ions are nearly identical: 1.957, 2.072, 2.057, 2.033, 2.081, and 2.056, respectively (in units of 10^{-9} m^2 s^{-1}), so it is not surprising that D values for dilute KCl, KBr, KI, RbCl and CsCl solutions are grouped together. By coincidence, however, the diffusion coefficients of Na^+ and F^- ions are similar:[1] 1.334 x 10^{-9} and 1.475 x 10^{-9} m^2 s^{-1}, respectively. Hence KF, NaCl, NaBr and NaI form a second group of salts with similar diffusion coefficients in dilute solution. By further coincidence, LiBr, LiCl and NaF form a third group of salts with similar D values below 0.1 mol dm^{-3}. Li^+ and F^- ions have the smallest diffusion coefficients of all the ions in the alkali halide series.[1,23] Consequently, LiF stands alone as the slowest alkali halide.

The simple pattern of diffusion coefficients observed for dilute solutions clearly breaks down at high salt concentrations. For example, the diffusion coefficients of LiBr, NaI, KCl,

KBr, KI, RbCl and CsCl increase relatively rapidly with concentration, producing a number of crossovers. The complicated concentration dependence of D can be attributed in part to the fact diffusion coefficients relate solute fluxes to solute concentration gradients, whereas chemical potential gradients are the fundamental driving forces for diffusion.[2,3] Concentrated salt solutions tend to be strongly nonideal. Changes in activity coefficients can therefore produce large changes in the chemical-potential driving force per unit concentration gradient. In order to understand the concentration dependence of D it is helpful to use the resistance coefficient [2]

$$\varphi = \frac{-\nabla\mu_1}{v_1 - v_0} = \frac{d\mu_1/d\ln m_1}{D} \tag{4.2}$$

to factor out the thermodynamic contribution to D. A measure of the frictional drag per mole of diffusing salt, φ gives the driving force per mole of salt ($-\nabla\mu_1$) required to maintain unit relative velocity ($v_1 - v_0$) between the diffusing salt(1) and solvent(0) components. μ_1 and m_1 denote the salt chemical potential and molality.

For the solutions considered here $d\mu_1/d\ln m_1 = 2RT(1 + d\ln\gamma/d\ln m_1)$, where γ is the mean ionic activity coefficient, and hence

$$\varphi = \frac{2RT}{D}\left(1 + \frac{d\ln\gamma}{d\ln m_1}\right) \tag{4.3}$$

φ is inversely related to the "thermodynamic diffusion coefficient" M used by some authors:[7,8,10,11] $\varphi/2RT = 1/M$.

No activity data appear to be available for aqueous LiF solutions, but accurate activity

coefficients have been reported for aqueous NaF and KF. Table 4.1 gives values of $1 + d\ln\gamma/d\ln m_1$ for these solutions calculated from the γ values recommended by Hamer and Wu.[24] Published densities[25] were used to convert salt molalities (m_1) to molarities (C). Values of $\varphi/2RT$ calculated from the measured diffusion coefficients by using eqn. (4.3) are also presented in Table 4.1. Over the concentration range from 0.0 to 8.0 mol dm^{-3} the resistance coefficient of aqueous KF increases by a factor of about 2.5, a substantial variation. Over a more limited concentration range, 0.0 to 0.9 mol dm^{-3}, the resistance coefficient of aqueous NaF varies by only 4%.

Activity [7,24] data taken from the literature were used to evaluate the thermodynamic factors shown in Fig. 4.2 for the other alkali halide solutions. Values of $1 + (d\ln\gamma/d\ln m_1)$ for concentrated LiCl and LiBr solutions are especially large because the amount of "free" water is reduced by strong hydration of the Li^+ ions. These solutions are effectively more concentrated than suggested by simple stoichiometric concentrations, which in turn raises the salt activity coefficient and the thermodynamic driving force for diffusion. Hydration of aqueous F^- ions is also relatively strong. This is why thermodynamic factors for aqueous KF solutions rise more steeply than for KCl or KBr solutions.

Diffusion coefficients and thermodynamic factors for the aqueous alkali halides were used to calculate the $\varphi/2RT$ values shown in Fig. 4.3. It has been noted in previous studies[7,8,10,11] that the concentration dependence of thermodynamic diffusion coefficients (and hence φ) is more regular than the concentration dependence of D. Figures 4.1 and 4.3 amply illustrate this point. However, the concentration dependence of φ can be much stronger than that of D. As shown in Fig. 4.1, the values of D for each salt solution usually vary by considerably less than 50%. Yet the corresponding values of $\varphi/2RT$ plotted in Fig. 4.3 more

Fig. 4.2 Thermodynamic factors[7,24] at 25 °C for aqueous alkali halides plotted against the square root of the concentration of each salt. Published densities[7,8,10,11,14,25-28] were used to convert salt molalities (m_1) to molarities (C).

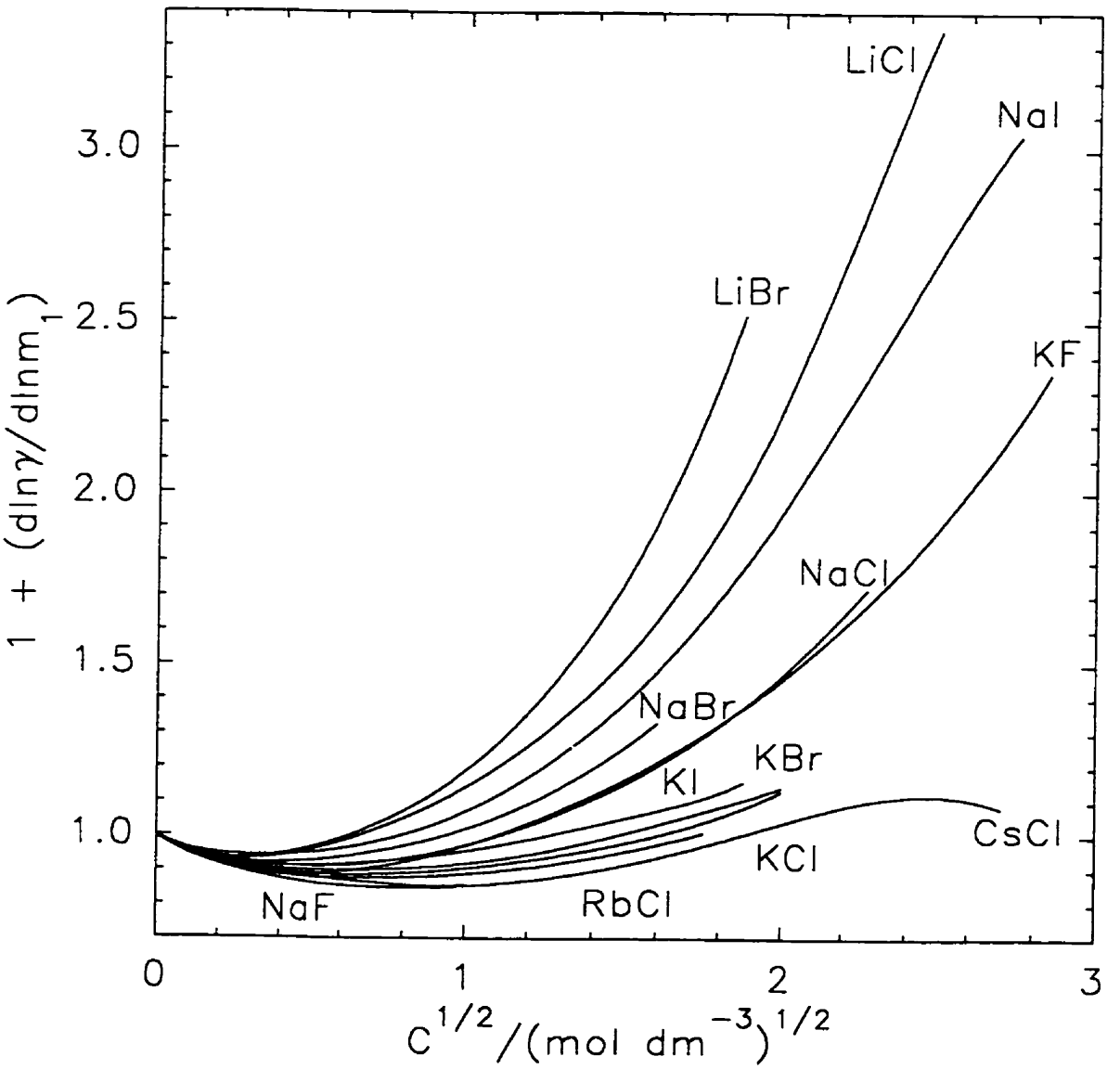
LiCl
NaI
LiBr
KF
NaCl
NaBr
KBr
KI
CsCl
KCl
NaF
RbCl
3.0
2.5
2.0
1.5
1.0
0
1
2
3
1 + (dlnγ/dlnm1)
c1/2/(mol dm−3)1/2

Fig. 4.3 Values of $\varphi/2RT$ for aqueous alkali halide solutions plotted against the square root of the concentration of each salt.

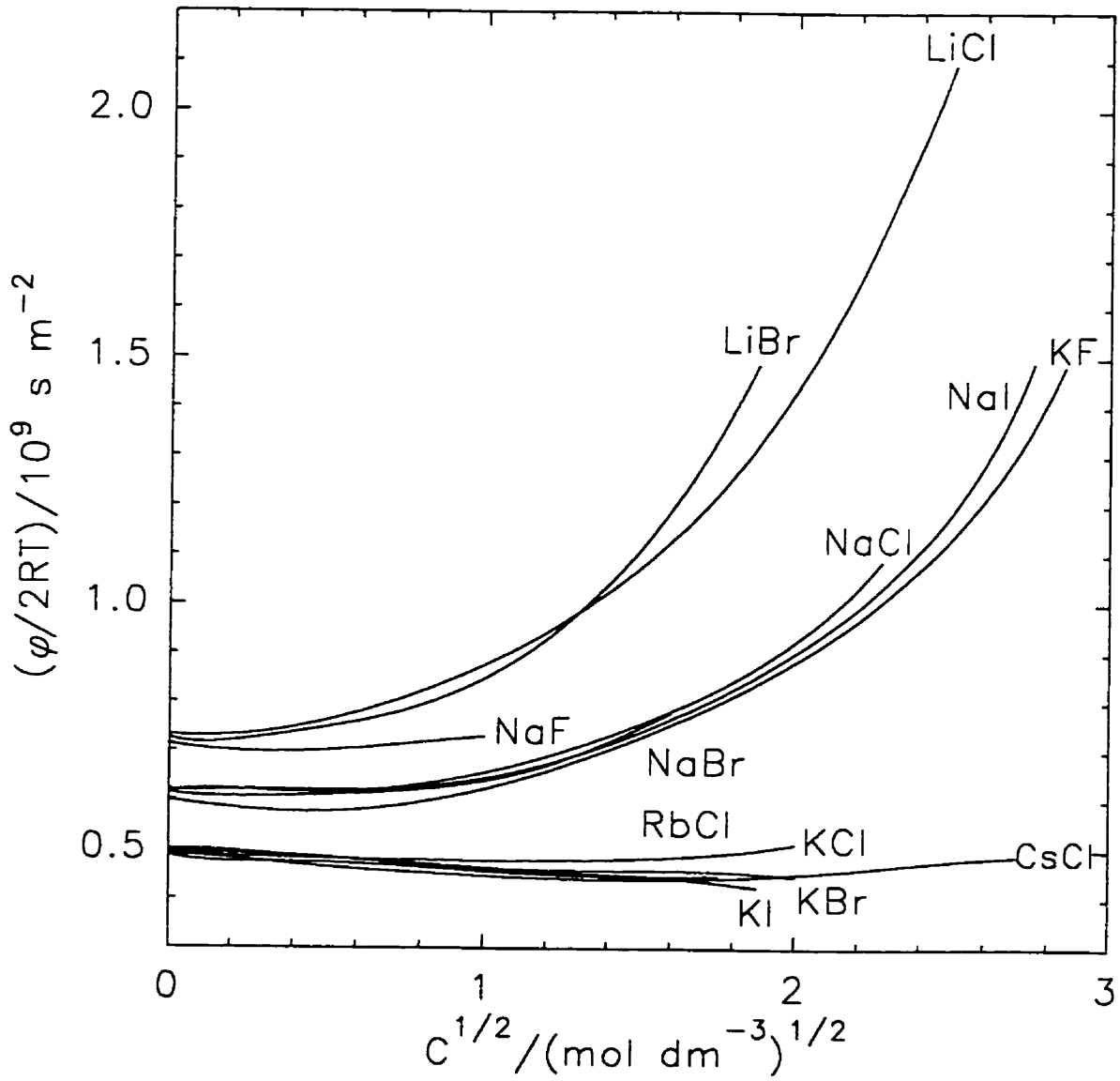
LiCl
LiBr
KF
NaI
NaCl
NaF
NaBr
RbCl
KCl
CsCl
KI
KBr
2.0
1.5
1.0
0.5
0
1
2
3
$(\varphi/2RT)/10^9$ s m^{-2}
$c^{1/2}/(\text{mol dm}^{-3})^{1/2}$

than double for LiBr, NaI and KF solutions, and there is a three-fold increase in the resistance coefficient for the LiCl solutions. Factoring out the thermodynamic contribution to D can therefore magnify the concentration dependence of the resulting resistance coefficient or thermodynamic diffusion coefficient.

The importance of the thermodynamic contribution to D has been emphasised in recent studies of diffusion in concentrated salt solutions.[7,8,10,11] It is known, however, that changes in the solution viscosity [1,2] are important too. In fact, the viscosity dominates the concentration dependence of D for some systems.[1,33]

To explore the relationship between the resistance coefficients and the viscosities of alkali halide solutions, published data [13,27-32] were used to calculate the relative viscosities plotted in Fig. 4.4. A direct relation between φ and η is not expected. In dilute solutions, for example, the viscosity usually increases more rapidly than the resistance coefficient.[1,2] But the plot of the relative viscosities of the alkali halide solutions (Fig. 4.4) does bear a qualitative resemblance to the plot of $\varphi/2RT$ values (Fig. 4.3). In particular, the relatively large resistance coefficients of concentrated solutions of LiCl, LiBr, NaCl, NaI and KF are consistent with the relatively large viscosities of these solutions.

To emphasise that the viscosity accounts for the bulk of the concentration dependence of the resistance coefficients, "viscosity-corrected" values of $(\varphi/2RT)(\eta^0/\eta)$ are plotted in Fig. 4.5 employing the same scale used for the plot of uncorrected $\varphi/2RT$ values (Fig. 4.3). As anticipated, the correlation between the resistance coefficient and the viscosity is not entirely satisfactory. For example, the resistance coefficients of LiBr and NaF solutions increase more rapidly and less rapidly, respectively, than the solution viscosity. Nevertheless, the results illustrate that both thermodynamic and viscosity factors should be used to interpret mutual

Fig. 4.4 Relative viscosities[13,27-32] at 25 °C for aqueous alkali halide solutions.

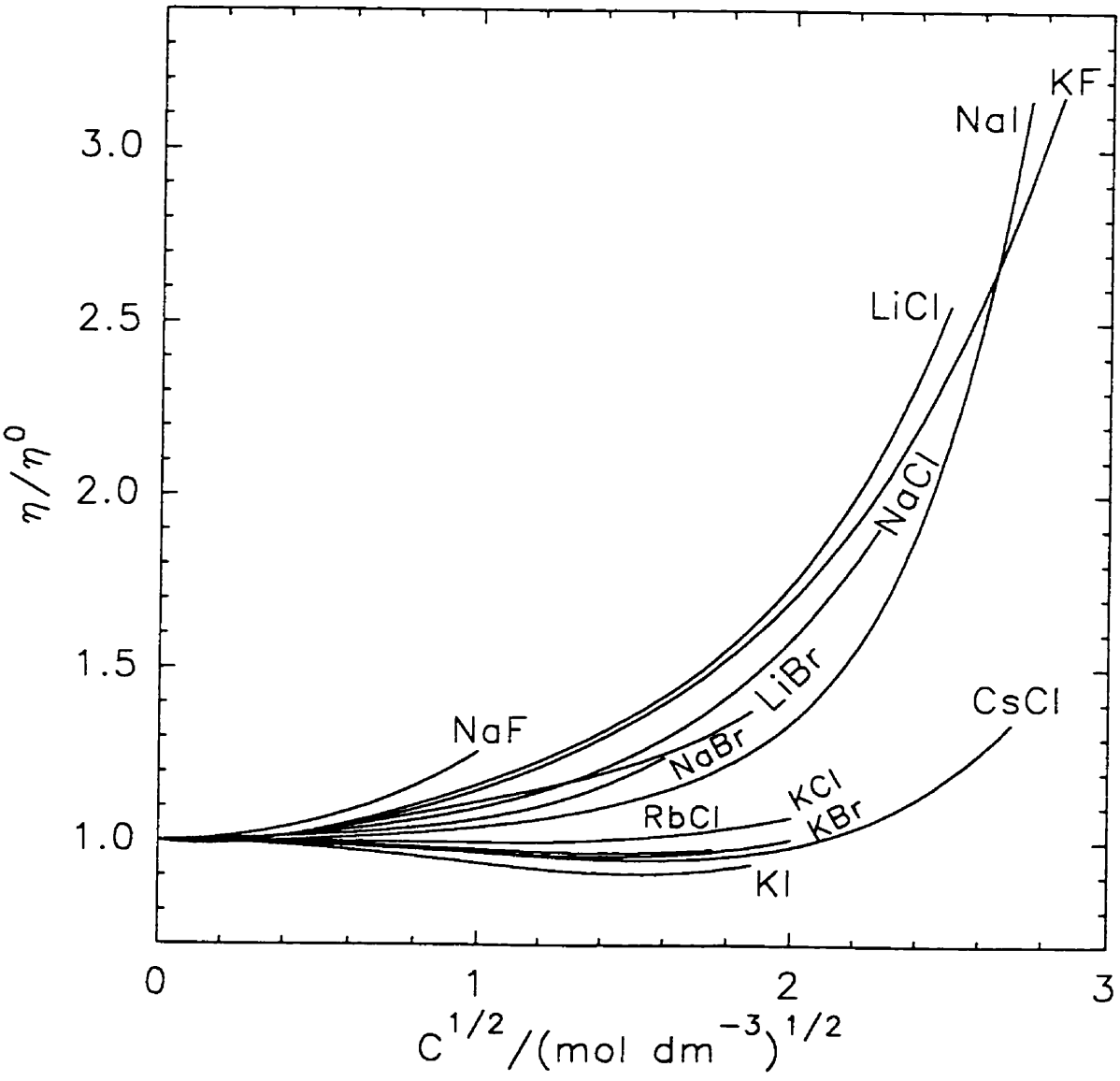
3.0
2.5
2.0
1.5
1.0
η/η^0
0
1
2
3
$c^{1/2}/(\text{mol dm}^{-3})^{1/2}$
KF
NaI
LiCl
NaCl
LiBr
CsCl
NaF
NaBr
KCl
RbCl
KBr
KI

Fig. 4.5 Values of $\varphi/2RT$ multiplied by the empirical viscosity correction factor η^0/η. The scale of this plot is deliberately chosen to match the scale of uncorrected $\varphi/2RT$ values plotted in Fig. 4.3.

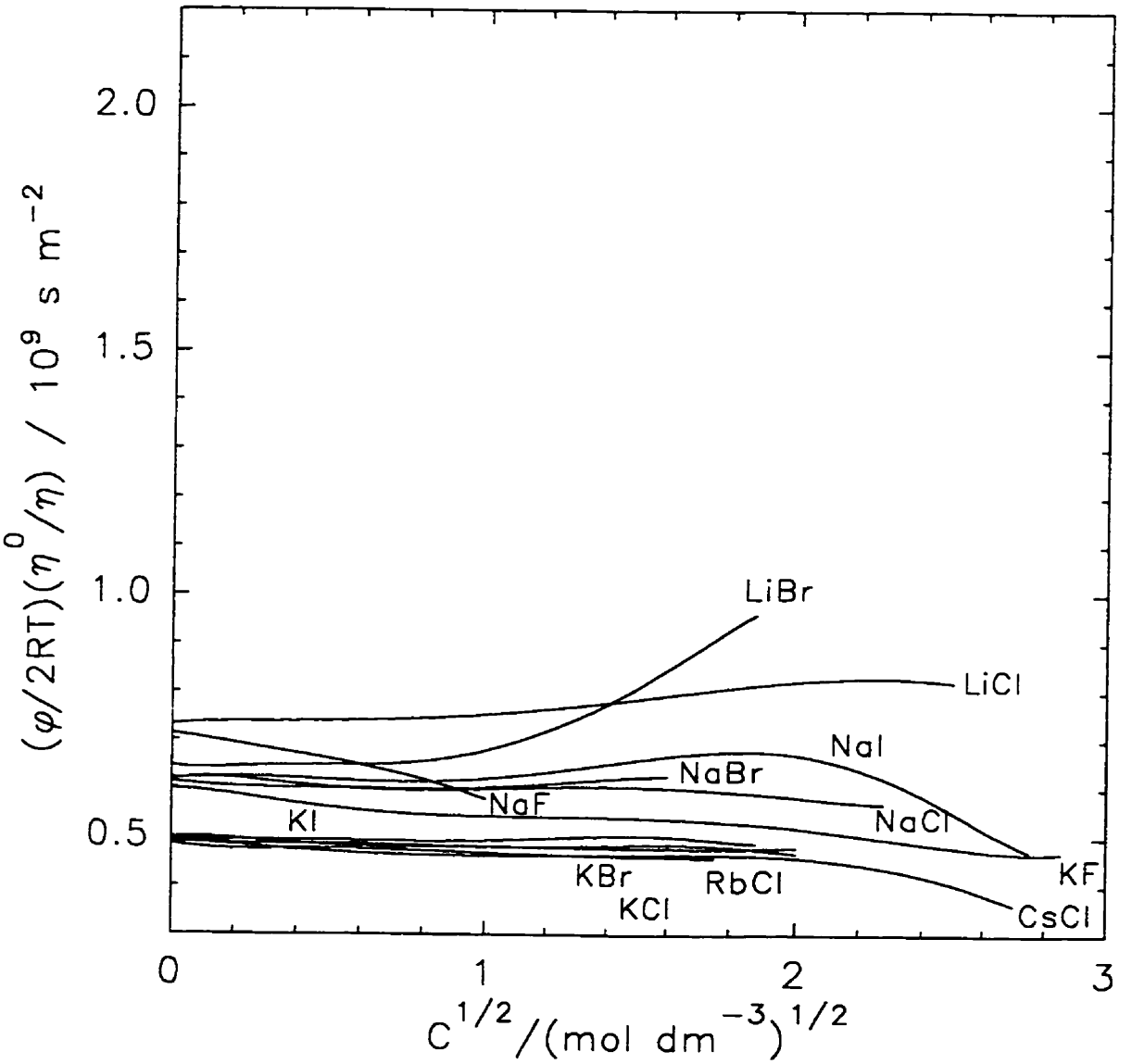
2.0
1.5
1.0
0.5
0
1
2
3
$(\varphi/2RT)(\eta^0/\eta)$ / 10^9 s m^{-2}
$c^{1/2}$/(mol dm^{-3})$^{1/2}$
LiBr
LiCl
NaI
NaBr
NaF
NaCl
KI
KF
KBr
RbCl
KCl
CsCl

diffusion in concentrated salt solutions.

4.4. References

1 R. A. Robinson and R. H. Stokes, *Electrolyte Solutions*, Academic, New York, 2nd edn., 1959.

2 H. J. V. Tyrrell and K. R. Harris, *Diffusion in Liquids*, Butterworths, London, 1984.

3 R. Haase, *Thermodynamics of Irreversible Processes*, Dover, New York, 1990.

4 J. S. Newman, *Electrochemical Systems*, Prentice-Hall, Englewood Cliffs, N.J., 1973.

5 H. S. Harned and C. L. Hildreth, *J. Am. Chem. Soc.*, 1951, **73**, 650.

6 V. Vitagliano, *Gaz. Chim. Ital.*, 1960, **90**, 876.

7 J. A. Rard and D. G. Miller, *J. Solution Chem.*, 1983, **12**, 413.

8 J. A. Rard and D. G. Miller, *J. Solution Chem.*, 1979, **8**, 701.

9 H. S. Harned and R. L. Nutall, *J. Am. Chem. Soc.*, 1949, **71**, 1460.

10 J. A. Rard and D. G. Miller, *J. Chem. Eng. Data*, 1980, **25**, 211.

11 J. A. Rard and D. G. Miller, *J. Chem. Soc., Faraday Trans. 1*, 1982, **78**, 887.

12 R. H. Stokes, *J. Am. Chem. Soc.*, 1950, **72**, 2243.

13 P. J. Dunlop and R. H. Stokes, *J. Am. Chem. Soc.*, 1951, **73**, 5456.

14 S. K. Jalota and R. Paterson, *J. Chem. Soc., Faraday Trans. 1*, 1973, **69**, 1510.

15 R. A. Noulty and D. G. Leaist, *Electrochim. Acta*, 1985, **30**, 1095.

16 K. L. Elmore, J. D. Hatfield, C. M. Mason and A. D. Jones, *J. Am. Chem. Soc.*, 1949, **71**, 2710.

17 G. D. Parkes, *Mellor's Modern Inorganic Chemistry*, Longmans and Green,

London, 1967, p. 527.

18 J. E. Tyler, *Caries Res.*, 1970, **4**, 23.

19 A. Alizadeh, C. A. Nieto de Castro and W. A. Wakeham, *Int. J. Thermophys.*, 1980, **1**, 243.

20 D. G. Leaist, *J. Chem. Soc., Faraday Trans.*, 1991, **87**, 597.

21 A. Vogel, *Vogel's Textbook of Quantitative Inorganic Analysis*, Longman, London, 4th edn., 1978.

22 J. H. Payne, *J. Am. Chem. Soc.*, 1937, **59**, 947.

23 W. C. Duer, R. A. Robinson and R. G. Bates, *J. Chem. Soc., Faraday Trans. 1*, 1972, **68**, 716.

24 W. J. Hamer and Y. Wu, *J. Phys. Chem. Ref. Data*, 1972, **1**, 1047.

25 C. Synowietz in *Landolt-Börnstein Tabellen*, Group IV, Vol. 1, Part b, ed. K. Schäfer, Springer-Verlag, Berlin, 1977, p. 45, 50, 58, 78, 82.

26 S. Lengyel, J. Tamás, J. Giber and J. Holderith, *Acta Chim. Sci. Hung.*, 1964, **40**, 125.

27 F. A. Gonçalves and J. Kestin, *Ber. Bunsenges. Phys. Chem.*, 1977, **81**, 1156.

28 J. E. Desnoyers, M. Arel, G. Perron and C. Jolicoeur, *J. Phys. Chem.*, 1969, **73**, 3346.

29 S. A. Bogatykh and I. D. Evnovich, *Zh. Prikl. Khim.*, 1963, **36**, 1867.

30 J. E. Desnoyers and G. Perron, *J. Solution Chem.*, 1972, **1**, 199.

31 D. E. Goldsack and R. Franchetto, *Can. J. Chem.*, 1977, **55**, 1062.

32 D. E. Goldsack and R. Franchetto, *Can. J. Chem.*, 1978, **56**, 1442.

33 D. G. Leaist and R. Lu, *J. Chem. Soc., Trans. Faraday Soc.*, 1997, **93**, 1755.

CHAPTER 5

CROSSOVER FROM MOLECULAR TO IONIC DIFFUSION IN DILUTE AQUEOUS SOLUTIONS OF HYDROLYSED ETHYLAMINE, DIETHYLAMINE AND TRIETHYLAMINE

5.1. Introduction

Electrolyte diffusion has been the subject of numerous experimental and theoretical studies.[1-10] Most of the work has focused on "strong" electrolytes, such as aqueous NaCl.[10] It is well known, however, that the diffusion of incompletely dissociated ("weak") electrolytes plays an essential role in many industrial, environmental, and biochemical processes. Moreover, ion association has important implications for electrolyte transport because it changes both the mobility and the thermodynamic driving force for diffusion.[2,11,12]

Mutual diffusion coefficients (D) have been reported previously for aqueous acetic acid [13,14] and for several other weak acids. [12,15-17] Although the dissociation $HA \rightleftharpoons H^+ + A^-$ produces two additional solute species, $H^+ + A^-$, there are two additional constraints: electroneutrality and local equilibrium of the dissociation reaction. As a result, there is still only one independent solute flux. Diffusion of a weak acid can therefore be described by a single binary mutual diffusion coefficient, D, which relates the flux of total acid (molecular plus ionized forms) to the gradient in total acid concentration: $J = -D\nabla C$.

One of the remarkable properties of aqueous weak acids is the sharp drop in the mutual diffusion coefficient caused by ion association. Over the narrow concentration interval from 0.000 to 0.001 mol dm^{-3}, for example, the mutual diffusion coefficient of aqueous acetic

acid[14] drops from 1.95×10^{-5} to 1.26×10^{-5} $cm^2\ s^{-1}$ at 25° C. Another interesting feature concerns the relative contributions to the mutual diffusion coefficient from the molecular and ionic forms of a weak electrolyte. For a univalent weak acid at total concentration C and extent of dissociation α, it seems reasonable, at first glance, to weight the molecular and ionic diffusion coefficients (D_{HA} and $D_{\pm}$ respectively) in proportion to the molecular and ionic fractions of the total acid.

$$D(c) = (1 - \alpha)D_{HA} + \alpha D_{\pm} \qquad (5.1)$$

However, eqn. (5.1) is not supported by theory or experiment. Because mutual diffusion fluxes are proportional to chemical concentration gradients, the molecular and ionic contributions to D are weighted in proportion to the concentration derivatives $d[(1-\alpha)C]/dC$ and $d(\alpha C)/dC$, not according to the molecular and ionic concentrations $(1-\alpha)C$ and αC. The correct weighting scheme leads to the approximate expression[2,14-17]

$$D(c) = \left[(1 - \alpha)D_{HA} + \frac{\alpha}{2}D_{\pm}\right]\frac{2}{2 - \alpha} \qquad (5.2)$$

for the concentration dependence of the mutual diffusion coefficient of a dilute univalent weak acid. Corrections for electrophoresis, viscosity changes, and non-ideal solution behaviour can be added to eqn. (5.2) for a more accurate description[2,14-17] of the diffusion behaviour. In addition, eqn. (5.2) can be extended to polyvalent or mixed weak acids.[18]

The theory developed for the diffusion of weak acids should apply equally well to weak bases, such as aqueous triethylamine: $(Et)_3N + H_2O \rightleftharpoons (Et)_3NH^+ + OH^-$. In this chapter binary mutual diffusion coefficients are reported for dilute aqueous solutions of

ethylamine, diethylamine, and triethylamine. The results are analysed to determine the diffusion coefficients of the molecular $(Et)_nNH_{3-n}$ species and the corresponding $(Et)_nNH^+_{4-n}$ ions.

5.2. Experimental

The diffusion measurements reported here were made by the Taylor dispersion (peak-broadening) method.[1,19] At the start of each run a narrow band of solution at concentration $C + \Delta C$ is injected into a laminar carrier stream at concentration C. Diffusion coefficients are calculated from absorbance or refractive-index profiles measured across the eluted sample peak. In practice, small initial concentration differences are employed so that the measured diffusion coefficients are independent of ΔC and therefore represent differential diffusion coefficients at the carrier-stream concentration. For dilute solutions of the aqueous amines, however, the strong concentration dependence of D causes the measured diffusion coefficients to drop with increasing values of ΔC, even for the smallest practicable initial concentration differences. The approach taken here is to measure apparent diffusion coefficients for several different initial concentration differences and then interpolated or extrapolated to $\Delta C = 0$ to give the true differential diffusion coefficient for each carrier stream.

A metering pump maintained a steady laminar flow of carrier solution through a Teflon dispersion tube (length 3334 cm, internal diameter 0.0947_6 cm). Slugs of solution of slightly higher or lower concentration (-15 mmol dm^{-3} $\leq \Delta C \leq +15$ mmol dm^{-3}) were introduced at the tube inlet through a six-port injection valve fitted with a 20 mm^3 sample loop. A flow-through differential refractometer at the tube outlet monitored the broadened

distribution of the dispersed samples. Mutual diffusion coefficients were evaluated by fitting eqn. (3.5) to the refractometer voltages $V(t)$. Details of the equipment and procedure have been described previously.[20,21]

Stock solutions of diethylamine and triethylamine (*ca.* 0.2 mol dm^{-3}) were prepared by dissolving the appropriate solute (Aldrich, 99.5 % purity) in distilled, deionized water. Ethylamine stock solutions were prepared by diluting a concentrated aqueous solution (Aldrich). Each stock solution was analysed by titrating weighed solution samples against standardized hydrochloric acid. Weighed amounts of each stock were diluted with freshly distilled, deionized water in calibrated volumetric flasks to prepare the solutions for the diffusion measurements. A few viscosities and densities were measured with an Ubbelohde viscometer and a single-stem pycnometer.

Binary mutual diffusion coefficients of aqueous ethylamine, diethylamine, and triethylamine were measured at concentrations from 0.2 to 100 mmol dm^{-3} at 25 °C. At least six injections were made into each carrier stream. Values of D from replicate injections were usually consistent within 1% or better for carrier-stream concentrations $C \geq 1.0$ mmol dm^{-3}. In this region peaks generated by different initial concentration differences gave identical diffusion coefficients within the precision of the measurements. These D values were averaged to determine the differential mutual diffusion coefficient for each carrier-stream composition.

Below 1.0 mmol dm^{-3}, however, the strong concentration dependence of D caused the measured diffusion coefficients to decrease as the injected solutions became more concentrated. In this region three or four solutions of different composition were injected into each carrier stream. Relatively small initial concentration differences were used ($\Delta C \leq$

Fig. 5.1 Apparent diffusion coefficients measured for a 0.50 mmol dm^{-3} triethylamine carrier solution. The injected solution contained 0.00, 1.50, or 2.50 mmol dm^{-3} triethylamine (ΔC = -0.50, 1.00, and 2.00 mmol dm^{-3}, respectively). Linear interpolation to zero initial concentration difference gives $1.04_4 \times 10^{-5}$ cm^2 s^{-1} for the differential mutual diffusion coefficient of 0.50 mmol dm^{-3} aqueous triethylamine.

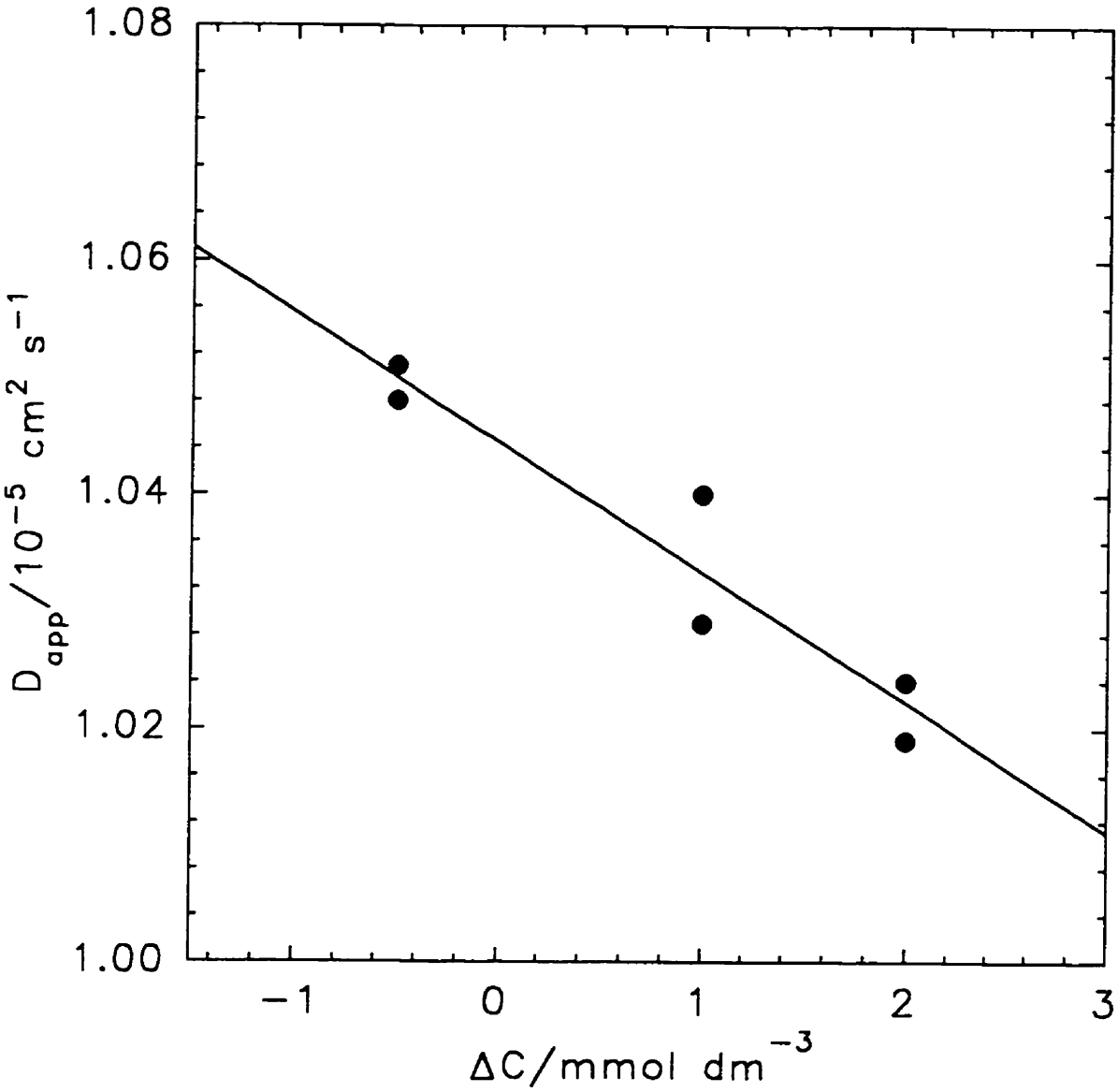
1.08
1.06
1.04
1.02
1.00
−1
0
1
2
3
$D_{app}/10^{-5}$ cm^2 s^{-1}
ΔC/mmol dm^{-3}

3 mmol dm^{-3}) to ensure that the changes in the apparent diffusion coefficients (D_{app}) were linear in ΔC. The D_{app} values were interpolated or extrapolated to $\Delta C = 0$ to give the differential diffusion coefficient for each carrier solution. This procedure is illustrated in Fig. 5.1 for a 0.50 mmol dm^{-3} triethylamine carrier stream. The diffusion measurements for the ethylamine solutions below 1.00 mmol dm^{-3} were not reproducible because the relatively small refractive-index increment for this system resulted in smaller dispersion peaks and hence poorer signal-to-noise ratios.

5.3. Results

The results of the diffusion measurements are summarized in Table 5.1. To help interpret the concentration dependence of D, Table 5.1 includes extents of hydrolysis (β)

$$M[(1 - \beta)C] + H_2O \rightleftharpoons MH^+(\beta C) + OH^-(\beta C) \qquad (I)$$

calculated for each amine: M = ethylamine, diethylamine, or triethylamine.

$$K = \frac{C_{MH^+} \cdot C_{OH^-}}{C_M} \gamma_\pm^2 = \frac{\beta^2 C}{1 - \beta} \gamma_\pm^2 \qquad (5.3)$$

The respective equilibrium constants 4.292×10^{-4}, 8.604×10^{-4}, and 7.391×10^{-4} were evaluated from reported molal-scale hydrolysis constants[2,22] (K_m) and the density of pure water ($\rho_0 = 0.99705$ kg dm^{-3}) according to the relation[2] $K = \rho_0 K_m$. Mean ionic activity coefficients for the hydrolysed portion of each amine were calculated from the semi-empirical relation[23]

Table 5.1[a] Binary mutual diffusion coefficients, mobilities, and thermodynamic factors for aqueous ethylamine, diethylamine, and triethylamine at 25 °C

C	D	β	$(C\,RT)d\mu/dC$	RTU	$-\Delta_1$	η/η^0
			Ethylamine			
0.00	$(1.94)^b$	1.000	2.000	0.97	0.000	1.000
1.00	1.37_8	0.483	1.313	1.05	0.006	1.000
2.00	1.31_3	0.377	1.228	1.07	0.008	1.000
5.00	1.26_3	0.262	1.147	1.10	0.011	1.001
10.0	1.20_2	0.195	1.105	1.09	0.014	1.002
25.0	1.18_1	0.130	1.067	1.11	0.018	1.004
50.0	1.15_7	0.095	1.048	1.10	0.022	1.008
100.0	1.14_4	0.069	1.034	1.11	0.027	1.016
			Diethylamine			
0.00	$(1.59)^b$	1.000	2.000	0.80	0.000	1.000
0.20	1.40_4	0.840	1.716	0.82	0.005	1.000
0.50	1.27_2	0.715	1.547	0.82	0.008	1.000
1.00	1.15_5	0.602	1.422	0.81	0.010	1.000
2.00	1.10_4	0.487	1.314	0.84	0.013	1.001
5.00	1.06_2	0.350	1.206	0.88	0.017	1.002
10.0	0.98_6	0.266	1.148	0.86	0.021	1.004

Table 5.1 (cont.)

25.0	0.94_4	0.181	1.095	0.87	0.027	1.010
50.0	0.91_5	0.133	1.068	0.88	0.033	1.021
100.0	0.88_9	0.098	1.049	0.89	0.040	1.042
			Triethylamine			
0.00	(1.32)[b]	1.000	2.000	0.66	0.000	1.000
0.20	1.11_2	0.822	1.690	0.66	0.006	1.000
0.50	1.04_4	0.691	1.519	0.69	0.008	1.000
1.00	0.93_4	0.576	1.396	0.67	0.011	1.001
2.00	0.88_0	0.462	1.294	0.68	0.014	1.001
5.00	0.80_2	0.330	1.192	0.67	0.018	1.003
10.0	0.77_6	0.249	1.138	0.68	0.022	1.006
25.0	0.74_4	0.168	1.088	0.68	0.029	1.015
50.0	0.71_4	0.124	1.063	0.67	0.035	1.030
100.0	0.70_4	0.091	1.045	0.67	0.043	1.060

[a] Units: C in mmol dm^{-3}; D, RTU and Δ_1 in 10^{-9} m^2 s^{-1}.

[b] Extrapolated value.

$$\ln\gamma_{\pm} = -1.17I^{1/2}/(1 + I^{1/2}) \qquad (5.4)$$

where $I = \beta C$ is the ionic strength in units of mol dm^{-3}. Because all the solutions were dilute the activity of water and the activity coefficient of the molecular amine species were set equal to unity.

Hydrolysis increases the number of free solute particles, which in turn increases the free-energy gradient, the driving force for diffusion. The dimensionless thermodynamic factor[15] $(C/RT)\mathrm{d}\mu/\mathrm{d}C$ provides a convenient measure of the changing driving force. R is the gas constant, T the temperature, and μ the solute chemical potential.

$$\mu = \mu^0 + RT\ln(\beta^2 C^2 \gamma_{\pm}^2) \qquad (5.5)$$

Differentiation of eqns. (5.3) and (5.5) shows that the thermodynamic factor equals $2/(2 - \beta)$ for an ideal solution ($\gamma_{\pm} = 1$). In the limiting case of zero hydrolysis, $2/(2 - \beta)$ equals 1; it increases to 2 for complete hydrolysis. The thermodynamic factors listed in Table 5.1 were calculated from the more accurate expression

$$\frac{C}{RT}\frac{\mathrm{d}\mu}{\mathrm{d}C} = \frac{2}{2 - \beta}\left(1 + \beta C\frac{\mathrm{d}\ln\gamma_{\pm}}{\mathrm{d}C}\right) \qquad (5.6)$$

which includes the mean ionic activity coefficient to allow for non-ideal behaviour.

Hydrolysis also changes the solute mobility, the diffusion speed per unit driving force. Molar mobility (U) can be calculated from thermodynamic factors and the measured mutual diffusion coefficients by using the identity $D = UC\,\mathrm{d}\mu / \mathrm{d}C$. The hydroxide ion, one of the hydrolysis products, has a relatively large mobility in water. Nevertheless, as shown in Table

5.1, hydrolysis decreases the mobility of each amine. Evidently the motion of separate MH^+ and OH^- ions suffers more frictional resistance than the motion of a single M molecule.

5.4. Discussion

Hydrolysis becomes more complete as the concentration of each amine drops to zero. Extrapolation of D against C to zero concentration to determine the limiting diffusion coefficients of the completely hydrolysed amines is clearly unreliable in view of the non-linear concentration dependence. As shown in Fig 5.2, extrapolation against $C^{1/2}$ is also unsuitable.

A better extrapolation of the data can be guided by the modified version of eqn. (5.2)

$$D(C) = \left[(1 - \beta)D_M + \frac{\beta}{2}D_\pm\right]\frac{2}{2 - \beta} \qquad (5.7)$$

in which the degree of dissociation of a weak acid has been replaced by the degree of hydrolysis of a weak base. Here D_M is the limiting molecular amine diffusion coefficient and $D_\pm$ is the limiting Nernst diffusion coefficient[1,2] for the completely hydrolysed amine.

$$D_\pm = \frac{2D_{MH^+}D_{OH^-}}{D_{MH^+} + D_{OH^-}} \qquad (5.8)$$

The limiting diffusion coefficient of the aqueous hydroxide ion ($D_{OH^-} = 5.28 \times 10^{-5}$ cm^2 s^{-1})[2] is known accurately from its limiting conductivity. It follows, from eqn. (5.7), that the mobility of a partially hydrolysed amine is given approximately by $(RT)^{-1}[(1 - \beta)D_M + (\beta D_\pm/2)]$.

For a more accurate analysis of the concentration dependence of D, we will use the

Fig. 5.2 Binary mutual diffusion coefficients of aqueous solutions of ethylamine, diethylamine, and triethylamine plotted against the square root of the concentration: ●, measured values; ——, fitted values, eqn. (5.9); --------, fitted values, eqn. (5.9) with the viscosity factor η^0/η omitted. The results are plotted against $C^{1/2}$ instead of C to avoid crowding the data points at the lower concentrations.

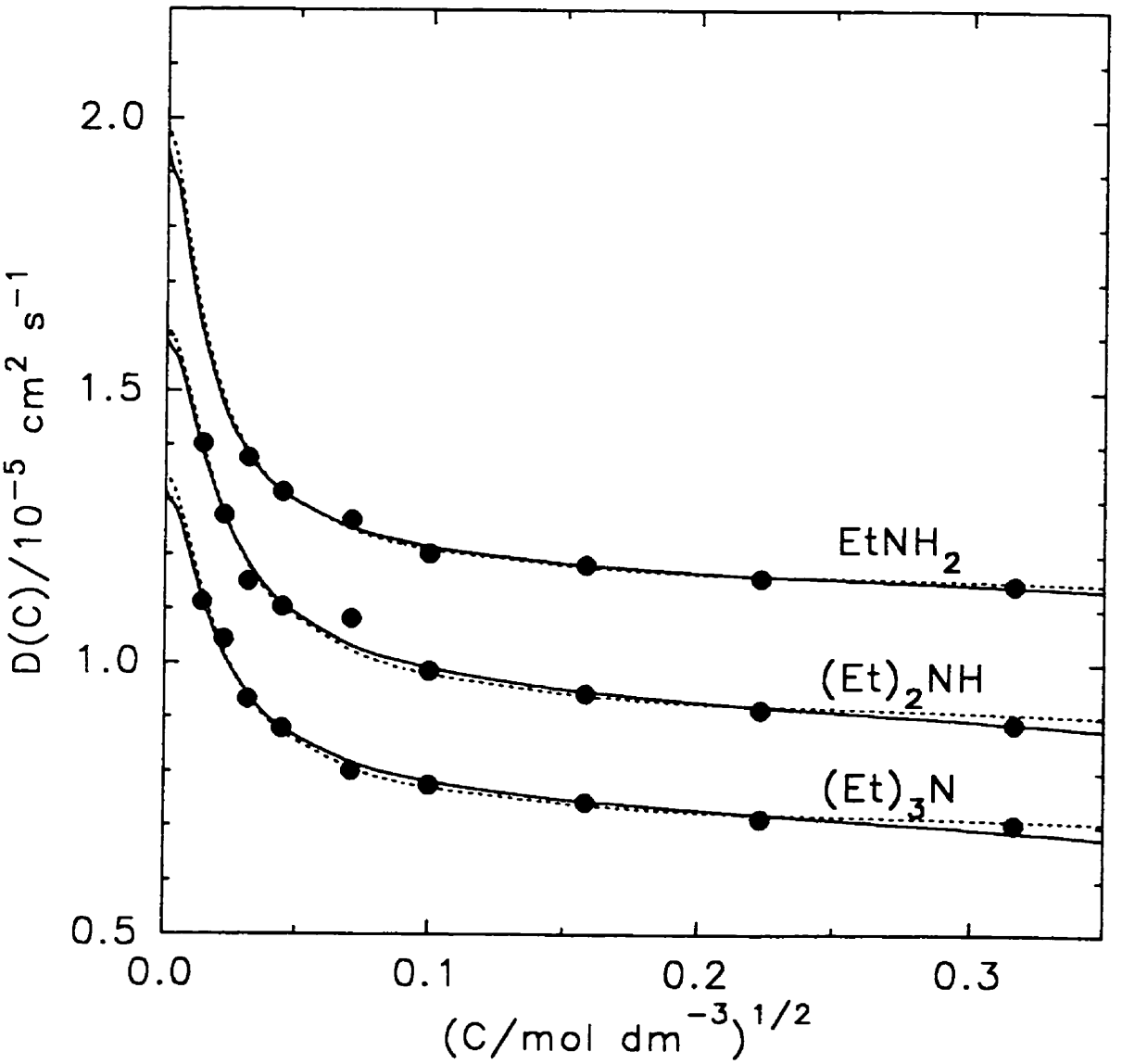
2.0
1.5
1.0
0.5
D(C)/10^{-5} cm^2 s^{-1}
0.0
0.1
0.2
0.3
(C/mol dm^{-3})$^{1/2}$
EtNH$_2$
(Et)$_2$NH
(Et)$_3$N

extended version[2,14,15] of eqn. (5.7)

$$D(C) = \left[(1 - \beta)D_M + \frac{\beta}{2}(D_= - \Delta_1)\right]\frac{\eta^0}{\eta}\frac{2}{2 - \beta}\left(1 + \beta C\frac{d\ln\gamma_=}{dC}\right) \qquad (5.9)$$

in which the mobility is corrected for electrophoresis and viscosity changes of the solution

$$U = (RT)^{-1}\left[(1 - \beta)D_M + \frac{\beta}{2}(D_= + \Delta_1)\right]\frac{\eta^0}{\eta} \qquad (5.10)$$

and the thermodynamic factor is corrected for non-ideal behaviour [see eqn. (5.6)]. Here η^0 and η are the viscosities of the pure solvent and the solution, and Δ_1 is the first-order electrophoretic correction. Because the ionic strengths of the solutions are very low, the simplified relation[2]

$$\Delta_1/\mathrm{cm}^2\ \mathrm{s}^{-1} = -8.07 \times 10^{-6}\left(\frac{D_{RH^+} - D_{OH^-}}{D_{RH^+} + D_{OH^-}}\right)^2 I^{1/2} \qquad (5.11)$$

was used to calculate Δ_1 with sufficient accuracy. The second-order electrophoretic correction was negligible.

Rearrangement of eqn. (5.9) gives the transformed diffusion coefficient

$$D'(C) \equiv \frac{(\eta/\eta^0)D(C)}{\frac{2}{2 - \beta}(1 + \beta C\frac{d\ln\gamma_=}{dC})} - \frac{\beta}{2}\Delta_1 = (1 - \beta)D_M + \frac{\beta}{2}D_= \qquad (5.12)$$

By design $D'(C)$ is linear in β and therefore well suited for extrapolation to the limiting values D_M and $D_=/2$ at $\beta = 0$ and $\beta = 1$, respectively.

The first step in the analysis was to estimate values of $D'(C)$ from the measured values of $D(C)$, ignoring the small electrophoretic corrections. Linear least-squares extrapolation of these $D'(C)$ values to $\beta = 1$ gave an approximate value of $D_-/2$ for each amine. This information was used to estimate the limiting diffusion coefficients of the $N(Et)_nH_{4-n}^+$ ions by using eqn. (5.8) together with the known diffusion coefficient of the hydroxide ion. Electrophoretic corrections and hence values of $D'(C)$ could then be calculated.

Fig. 5.3 shows values of $D'(C)$ plotted against β for each amine. The molecular and ionic diffusion coefficients derived by extrapolation to zero hydrolysis and complete hydrolysis are given in Table 5.2 . In Fig. 5.2, mutual diffusion coefficients calculated from eqn. (5.9) (solid curves) are compared with the measured D values. The fit appears to be adequately good for each amine.

The empirical factor η^0 / η in eqn. (5.9) is based on the assumption that an increase in the relative viscosity produces a corresponding decrease in the relative mobility of each amine. In general, however, the relative mobility changes more slowly[1,2] than the relative viscosity. Thus η^0 / η probably "overcorrects" for the viscosity changes. Fortunately, the viscosity corrections used in the present study are relatively small ($\eta^0 / \eta \leq 1.06$) and therefore not an important source of error. To illustrate this point, the diffusion data were reanalysed with the factor η^0 / η omitted from eqn. (5.9). The diffusion coefficients of the $(Et)_nNH_{3-n}$ and $(Et)_nNH_{4-n}^+$ species estimated by this procedure are compared, in Table 5.2, with the values obtained with the viscosity factor included in eqn. (5.9). The two sets of diffusion coefficients differ by only 0.01×10^{-5} to 0.02×10^{-5} $cm^2\ s^{-1}$. Fig. 5.2 shows that the omission of the viscosity factor does not decrease the ability of eqn. (5.9) to account for the concentration dependence of D for each amine.

Fig. 5.3 Transformed diffusion coefficients $D'(C)$ [eqn. (5.12)] against the extent of hydrolysis. Linear extrapolation of $D'(C)$ to $\beta = 1$ gives 0.97 x 10^{-5}, 0.80 x 10^{-5} and 0.66 x 10^{-5} cm^2 s^{-1} for the values of $D_{-}/2$ for ethylamine, diethylamine, and triethylamine, respectively. The values of $D'(C)$ extrapolated to $\beta = 0$ give 1.13 x 10^{-5}, 0.89 x 10^{-5} and 0.70 x 10^{-5} cm^2 s^{-1} for the diffusion coefficients of the corresponding molecular amines.

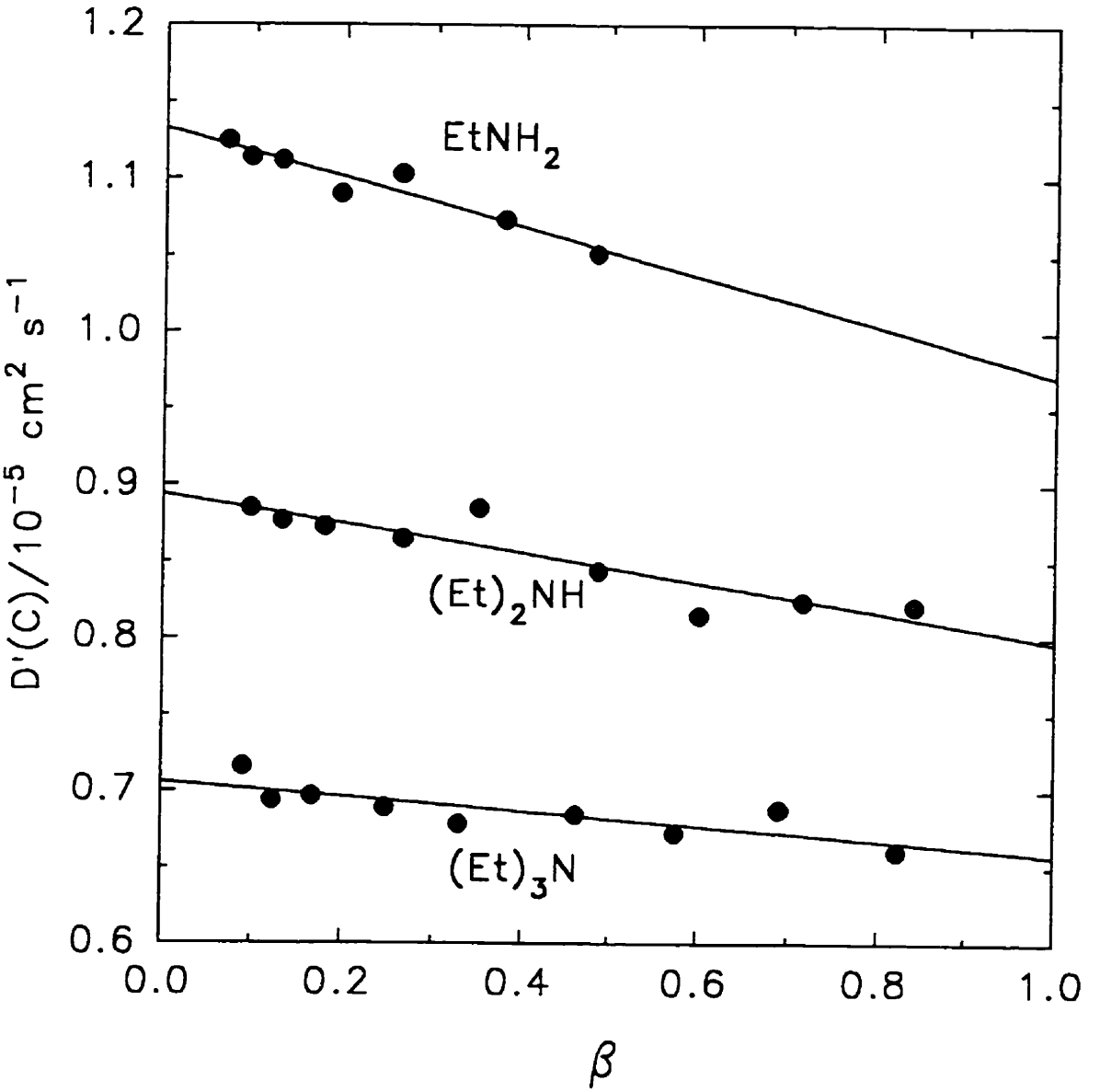
1.2
1.1
1.0
0.9
0.8
0.7
0.6
D'(C)/10^{-5} cm^2 s^{-1}
EtNH$_2$
(Et)$_2$NH
(Et)$_3$N
0.0
0.2
0.4
0.6
0.8
1.0
β

Table 5.2 Limiting diffusion coefficients of aqueous ions and molecules at 25 °C

ion, MH^+	$D_{MH^+}/10^{-5}$ cm^2 s^{-1}	molecule	$D_M/10^{-5}$ cm^2 s^{-1}
NH_4^+	1.959[a]	NH_3	2.08[b]
$EtNH_3^+$	1.19(1.21)[c]	$EtNH_2$	1.13(1.12)[c]
$(Et)_2NH_2^+$	0.94(0.95)[c]	$(Et)_2NH$	0.89(0.87)[c]
$(Et)_3NH^+$	0.75(0.77)[c]	$(Et)_3N$	0.70(0.68)[c]
$(Et)_4N^+$	0.870[a]	-	

[a] Ref. 2. [b] Ref. 24. [c] Viscosity factor omitted from eqn. (5.9).

Table 5.2 includes, for comparison with the present results, the previously reported limiting diffusion of molecular ammonia,[24] as well as the limiting diffusion coefficients of the ammonium and tetraethylammonium ions calculated from their limiting conductivities.[2] As might be anticipated, the diffusion coefficients of the $(Et)_nNH_{3-n}$ molecules decrease smoothly as the number of ethyl substituents, and hence the molecular size, increases. For the corresponding ions, there is a smooth decrease in the diffusion coefficients on moving from NH_4^+ to $(Et)_3NH^+$ in the series. It is interesting, however, that the diffusion coefficient of the symmetrical $(Et)_4N^+$ ion is about 15% larger than the diffusion coefficient of the $(Et)_3NH^+$ ion, despite the extra ethyl group carried by the former. $(Et)_4N^+$ ions may experience less frictional resistance because of their nonpolar nature and hence weaker interaction with the surrounding water molecules. In any event this result illustrates accurate diffusion for aqueous species are not easily predicted.

In conclusion, equations developed previously for weak-acid diffusion adequately describe the concentration dependence of mutual diffusion coefficients for aqueous amine weak bases. The equations can be used to extrapolate with confidence, in order to evaluate diffusion coefficients for very dilute solutions beyond the capability of current measurement techniques. Analysis of the results provides the diffusion coefficients of the molecular amines and the corresponding protonated species. In addition, the present work shows that Taylor dispersion can be used to measure diffusion coefficients in difficult cases where D changes rapidly with the concentration of the diffusing substance.

5.5. References

1 H. J. V. Tyrrell and K. R. Harris, *Diffusion in Liquids*, Butterworths, London, 1984.

2 R. A. Robinson and R. H. Stokes, *Electrolyte Solutions*, Academic Press, New York, 2nd edn., 1959.

3 R. H. Stokes, *J. Amer. Chem. Soc.*, 1950, **72**, 2243.

4 B. F. Wishaw and R. H. Stokes, *J. Amer. Chem. Soc.*, 1954, **76**, 2065.

5 V. M. M. Lobo and J. L. Quaresma, *Electrolyte Solutions: Literature Data on Thermo-dynamic and Transport Properties*, Coimbra University Press, Coimbra (Portugal), 1981.

6 J. Anderson and R. Paterson, *J. Chem. Soc., Faraday Trans. 1*, 1975, **71**, 1335.

7 R. Mills, *Rev. Pure Appl. Chem. Aust.*, 1961, **11**, 78.

8 R. Mathew, J. G. Albright, D. G. Miller and J. A. Rard, *J. Phys. Chem.*, 1990, **94**, 6875.

9 J. A. Rard, D. G. Miller and C. M. Lee, *J. Chem. Soc., Faraday Trans. 1*, 1989, **85**, 3343.

10 J. A. Rard and D. G. Miller, *J. Solution Chem.*, 1979, **8**, 701.

11 H. S. Harned and R. M. Hudson, *J. Amer. Chem. Soc.*, 1951, **73**, 5880.

12 G. T. A. Müller and R. H. Stokes, *Trans. Faraday Soc.*, 1957, **53**, 642.

13 V. Vitagliano and P. A. Lyons, *J. Amer. Chem. Soc.*, 1956, **78**, 4538.

14 D. G. Leaist and P. A. Lyons, *J. Solution Chem.*, 1984, **13**, 77.

15 R. A. Noulty and D. G. Leaist, *J. Chem. Eng. Data*, 1987, **32**, 418.

16 D. G. Leaist, *J. Chem. Soc., Faraday Trans. 1*, 1984, **80**, 3041.

17 H. Lü and D. G. Leaist, *Can. J. Chem.*, 1990, **68**, 1317.

18 D. G. Leaist and L. Hao, *J. Chem. Soc., Faraday Trans.*, 1993, **89**, 2775.

19 A. Alizadeh, C. A. Nieto de Castro and W. A. Wakeham, *Int. J. Thermophys*, 1988,

1, 243.

20 D. G. Leaist, *J. Chem. Soc., Faraday Trans.*, 1991, **76**, 597.

21 D. G. Leaist and L. Hao, *J. Solution Chem.*, 1992, **21**, 345.

22 R. G. Bates and G. D. Pinching, *J. Res. Natl. Bur. Stand. (U.S.)*, 1949, **42**, 419.

23 E. A. Guggenheim, *Phil. Mag.*, 1935, **19**, 588.

24 D. G. Leaist, *Aust. J. Chem.*, 1985, **38**, 249.

CHAPTER 6

DIFFUSION IN AQUEOUS SOLUTIONS OF AMINOBENZOIC ACIDS AT 25°C

6.1. Introduction

Mutual diffusion coefficients for a number of aqueous weak electrolyte systems have been reported in previous studies.[1-3] However, relatively few studies have dealt with the diffusion of amino acids, despite their practical importance (in protein synthesis and drug manufacture,[4] for example). In addition, amino acids are used to inhibit metal corrosion.[5]

The interpretation of amino acid reaction and dissolution rates requires solubility and diffusion data. The work reported in this chapter was undertaken to measure the mutual diffusion coefficients of aqueous solutions of 2-aminobenzoic acid (2-ABAH), 3-aminobenzoic acid (3-ABAH), and 4-aminobenzoic acid (4-ABAH) at concentrations from 0.05 to 10.0 mmol dm^{-3} at 25° C. Although accurate solubilities have been reported for aqueous aminobenzoic acids (an important class of amino acids),[6] no diffusion data appear to be available for these solutions. Another purpose of the work reported in this chapter is to predict the diffusion coefficients of these organic acids as a function of concentration and to verify the limiting law for diffusion in these systems.

Diffusion in an aqueous solution of an aminobenzoic acid is a binary process. In 4-ABAH solutions, for example, there are five solute species: $H_2N-C_6H_4-COOH$ molecules, the zwitterion $^+H_3N-C_6H_4-COO^-$, and the $^+H_3N-C_6H_4-COOH$, $H_2N-C_6H_4-COO^-$, H^+ ions. But only one solute flux is independent in view of the constraints imposed by electroneutrality

and by the local equilibrium of the isomerization and dissociation reactions: $H_2N-C_6H_4-COOH \rightleftharpoons {}^{+}H_3N-C_6H_4-COO^{-}$, ${}^{+}H_3N-C_6H_4-COOH \rightleftharpoons H^{+} + H_2N-C_6H_4-COOH$ and $H_2N-C_6H_4-COOH \rightleftharpoons H^{+} + H_2N-C_6H_4-COO^{-}$. Diffusion of an aminobenzoic acid can therefore be described by a single mutual diffusion coefficient, D.

Since highly mobile hydrogen ions are produced by dissociation of the acids , there should be a corresponding increase in the apparent diffusion coefficients of the aqueous aminobenzoic acid solutions, especially in dilute solutions where dissociation is extensive. Sharp increases in D might cause the experimental D values to vary with the initial concentration difference employed, instead of representing the true differential D value at the carrier-stream composition. This consideration prompted us to use the Taylor technique to determine the diffusion coefficients of the acids. In chapter 5, Taylor dispersion was successfully used to determine the diffusion of dilute amine solutions for which the measured D values vary with even the smallest practicable initial concentration differences. Taylor dispersion should also be suitable for measuring diffusion in aminobenzoic acid solutions.

6.2. Experimental

Diffusion coefficients reported in this chapter were measured by the Taylor dispersion (peak-broadening) method.[7,8] Details of the equipment have been described in previous chapters. A steady laminar flow of carrier solution at concentration C was confined within a Teflon dispersion tube (length 3334 cm, inner diameter 0.0947_6 cm). At the start of each run, a sample of solution at concentration $C + \Delta C$ (-20 mmol dm^{-3} $\leq \Delta C \leq$ +20 mmol dm^{-3}) was injected in the carrier stream. A differential refractometer detector monitored the broadened sample solutions at the tube outlet. Binary diffusion coefficients were determined

by fitting eqn. (3.5) to the detector voltages $V(t)$.

Binary diffusion coefficients of aqueous 2-ABAH, 3-ABAH, and 4-ABAH were measured at concentrations from 0.05 to 10.0 mmol dm^{-3}. From six to eight injections were made into each flow solution. D values obtained from different initial concentration differences were usually reproducible within $\pm 0.5\%$ for flow-solution concentrations in the range $C \geq 1.0$ mmol dm^{-3}. Mutual diffusion coefficients for these solutions were evaluated by simply averaging the measured D values.

For carrier-stream concentrations $C \leq 1.0$ mmol dm^{-3}, however, the strong concentration dependence of D caused the measured D values to decrease as the ΔC values increased, even for the smallest initial concentration differences that were used. In this region small initial concentration differences were used to ensure that the measured D values were linear in ΔC. These measured D values were then interpolated or extrapolated to $\Delta C = 0$ to determine the mutual diffusion coefficient at each flow-solution composition.

Reagent-grade 2-ABAH, 3-ABAH and 4-ABAH (Aldrich, >99.5% purity) were recrystallized from distilled, deionized water in a vacuum oven at 80°C. Solutions of acids were prepared by dissolving weighted amounts of acids in distilled, deionized water in calibrated volumetric flasks.

6.3. Results and Discussion

There are two important reaction equilibria in aqueous solutions of an aminobenzoic acid:

$$ABAH_2^+ \rightleftharpoons ABAH + H^+ \qquad K_1$$

$$ABAH \rightleftharpoons H^+ + ABA^- \qquad K_2$$

Values of the thermodynamic equilibrium constants K_1 and K_2 are given in Table 6.1.[9,10] Thus there are effectively four diffusing solute species to be considered: 0. ABAH; 1. $ABAH_2^+$; 2. ABA^-; 3. H^+. In terms of the degree of dissociation of the acid, $\alpha = [ABA^-]/C$, and the extent of formation of $ABAH_2^+$, which may be expressed as $\beta = [ABAH_2^+]/C$, the concentrations of various solute species are given by $[ABAH] = (1 - \alpha - \beta)C$, $[ABAH_2^+] = \beta C$, $[ABA^-] = \alpha C$, and $[H^+] = (\alpha - \beta)C$. Thermodynamics cannot distinguish the two neutral aminobenzoic acid species $H_2N-C_6H_4-COOH$ and $^-H_3N-C_6H_4-COO^-$. Therefore, following the usual convention, we use [ABAH] to represent the sum of the concentrations of the $H_2N-C_6H_4-COOH$ and $^-H_3N-C_6H_4-COO^-$ species.

Values of α and β are calculated from the equilibrium relations

$$K_1 = \frac{[ABAH][H^+]}{[ABAH_2^+]}\frac{\gamma_m\gamma_{H^+}}{\gamma_{ABAH_2^+}} = \frac{(1 - \alpha - \beta)(\alpha - \beta)C}{\beta} \qquad (6.1)$$

$$K_2 = \frac{[ABA^-][H^+]}{[ABAH]}\frac{\gamma_{ABA^-}\gamma_{H^+}}{\gamma_m} = \frac{\alpha(\alpha - \beta)C}{(1 - \alpha - \beta)}\gamma_\pm^2 \qquad (6.2)$$

where $C = [ABAH] + [ABAH_2^+] + [ABA^-]$ is the total concentration of diffusing solute, and γ_i is the activity coefficient of species i. At the low concentrations used in the present study the activity coefficients of the molecular acid species γ_m can be set equal to unity without significant error. The mean ionic activity coefficients $\gamma_\pm$ were estimated from the convenient relation[11]

$$\ln\gamma_\pm = -1.17I^{1/2}/(1 + I^{1/2}) \qquad (6.3)$$

Table 6.1[a] Equilibrium constants of aqueous aminobenzoic acid at 25 °C

Acid	K_1	K_2
2-aminobenzoic	0.00780	0.0000113
3-aminobenzoic	0.000752	0.0000180
4-aminobenzoic	0.00386	0.0000140

[a] Ref. 9,10.

where $I = \alpha C$ denotes the ionic strength in units of mol dm^{-3}. Note that activity coefficients are omitted in eqn. (6.1). This approximation is based on the fact that γ_{H^+} in the numerator nearly cancels $\gamma_{ABAH_2^+}$ in the denominator. The calculated values of α and β are recorded in Table 6.2. In very dilute solutions the concentrations of H^+ and ABA^- are approximately equal in view of the relatively minor concentration of $ABAH_2^+$.

For a binary solution, the diffusion coefficient is the product of a mobility and a thermodynamic factor[12]

$$D = U\frac{d\mu}{d\ln C} \tag{6.4}$$

where

$$\frac{d\mu}{d\ln C} = RT\frac{d\ln[(1 - \alpha - \beta)C]}{d\ln C} \tag{6.5}$$

This result is obtained by differentiation of the expression

$$\mu = \mu^0_{ABAH} + RT\ln[ABAH] = \mu^0_{ABAH} + RT\ln[(1 - \alpha - \beta)C] \tag{6.6}$$

for the chemical potential μ of the aqueous acid.

The measured diffusion coefficients are listed in the second column of Table 6.2. Thermodynamic values calculated from eqn. (6.5) are listed in the sixth column. At low concentrations, the strong concentration dependence of the thermodynamic factor is evident. This behaviour is reasonable since the extensive dissociation of each acid in dilute solutions strongly increases the number of solute species per formula weight of the electrolyte, thereby increasing the free-energy force which drives the solute through the solvent.

Mobility factors derived for the solutes from the measured diffusion coefficients are

Table 6.2[a] Binary mutual diffusion coefficients, mobilities, and thermodynamic factors of aqueous 2-aminobenzoic acid, 3-aminobenzoic acid and 4-aminobenzoic acid solutions 25 °C

C	D_{obs}	D_{cal}	α	β	$(C/RT)d\mu/dC$	RTU
			2-Aminobenzoic Acid			
0.00	—	1.469[b]	1.000	0.000	2.000	0.735
0.05	1.025	1.005	0.377	0.002	1.229	0.834
0.10	0.949	0.959	0.287	0.003	1.164	0.815
0.20	0.943	0.924	0.214	0.004	1.113	0.847
0.50	0.894	0.892	0.144	0.007	1.070	0.836
1.00	0.885	0.875	0.107	0.011	1.045	0.847
2.00	0.873	0.862	0.081	0.015	1.026	0.851
5.00	0.858	0.851	0.059	0.022	1.011	0.849
10.00	0.844	0.846	0.049	0.027	1.004	0.841
			3-Aminobenzoic Acid			
0.00	—	1.548[b]	1.000	0.000	2.000	0.774
0.05	0.958	0.973	0.449	0.0154	1.264	0.758
0.10	0.902	0.913	0.351	0.0268	1.175	0.768
0.20	0.860	0.867	0.272	0.0420	1.105	0.779
0.50	0.832	0.826	0.201	0.0658	1.046	0.796
1.00	0.817	0.808	0.167	0.0832	1.020	0.801

Table 6.2 (cont.)

2.00	0.794	0.800	0.146	0.0975	1.006	0.789
5.00	0.794	0.795	0.132	0.110	1.002	0.795
10.00	0.797	0.793	0.128	0.116	1.000	0.801
			4-Aminobenzoic Acid			
0.00	—	1.588[b]	1.000	0.000	2.000	0.794
0.05	0.992	1.049	0.409	0.003	1.252	0.793
0.10	0.961	0.995	0.314	0.005	1.178	0.816
0.20	0.949	0.955	0.236	0.009	1.124	0.845
0.50	0.911	0.917	0.161	0.016	1.069	0.852
1.00	0.900	0.897	0.123	0.022	1.042	0.864
2.00	0.892	0.883	0.096	0.030	1.021	0.874
5.00	0.882	0.872	0.075	0.040	1.007	0.876
10.00	0.868	0.868	0.066	0.046	1.001	0.867

[a] Units: C in mmol dm^{-3}; D_{obs}, D_{cal} and RTU in 10^{-9} m^2 s^{-1}.

[b] Limiting diffusion value for fully dissociated aminobenzoic acid calculated from eqn. (6.17).

given in the seventh column of Table 6.2. Despite the highly mobile hydrogen ions produced by dissociation of the acids, the overall mobility of each aminobenzoic acid actually *decreases* as the degree of dissociation increases. This counterintuitive behavior is a result of the fact that the motion of two separate ABA^- and H^+ ions through the solvent experiences more frictional resistance than the motion of a single ABAH molecule.

After determination of the thermodynamic and mobility factors for the diffusing acids, we now turn to the problem of predicting the diffusion coefficients of each acid as a function of concentration. The flux of aminobenzoic acid is the sum of fluxes of molecular ABAH and dissociated $ABAH_2^+$ and ABA^- species.

$$J = j_0(\mathrm{ABAH}) + j_1(\mathrm{ABAH_2^+}) + j_2(\mathrm{ABA^-}) \tag{6.7}$$

It follows that

$$L\nabla\tilde{\mu}_0 = l_0\nabla\tilde{\mu}_0 - l_1\nabla\tilde{\mu}_1 - l_2\nabla\tilde{\mu}_2 \tag{6.8}$$

where L is the Onsager transport coefficient of the total acid component and l_i is the Onsager transport coefficient of solute species i.

The flow of electric charge is zero in pure diffusion, and hence

$$l_1\nabla\tilde{\mu}_1 - l_3\nabla\tilde{\mu}_3 = l_2\nabla\tilde{\mu}_2 \tag{6.9}$$

From equilibrium conditions, we have

$$\nabla\tilde{\mu}_0 = \nabla\tilde{\mu}_2 + \nabla\tilde{\mu}_3 \tag{6.10}$$

$$\nabla\tilde{\mu}_1 = \nabla\tilde{\mu}_0 + \nabla\tilde{\mu}_3 \tag{6.11}$$

Combining eqns. (6.9) to (6.11) gives

$$\nabla\tilde{\mu}_3 = \frac{l_2 - l_1}{l_1 + l_2 - l_3}\nabla\tilde{\mu}_0 \qquad (6.12)$$

Substituting eqn. (6.12) into eqn. (6.8) leads to the equation

$$L = l_0 + \frac{4l_1l_2 + l_1l_3 + l_2l_3}{l_1 + l_2 + l_3} \qquad (6.13)$$

Since $l_i = c_iD_i / RT$, and $U = L / C$

$$RTU = (1 - \alpha - \beta)D_0 + \frac{4\alpha\beta D_1D_2 + \beta(\alpha - \beta)D_1D_3 + \alpha(\alpha - \beta)D_2D_3}{\beta D_1 + \alpha D_2 + (\alpha - \beta)D_3} \qquad (6.14)$$

Substituting eqns. (6.14) and (6.5) into eqn. (6.4) finally yields

$$D = \left[(1 - \alpha - \beta)D_0 + \frac{4\alpha\beta D_1D_2 + \beta(\alpha - \beta)D_1D_3 + \alpha(\alpha - \beta)D_2D_3}{\beta D_1 + \alpha D_2 + (\alpha - \beta)D_3}\right] \times \frac{d\ln[(1 - \alpha - \beta)C]}{d\ln C} \qquad (6.15)$$

This result is used to predict the diffusion coefficients of aqueous aminobenzoic acid. Although the electrophoretic and viscosity corrections for the solute mobilities are not included in the equation, the estimated D values should be reliable since the acid concentrations used here are low ($\leq$ 10 mmol dm^{-3}) and the ion-ion interactions and viscosity changes of the solution are therefore very small. Notice that D is not a simple concentration-weighted average of the diffusion coefficients of the solute species [*ie*, $D \neq (1 - \alpha - \beta)D_{AB,AH}$

$- \alpha D_{ABA^-} - \beta D_{ABAH_2^+}]$

For very dilute solutions where the concentration of $ABAH_2^+$ is negligible ($\beta \approx 0$), eqn. (6.15) simplifies to

$$D = \left[(1 - \alpha)D_0 + \frac{\alpha}{2}D_2\right]\frac{d\mu}{d\ln C} \qquad (6.16)$$

where

$$D_2 = \frac{2D_2D_3}{D_2 + D_3} \qquad (6.17)$$

is the limiting diffusion coefficient[7,9] of fully ionized $ABA^- - H^+$. Eqns. (6.16) and (6.17) are identical to the expressions for the concentration dependence of the diffusion coefficient of a simple univalent weak acid, such as acetic acid.[1]

The limiting diffusion coefficient of the H^+ ion is accurately known from conductivity data:[9,13] $D_3 = 9.33 \times 10^{-9}$ m^2 s^{-1}. No diffusion data seem to have been reported for aminobenzoic acid species. We use here the values $D_0 = 0.844 \times 10^{-9}$, 0.797×10^{-9} and 0.868×10^{-9} $m^2 s^{-1}$ for molecular 2-ABAH, 3-ABAH, and 4-ABAH, respectively. These values were obtained by fitting eqn. (6.15) to the measured D values by using least squares (see Fig. 6.1). Based on the fact that limiting diffusion coefficient of a molecular acid species is always very close to that of the corresponding ionic species (which are nearly identical in size and shape), we assume here the diffusion coefficients D_1, and D_2 for $ABAH_2^+$ and ABA^- species are identical to that of the corresponding molecular species, ABAH.

Based on the above values, the limiting diffusion coefficients for fully dissociated 2-

Fig. 6.1 Comparison of measured and predicted diffusion coefficients of aminobenzoic acids at 25°C: 2-aminobenzoic acid: ●, measured values; ———, predicted values; 3-aminobenzoic acid: ▲, measured values; ·····, predicted values; 4-aminobenzoic acid: ▼, measured values; --------, predicted values.

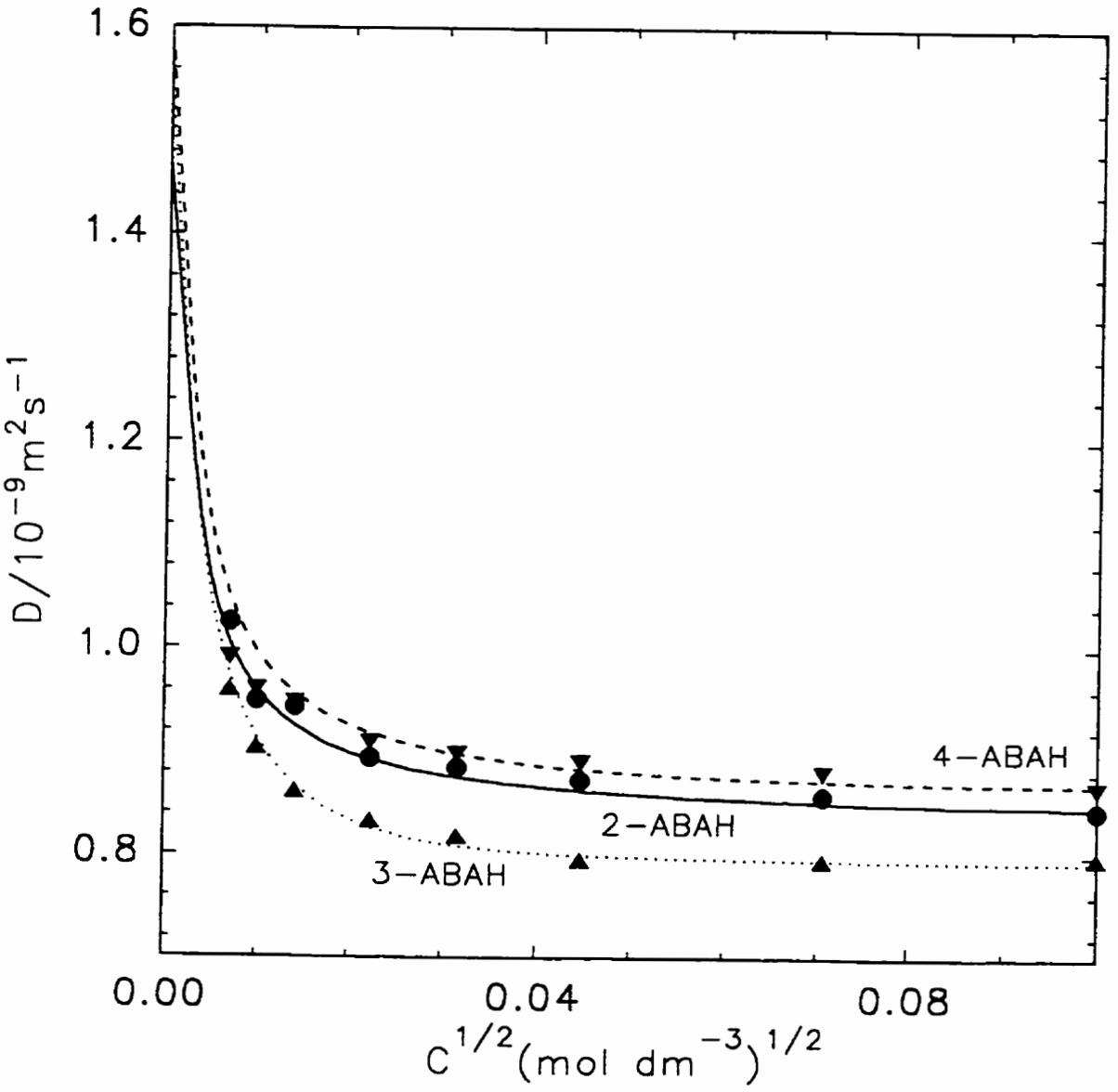
1.6
1.4
1.2
1.0
0.8
D/10⁻⁹m²s⁻¹
0.00
0.04
0.08
C^1/2(mol dm⁻³)^1/2
4−ABAH
2−ABAH
3−ABAH

ABAH, 3-ABAH, 4-ABAH are 1.548 x 10^{-9}, 1.469 x 10^{-9}, and 1.588 x 10^{-9} m^2 s^{-1} respectively (calculated by using eqn. (6.17)). Upon the substitution of the limiting diffusion coefficient of each diffusing solute species into eqn. (6.15), we obtained the predicted diffusion coefficients of the total acid component listed in the third column of Table 6.2. Observed and predicted mutual diffusion results are compared in Fig. 6.1. It is evident from the figure that the Taylor dispersion data bring theory and experiment into good agreement down to concentrations as low as 0.05 mmol dm^{-3}. At this concentration about 40% of acid molecules are dissociated. It would of course be interesting to measure D at lower concentrations in order to provide a more extensive test of eqn. (6.15). However, D values measured below 0.05 mmol dm^{-3} were not reproducible because the very small dispersion peaks had poor signal-to-noise ratios.

In summary, the work reported in this chapter has shown that the Taylor dispersion method can be used to determine accurate diffusion coefficients in difficult cases where the diffusion coefficients change rapidly with composition. Equations developed for diffusion of simple weak electrolytes, such as aqueous acetic acid,[1] can be adequately extended to predict reliable diffusion coefficients of more complicated systems, such as aqueous aminobenzoic acid solutions.

6.4. References

1 D. G. Leaist and P. A. Lyons, *J. Solution Chem.*, 1984, **13**, 77.

2 D. G. Leaist, *J. Chem. Soc., Faraday Trans. 1*, 1984, **80**, 3041.

3 R. A. Noulty and D. G. Leaist, *J. Chem. Eng. Data*, 1987, **32**, 418.

4 G. Lubec and G. A. Rosenthal, *Amino acids Chemistry, Biology and Medicine*,

ESCOM Science Publishers B. V., Leiden (Netherland), 1990.

5 A. Akiyama and K. Nobe, *Corrosion*, 1970, **26**, 439.

6 R. M. Dannenfelser and S. H. Yalkowsky, *Sci. Total Environ.*, 1991, **109/110**, 625.

7 H. J. V. Tyrrell and K. R. Harris, *Diffusion in Liquids*, Butterworths, London, 1984.

8 A. Alizadeh, C. A. Nieto de Castro and W. A. Wakeham, *Int. J. Thermophys*, 1988, **1**, 243.

9 R. A. Robinson and R. H. Stokes, *Electrolyte Solutions*, Academic Press, New York, 2nd edn., 1959.

10 R. A. Robinson and A. I. Biggs, *Aust. J. Chem.*, 1957, **10**, 128.

11 E. A. Guggenheim, *Phil. Mag.*, 1935, **19**, 588.

12 A. Katchalsky and P. F. Curran, *Non-equilibrium Thermodynamic in Biophysics*, Harvard University Press, Cambridge, Mass., 1965.

13 B. B. Owen and F. H. Sweeton, *J. Am. Chem. Soc.*, 1941, **63**, 2811.

CHAPTER 7

DIFFUSION COEFFICIENTS MEASURED BY TAYLOR DISPERSION IN A FOURIER RING. AQUEOUS LANTHANUM CHLORIDE AT 25 °C

7.1. Introduction

Diffusion in liquids can be measured reliably and conveniently by the Taylor dispersion (peak-broadening) method.[1-10] A relative newcomer to diffusion studies, the full potential of this technique may not have been exploited. The usual procedure is to inject a slug of solution at concentration $C + \Delta C$ into a laminar flow of carrier solution at a slightly different concentration, C. Convection and diffusion shape the initial concentration pulse into a nearly Gaussian distribution as the injected sample is pumped through a long capillary tube. Diffusion coefficients are calculated from optical absorbance or refractive index profiles measured across the broadened sample peaks at the tube outlet.

Dispersion tubes have been used to measure binary mutual diffusion coefficients[1-10] for a number of electrolyte and nonelectrolyte systems. In addition, tracer[11] and multicomponent diffusion coefficients[12-17] (including cross-coefficients for coupled diffusion) have been measured for three- and four-component systems. A few self-diffusion measurements[18-20] have been made by injecting labelled samples into unlabelled carrier streams of identical chemical composition.

Though not as accurate as Gouy or Rayleigh interferometry, dispersion measurements have important advantages. For example, dispersion measurements are free of errors from convection because the solutions are confined within fine-bore tubing. This

feature is especially important for multicomponent solutions because coupled diffusion in these systems can spoil free-diffusion columns by generating unwanted density inversions or dynamic instabilities.[21,22] In practice, dispersion experiments are relatively inexpensive and easily automated. Moreover, the apparatus is readily assembled from commercial tubing, detectors, pumps, and injection valves manufactured for liquid chromatography.

Dilution with the carrier stream causes the concentration of diffusing solute to drop from the initial value $C + \Delta C$ to the background concentration C during a dispersion run. In order to measure a clearly defined diffusion coefficient (the differential coefficient at C), it is common practice to use small initial concentration differences which in turn demands sensitive detectors. Drifting detector baseline signals can therefore be a source of error, especially for slowly diffusing materials which generate relatively broad peaks. To help achieve stable baselines, dispersion tubes and detectors are usually flushed with copious amounts of carrier solution. Allowing for replicate injections, from 0.3 to 0.5 dm^3 of solution is usually required to measure diffusion at a given composition. This amount can be prohibitive for concentrated solutions of certain biochemicals and for other materials that are costly, difficult to purify or highly toxic.

With these considerations in mind, the work reported here was undertaken to develop a new dispersion experiment that can be used to measure diffusion with less-sensitive detectors and only a few millilitres of solution. Instead of "once through" flow in a long capillary tube, the idea is to recirculate solution continuously in a "racetrack" flow path. Closed-circuit flow is achieved by connecting the outlet of a short dispersion tube to the pump inlet. At the start of each run, one half of the circuit is filled with solution at concentration $C + (\Delta C/2)$, the other half is filled with solution at concentration $C - (\Delta C/2)$

and the pump is started. Because the average concentration of the diffusing material ($\bar{C}$) is constant, larger concentration differences and less sensitive detectors may be used while still measuring the differential diffusion coefficient. Moreover, recirculation will greatly reduce the required volume of solution.

Closed-circuit dispersion measurements are reported here for binary aqueous solutions of sucrose, glycine, urea, NaCl and KCl at 25 °C. In addition, the binary mutual diffusion coefficient of aqueous lanthanum chloride is measured at concentrations up to 2.8 mol dm^{-3} to provide quantitative information on the transport of a high-valent salt in concentrated solutions. Diffusion in aqueous lanthanum chloride solutions has been studied previously by Harned's conductivity method;[23,24] but data for concentrated solutions of the salt do not appear to be available.

In the following section, equations are developed to predict rates of dispersion in closed circuits. This problem bears a striking resemblance to the famous problem of the temperature distribution produced by heat conduction in a ring;[25] the first application of Fourier's mathematical theory. Ring problems are particularly suggestive illustrations of Fourier analysis because the ring circumference must be an integral multiple of the wavelengths of the sine and cosine terms in the series.

7.2. Taylor Dispersion in a Ring

Before dispersion in a ring is considered, the relevant equations for straight tubes will be summarized briefly. Steady laminar flow of a binary liquid solution in a tube of circular cross-section is assumed. The radially averaged concentration of the solution at time t and position z along the tube will be designated by $C(z,t)$.

Solution near the centerline of the tube moves ahead of the slower solution near the tube wall. This convective mixing gradually smooths out any concentration differences along the flow path. The rate of dispersion is most easily described by transforming to the frame of reference

$$y = z - Ut \tag{7.1}$$

moving at the mean speed (U) of the flowing solution. For sufficiently large values of t, dispersion is accurately represented by an equation of the form[26,27]

$$\frac{\partial C(y,t)}{\partial t} = K\frac{\partial^2 C(y,t)}{\partial y^2} \tag{7.2}$$

The dispersion coefficient K is given by

$$K = r_0^2 U^2/48D \qquad (t > 3.5\ r_0^2/D) \tag{7.3}$$

where D the mutual diffusion coefficient and r_0 is the inner radius of the tube.

Dispersion in a Ring Suppose a straight tube of length L is bent into a circle. Also, the tube outlet is connected to the inlet to provide continuous recirculation in a closed circuit. The concentrations around the circuit are periodic, with period L in y.

$$C(y,t) = C(y \pm nL, t) \qquad n = 1, 2, 3, \ldots \tag{7.4}$$

Subject to these constraints and the assumption that the dispersion coefficient is constant, the general solution of the dispersion equation is the exponentially damped Fourier series[28]

$$C(y,t) = C + \sum_{n=1}^{\infty} \left[a_n \cos(2n\pi y/L) + b_n \sin(2n\pi y/L)\right] \exp(-4n^2\pi^2 Kt/L^2) \qquad (7.5)$$

Constants a_n and b_n are determined by the initial concentration distribution around the circuit. As $t \to \infty$, the concentration at each point decays to the mean value, C. (Fourier's expression for the temperature distribution in a ring[28] is obtained by replacing the dispersion coefficient with the thermal conductivity, the concentration with the temperature, and y with z.)

The rate of dispersion can be followed by placing a detector at a convenient position along the tube. At $z = 0$, for example, y equals $-Ut$ and the concentration detected at time t is

$$C(z=0,t) = C + \sum_{n=1}^{\infty} \left[a_n \cos(2n\pi Ut/L) - b_n \sin(2n\pi Ut/L)\right] \exp(-4n^2\pi^2 Kt/L^2) \qquad (7.6)$$

Symmetrical Initial Conditions Symmetrical step-function initial conditions, such as

$$C(0 < z < L/2,\ t = 0) = C + (\Delta C/2) \qquad (7.7)$$

$$C(L/2 < z < L,\ t = 0) = C - (\Delta C/2) \qquad (7.8)$$

have the desirable features mentioned in the introduction. Subject to initial conditions (7.7) and (7.8) the solution of eqn. (7.2) is the well known expression for the exponentially damped square wave[28]

$$C(z=0,t) = C^{\circ} - (2\Delta C/\pi) \sum_{n=1,3,5,\ldots}^{\infty} (1/n) \sin(2n\pi\omega t) \exp(-n^2 t/\tau) \qquad (7.9)$$

where ω is the frequency of the concentration oscillations (the inverse of the average time required for the solution to pass once around the circuit)

$$\omega = U/L \qquad (7.10)$$

and τ is an abbreviation for the decay time

$$\tau = L^2/4\pi^2 K \qquad (7.11)$$

The curvature of the tubing will be negligible for a large ring. In this case the dispersion coefficient is $r_0^2 U^2/48D$ and hence

$$\tau = \frac{12L^2 D}{\pi^2 r_0^2 U^2} = \frac{12D}{\pi^2 \omega^2 r_0^2} \qquad (7.12)$$

Eqn.(7.12) shows that the concentration oscillations decay more rapidly for solutions with small diffusion coefficients. This point is illustrated in Fig. 7.1 where calculated dispersion profiles are plotted for different D values. Increasing the flow rate or the tube radius will also increase the rate of decay of the oscillations. Increasing the tube length has the opposite effect.

7.3. Experimental

Practical Considerations The preceding equations apply to steady laminar flow in a closed

Fig. 7.1 Calculated dispersion profiles [eqns. (7.9) and (7.12)] for solutions with diffusion coefficients of 0.5×10^{-5}, 1.0×10^{-5}, and 2.0×10^{-5} cm^2 s^{-1}. In each case the mean flow speed (U), ring circumference (L), frequency (ω), and tube radius (r_0) are 0.5 cm s^{-1}, 500 cm, 1 mHz, and 0.05 cm, respectively. The top and bottom profiles have been offset vertically for clarity.

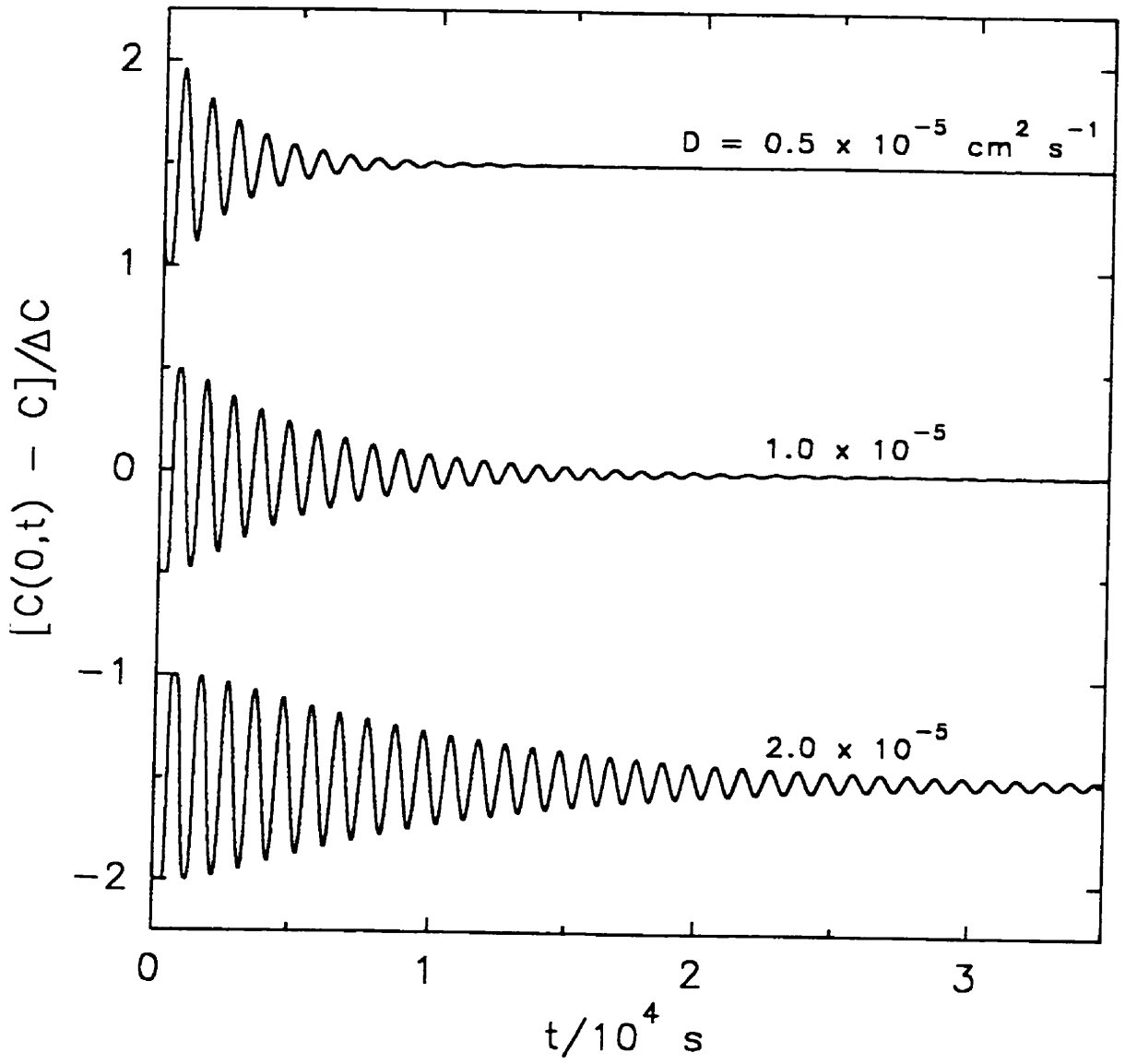
2
1
0
−1
−2
0
1
2
3
[C(0,t) − C]/ΔC
t/10^4 s
D = 0.5 x 10^−5 cm^2 s^−1
1.0 x 10^−5
2.0 x 10^−5

circuit of uniform tubing. In practice, however, a pump and detector cell will be included in the flow path together with valves for flushing and filling the circuit. Significant dispersion could be generated by the pump action and by the flow of solution through the detector and curved sections of tubing. Nevertheless, the "effective" length and radius of the flow path will be constant for a given flow rate, and hence according to eqn. (7.12)

$$\omega^2 \tau_{\text{eff}} \propto D \qquad (U \text{ fixed}) \qquad (7.13)$$

The approach taken here is to calibrate a dispersion ring by measuring effective decay times (τ_{eff}) for solutions that have accurately known diffusion coefficients. Diffusion coefficients for other solutions are evaluated by interpolation of calibration plots.

Equipment The flow circuit was constructed from matched sample loops connected to two 6-port liquid-chromatography injection valves (Rheodyne model 50) as shown in Fig. 7.2. This design minimized dead volume and facilitated flushing and filling the circuit. All connections were made with 1.59 mm o.d., 1.02 mm i.d. liquid-chromatography tubing (1/16 in o.d., 0.040 in i.d.) and flanged union fittings of equal bore. The pump and detector cell were connected in series in one of the loops (see Fig. 7.2). The length of the tubing in the other loop (136 cm) was adjusted so that its internal volume (1.10 ± 0.02 mL) matched that of the pump, detector, and connecting tubing in the first loop.

To avoid additional dispersion, a peristaltic pump (Gilson MiniPuls 3) was used instead of a piston model. In the pump head 10 stainless-steel rollers rotated at an adjustable rate against a 15.0 cm length of size 13 Viton peristaltic tubing. The rate of dispersion was followed by a deflection-type differential refractometer (Gilson model 131,

Fig. 7.2 Flow path for the closed-circuit dispersion experiments. After filling the sample loops with solution, the valves are switched to the "RUN" position and the pump is started at time $t = 0$.

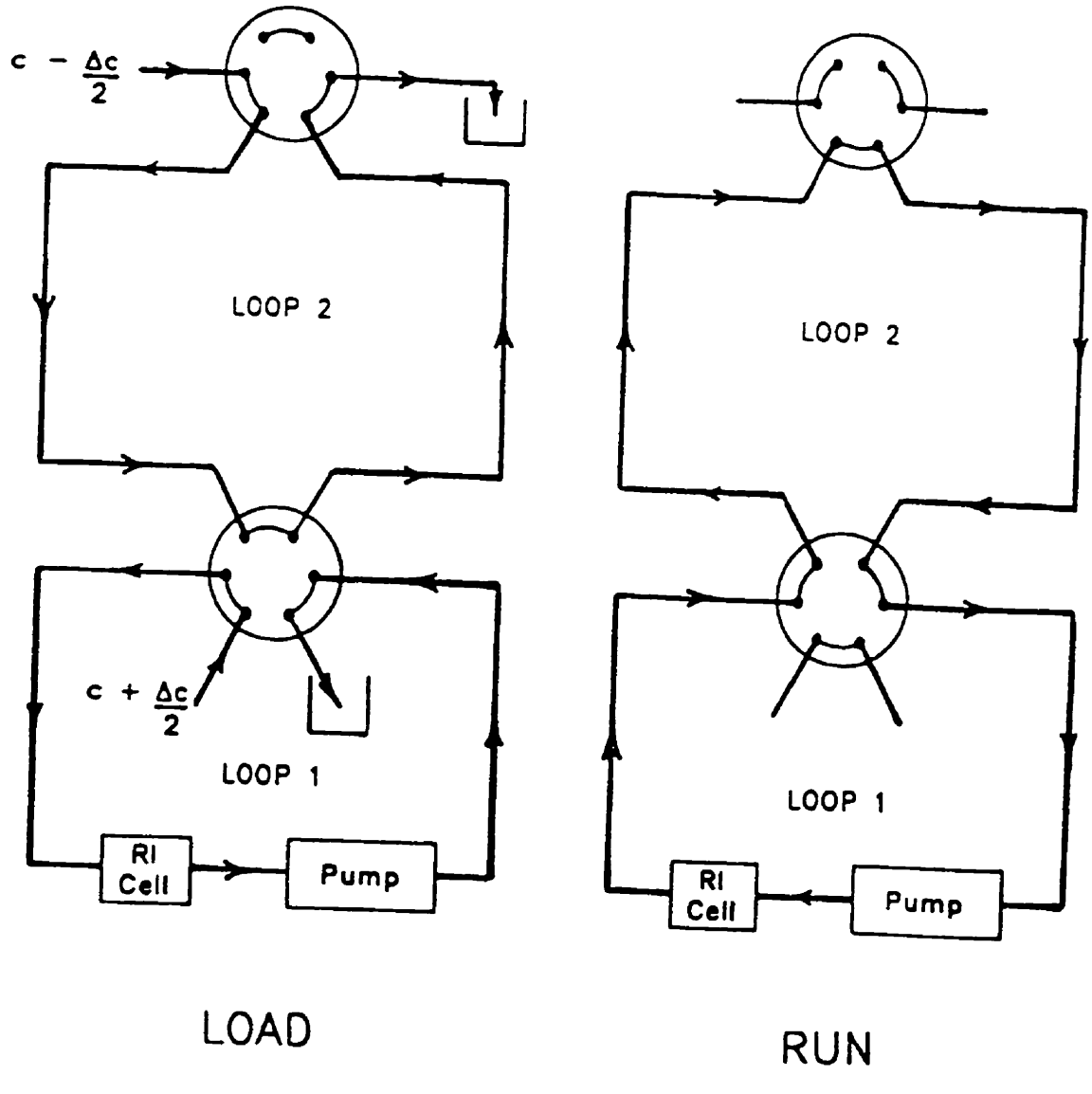

LOAD

RUN

10 mm^3 flow cells). A computer-controlled digital voltmeter (Hewlett Packard model 34401A) measured the refractometer output voltage, $v(t)$, at accurately timed intervals.

The pump, refractometer cells, injection valves and the connecting tubing were placed inside an insulated polyethylene box fitted with a foam lid. The temperature inside the box was held at 25.00 ± 0.05 °C by a proportional controller (YSI model 50) and a 100 W heater. A fan maintained efficient air circulation in the thermostat.

Procedure Prior to each run a needle and syringe were used to fill the refractometer reference cell with solution at concentration C. One of the sample loops was then rinsed and filled with solution at concentration $C + (\Delta C/2)$, and the other loop was rinsed and filled with solution at concentration $C - (\Delta C/2)$. After waiting a few minutes for thermal equilibration the valves were switched to the "run" position and the pump was started. Flow rates from 0.03 to 0.25 $cm^3\ min^{-1}$ were used, corresponding to mean flow speeds of 0.07 to 0.50 $cm\ s^{-1}$. Each run required about 10 cm^3 of solution.

Initial concentration differences (ΔC) from 0.01 to 0.05 mol dm^{-3} were used. Because the average concentration of diffusing solute was constant throughout each run, differential diffusion coefficients could be determined by using concentration differences 10 to 50 times larger than those measured in once-through dispersion experiments. After checking that changes in the refractometer output voltage (v) were proportional to changes in the concentration

$$v(t) = v_{\infty} + k[C(t) - C] \qquad (7.14)$$

the refractometer was operated at its lowest sensitivity (k) which corresponded to a full-

scale deflection for a refractive index difference of 0.003. Pulsation from the pump and baseline drift were negligible at this setting.

Binary aqueous solutions of sucrose, glycine, urea, NaCl, and KCl were prepared by dissolving weighed amounts of reagent-grade solutes in distilled, deionized water in calibrated volumetric flasks. Lanthanum chloride was supplied as a hydrate (AnalaR $LaCl_3 \cdot 7H_2O$). A concentrated stock solution of the salt (*ca.* 2.8 mol dm^{-3}) was filtered through a fine-porosity (5 μm) Pyrex frit and then titrated against silver nitrate to determine the mass percentage of $LaCl_3$. Solutions for the dispersion runs were prepared by mass dilution of the stock with water. Published densities[29,30] were used to calculate the volumetric concentrations of $LaCl_3$ at 25 °C. The viscosities of a few $LaCl_3$ solutions were measured with an Ubbelohde viscometer.

7.4. Results and Discussion

Calibration of the Dispersion Circuit Binary aqueous solutions of sucrose, glycine, urea, and KCl were used to calibrate the dispersion circuit. These systems were chosen because their diffusion coefficients are accurately known[31-35] and they span a useful range of D values, from about 0.5×10^{-5} to 1.8×10^{-5} $cm^2\ s^{-1}$. Table 7.1 lists the mean concentration, initial concentration difference and accepted value of D for each calibration solution.

Dispersion profiles measured for sucrose and glycine are shown in Fig. 7.3. At 25 °C the diffusion coefficient of aqueous glycine is about twice that of aqueous sucrose. As predicted by eqn. (7.12) the glycine profile (frequency $\omega = 1.090$ mHz) decays more slowly than the sucrose profile obtained at a similar flow rate (1.162 mHz). In addition, Fig. 7.3 shows that sucrose profiles decay more rapidly as the flow rate is increased, from 0.618 to

Table 7.1 Decay times measured for binary aqueous solutions of sucrose, glycine, urea, NaCl, and KCl at different flow rates

Sucrose, $D = 0.5094 \times 10^{-5}$ cm^2 s^{-1} ($C = 0.050$; $\Delta C = 0.010$ mol dm^{-3})		Glycine, $D = 1.041 \times 10^{-5}$ cm^2 s^{-1} ($C = 0.100$; $\Delta C = 0.050$ mol dm^{-3})	
ω/mHz	τ_{eff}/s	ω/mHz	τ_{eff}/s
1.521	1604	1.862	2055
1.442	1768	1.823	2108
1.162	2519	1.578	2736
1.158	2483	1.287	3788
1.143	2551	1.258	4054
1.115	2655	1.228	4108
1.068	2903	1.094	5127
0.883	3989	1.090	5233
0.618	7697	0.807	8768
0.407	16710	0.763	9777
0.258	40280		

Table 7.1 (cont.)

Urea, D = 1.378 x 10^{-5} cm^2 s^{-1} (C = 0.050; ΔC = 0.050 mol dm^{-3})		KCl, D = 1.838 x 10^{-5} cm^2 s^{-1} (C = 0.200; ΔC = 0.040 mol dm^{-3})	
ω/mHz	τ_{eff}/s	ω/mHz	τ_{eff}/s
1.666	3030	1.444	5172
1.554	3458	1.278	6354
1.306	4636	1.120	8016
1.223	5244	1.119	8026
0.719	14005	0.615	25110
0.654	16830	0.592	26590

Fig. 7.3 Measured refractometer voltages $v(t)$ plotted against the time for aqueous sucrose ($D = 0.5094 \times 10^{-5}$ cm^2 s^{-1}) and aqueous glycine ($D = 1.041 \times 10^{-5}$ cm^2 s^{-1}). The glycine and upper sucrose profiles have been offset for clarity.

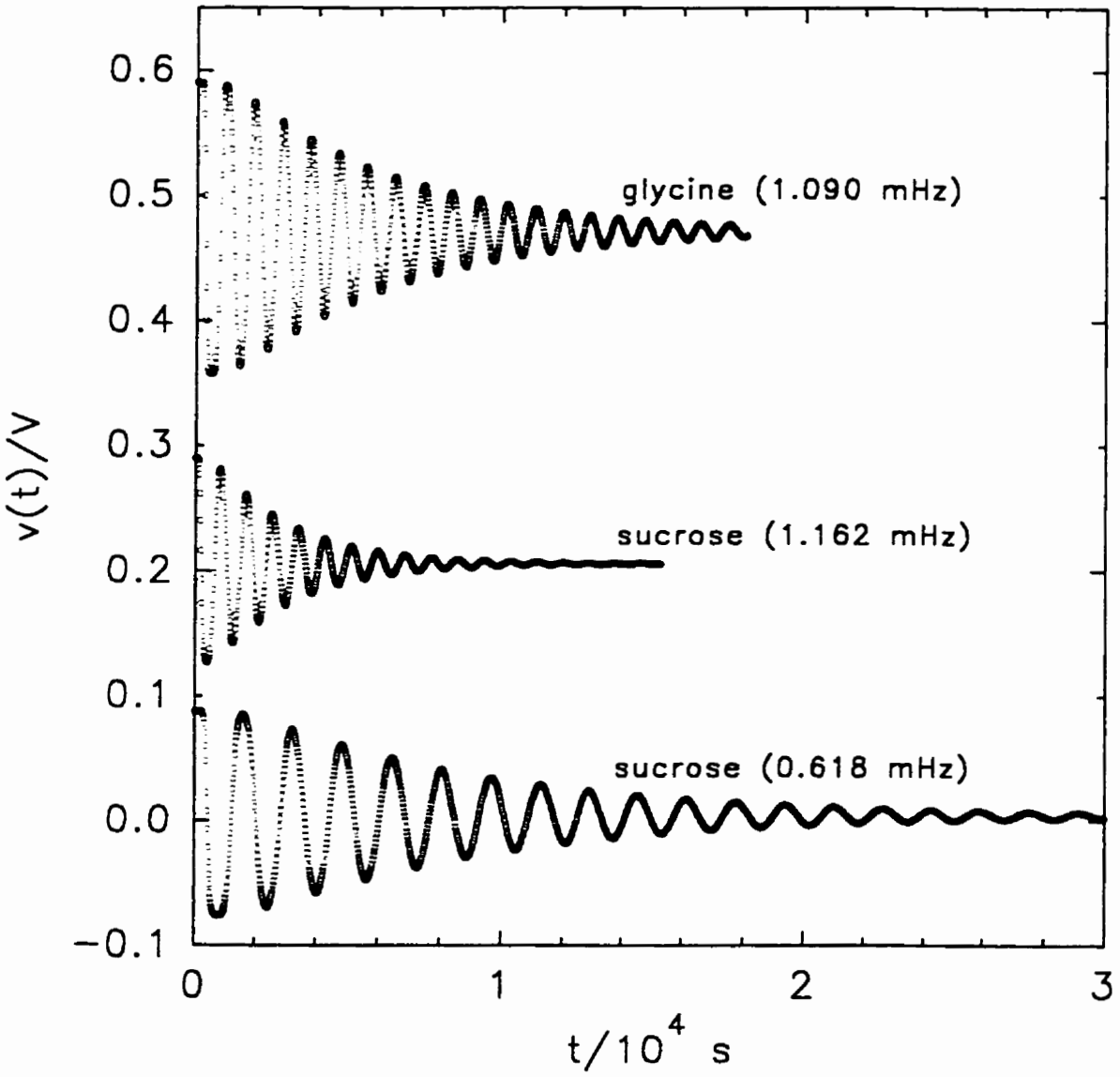
0.6
0.5
0.4
0.3
0.2
0.1
0.0
−0.1
v(t)/V
glycine (1.090 mHz)
sucrose (1.162 mHz)
sucrose (0.618 mHz)
0
1
2
3
t/10^4 s

1.162 mHz in this case. These results agree qualitatively with the behaviour predicted for dispersion in a closed circuit. Though not unexpected, the oscillations in the detector signal are noteworthy. In most diffusion experiments the measured concentration differences decay smoothly to zero.

Fourier-transform methods could be used to evaluate decay times and hence diffusion coefficients from measured dispersion profiles. In this study, however, the profiles were analysed more directly by fitting the Fourier series

$$v(t) = v_0 + \sum_{n=1}^{3} \left[A_n \cos(2n\pi\omega t) - B_n \sin(2n\pi\omega t)\right] \exp(-n^2 t/\tau_{eff}) \qquad (7.15)$$

to the detector signal. The following parameters were adjusted for each fit: the effective decay time τ_{eff}, frequency ω, baseline voltage v_0, Fourier coefficients A_n and B_n (n = 1, 2, 3). To ensure that higher-order terms ($n > 3$) were negligible, the fitting procedure was applied to data points in the range $t > 0.5\tau_{eff}$. According to eqn. (7.9), only odd-n terms are needed to describe the dispersion of a symmetrical step-function concentration distribution in an ideal closed circuit. As a precaution, however, guard terms with $n = 2$ were included in the fitting equation to allow for imperfections in the actual flow path, such as non-uniform dispersion around the circuit caused by the flow of solution through the pump and detector. In practice, the even fitting parameters A_2 and B_2 were small, usually < 1% of the magnitudes of A_1 or B_1. Contributions made by the third-order terms in A_3 and B_3 were even smaller because of the $\exp(-9t/\tau_{eff})$ weighting factor.

Measured and fitted dispersion profiles for aqueous urea are compared in Fig. 7.4. Fitting the data points in the range $t > 2500$ s gave $\tau_{eff} = 5244$ s. The decay times appeared

Fig. 7.4 Dispersion profiles for aqueous urea: o, measured; ———, fitted [eqn. (7.15)].

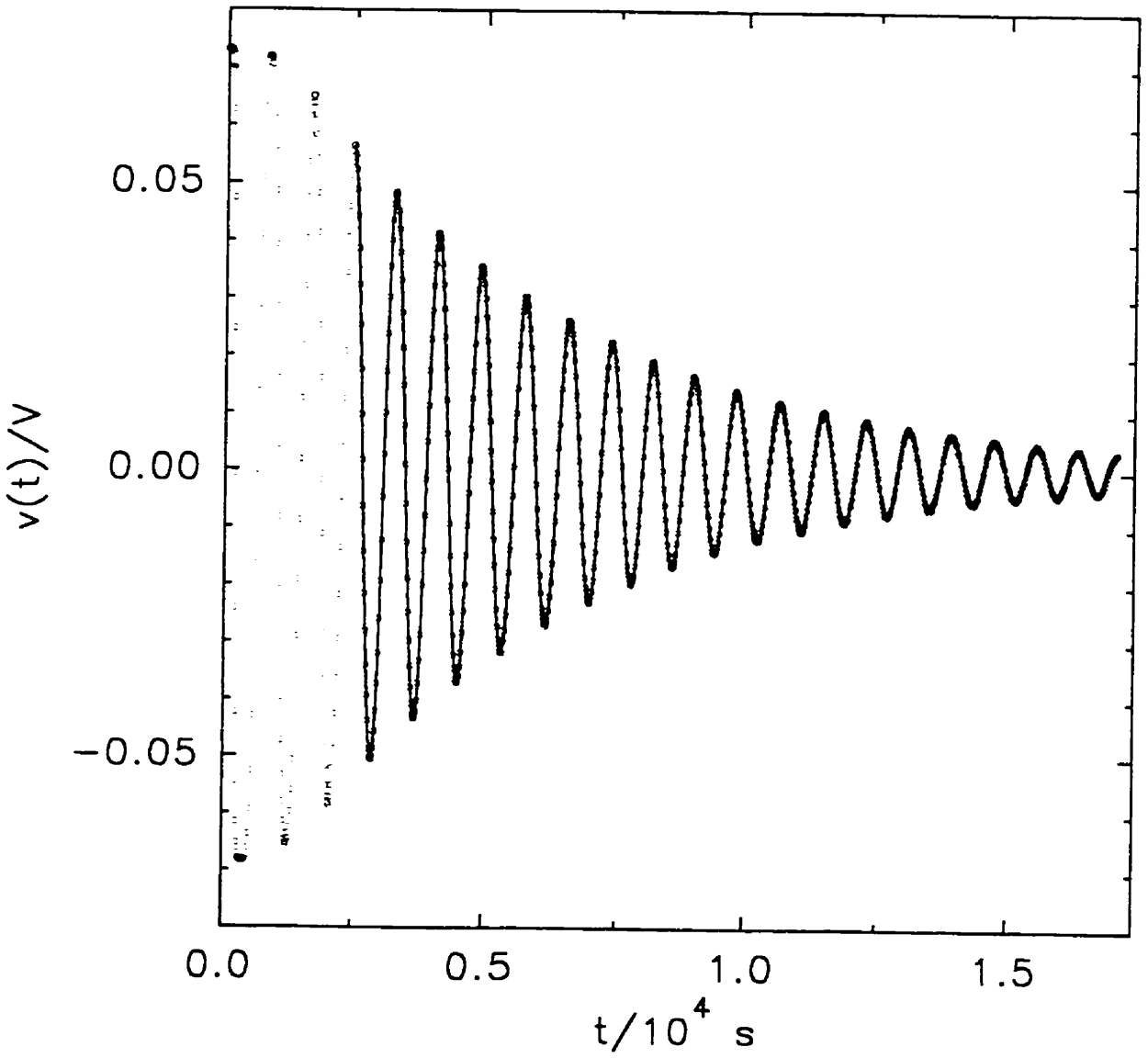
0.05
0.00
−0.05
v(t)/V
0.0
0.5
1.0
1.5
t/10^4 s

to be constant within experimental precision (1-2%) for each profile. For example, refitting the data in Fig. 7.4 in the range $t > 5000$ s gave $\tau_{eff} = 5239$ s.

The calibration results are summarized in Table 7.1. For a sufficiently large ring of tubing, the predicted value of $\omega^2\tau_{eff}$ is $12D/\pi^2 r_0^2$, a constant for each solution. Figure 7.5 shows, however, that the measured values of $\omega^2\tau_{eff}$ increase slightly with the flow rate. Moreover, the increase is linear in ω within the precision of the measurements. For interpolation purposes, it will be convenient to use a linear equation of the form

$$\omega^2\tau_{eff} = W_0 + W_1\omega \tag{7.16}$$

to represent the calibration results. Table 7.2 lists the least-square values of the intercept (W_0) and slope (W_1) for each calibration solution.

The pump used in this work traps short segments of solution in peristaltic tubing, temporarily "pinching off" the parabolic velocity profile and reducing the rate of dispersion. Extrapolation to $\omega = 0$, however, gives the value of $\omega^2\tau_{eff}$ at zero flow rate [intercept W_0 in eqn. (7.16)]. In this limit the flow disturbances generated by the pump are negligible. As shown in Table 7.2, the value of W_0 for each solution is approximately equal to $12D/\pi^2 r_0^2$.

The calibration data plotted in Fig. 7.6 confirm that $\omega^2\tau_{eff}$ is proportional to D at fixed flow rates. Given values of τ_{eff} and ω for a solution with an unknown diffusion coefficient, the value of D can be evaluated by straightforward linear interpolation. To illustrate this procedure, dispersion profiles were measured for aqueous NaCl ($C = 0.250$ mol dm^{-3}, $\Delta C = 0.050$ mol dm^{-3}), yielding decay times of 7212, 6280, and 6620 s for the respective frequencies 1.073, 1.154, and 1.122 mHz. Linear interpolation by eqn. (7.16),

Fig. 7.5 Measured values of $\omega^2 \tau_{eff}$ plotted against ω for aqueous solutions of sucrose (D = 0.5094 x 10^{-5} cm^2 s^{-1}), glycine (D = 1.041 x 10^{-5} cm^2 s^{-1}), urea (D = 1.378 x 10^{-5} cm^2 s^{-1}), NaCl (D = 1.475 x 10^{-5} cm^2 s^{-1}), and KCl (D = 1.838 x 10^{-5} cm^2 s^{-1}).

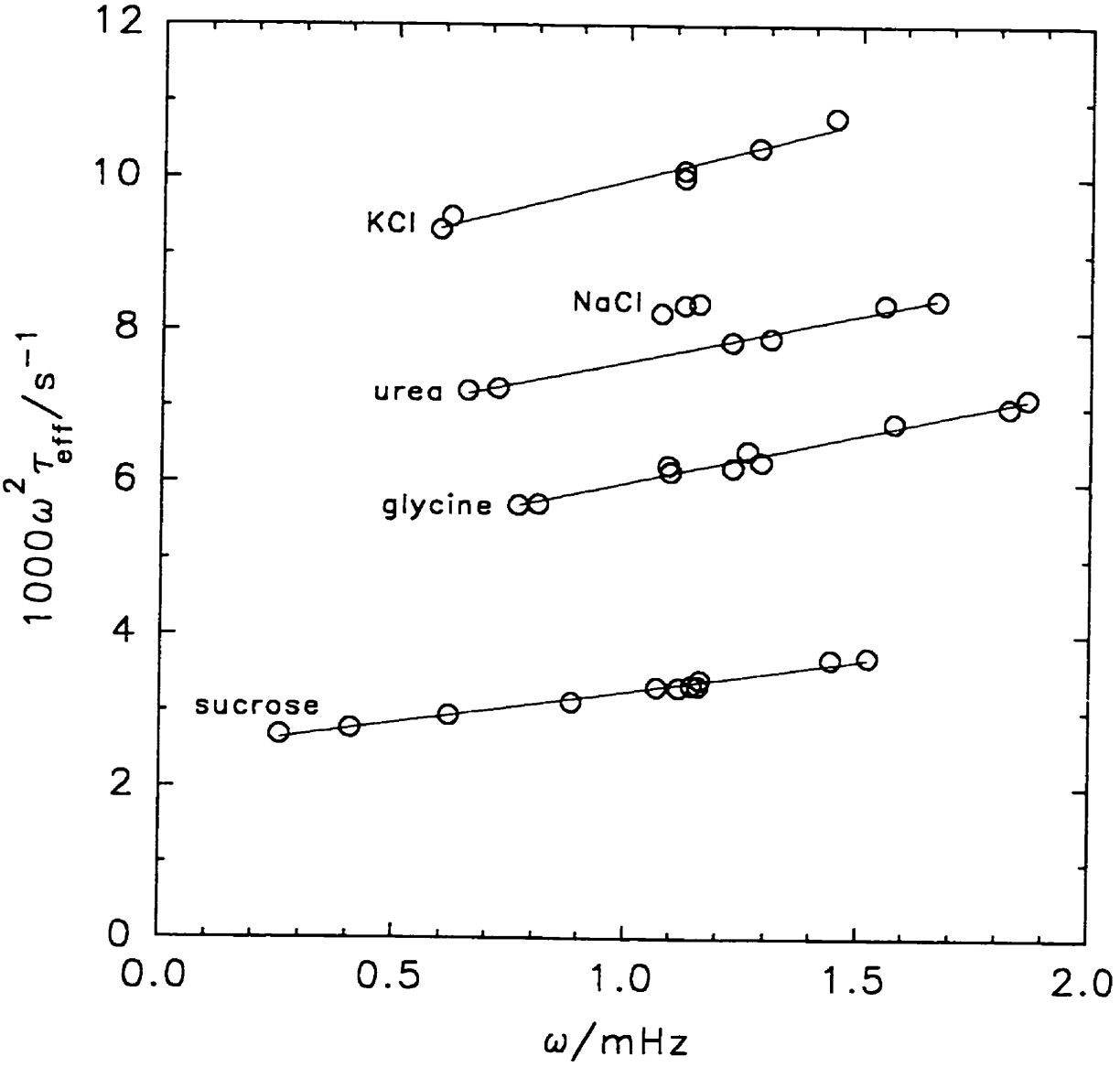
12
10
8
6
4
2
0
0.0
0.5
1.0
1.5
2.0
$1000\omega^2\tau_{eff}/s^{-1}$
ω/mHz
KCl
NaCl
urea
glycine
sucrose

Table 7.2 Calibration parameters for eqn. (7 16) for aqueous sucrose, glycine, urea, and KCl solutions

Solute	$(12D/\pi^2 r_0^2)/10^{-3}$ s^{-1}	$W_0/10^{-3}$ s^{-1}	W_1
sucrose	2.40	2.427	0.823
glycine	4.90	4.723	1.278
urea	6.49	6.360	1.234
KCl	8.66	8.414	1.558

Fig. 7.6 Calibration plots of D against $\omega^2\tau_{eff}$ for different flow rates calculated from eqn. (7.16). To determine the value of D for 0.250 mol dm^{-3} aqueous NaCl from the 1.154 mHz run (τ_{eff} = 6280 s), values of D for sucrose, glycine, urea, and KCl (○) are plotted against the values of $\omega^2\tau_{eff}$ calculated at this frequency for each calibration solute by using eqn. (7.16). Linear interpolation gives D = 1.478 x 10^{-5} cm^2 s^{-1} for NaCl (■) at $\omega^2\tau_{eff}$ = (1.154mHz)^2 (6280 s).

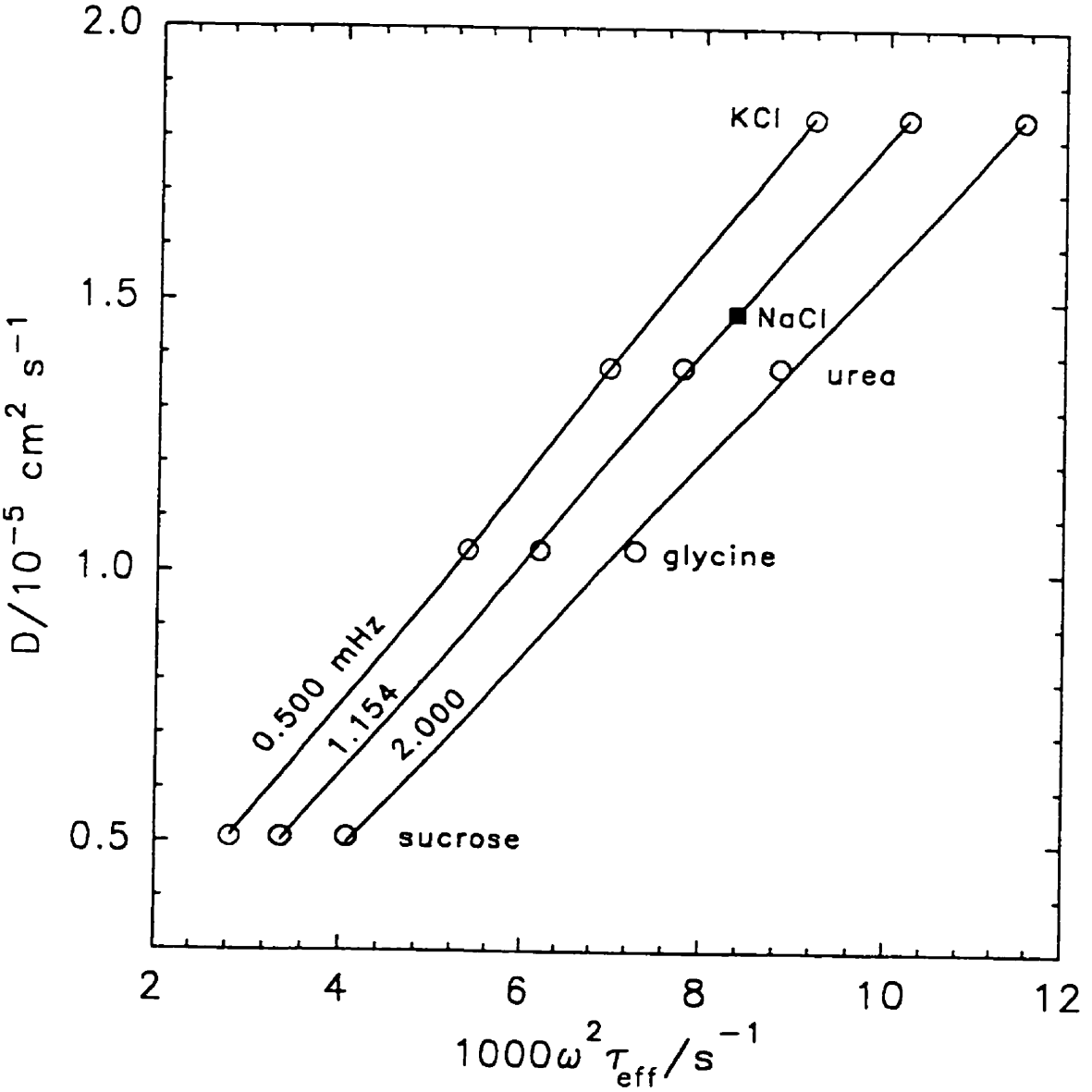
2.0
1.5
1.0
0.5
D/10^-5 cm^2 s^-1
2
4
6
8
10
12
1000ω^2τ_eff/s^-1
KCl
NaCl
urea
glycine
sucrose
0.500 mHz
1.154
2.000

as shown in Fig. 7.6 for one of the NaCl runs, gave 1.488×10^{-5}, 1.478×10^{-5}, and 1.481×10^{-5} cm^2 s^{-1} for the diffusion coefficient. Each of these results differs by < 1% from the value[34] 1.475×10^{-5} cm^2 s^{-1} obtained by optical interferometry for 0.250 mol dm^{-3} aqueous NaCl at 25 °C.

Aqueous $LaCl_3$ Solutions The calibrated dispersion circuit was used to measure the binary mutual diffusion coefficient of aqueous lanthanum chloride at concentrations from 0.015 to 2.784 mol dm^{-3} at 25° C. The results are summarized in Table 7.3. In Fig. 7.7 the measured D values are plotted against the square root of the salt concentration together with Harned and Blake's conductimetric results[23] for dilute solutions of the salt. There is a shallow minimum in D near 0.2 mol dm^{-3}, followed by a 50% drop in D as the concentration is increased from about 1.0 to 2.8 mol dm^{-3}. The precision of the reported D values is 1-2%, limited primarily by the precision of the fitted τ_{eff} values.

The mutual diffusion coefficient of aqueous $LaCl_3$ relates the flux of the salt to the gradient in its concentration. It is well known, however, that chemical potential gradients are the fundamental driving forces for mutual diffusion. Mutual diffusion coefficients can therefore be interpreted[1] as a product of a frictional factor as well as an equilibrium thermodynamic factor reflecting changes in the chemical-potential driving force with concentration.

$$D = \frac{m d\mu_1/dm}{\varphi} = \frac{4RT(1 + m d\ln\gamma/dm)}{\varphi} \qquad (7.17)$$

Table 7.3[a] Measured decay times and mutual diffusion coefficients of aqueous $LaCl_3$ at 25 °C

C	ΔC	ω	τ	D	$1 + m\mathrm{d}\ln\gamma/\mathrm{d}m$	φ/RT
0.000	-	-	-	(1.292)[b]	1.000	3.10
0.015	0.020	1.070	5395	1.07_1	0.785	2.93
0.015	0.020	1.071	5408	1.07_6	0.785	2.92
0.020	0.020	1.060	5496	1.07_3	0.776	2.89
0.025	0.010	1.008	5894	1.04_8	0.767	2.93
0.050	0.010	1.077	5092	1.01_6	0.767	3.02
0.050	0.010	1.067	5241	1.03_1	0.767	2.97
0.076	0.009	1.056	5324	1.02_6	0.772	3.01
0.097	0.010	1.044	5358	1.01_1	0.789	3.12
0.102	0.010	1.065	5193	1.01_6	0.793	3.12
0.198	0.010	1.083	5056	1.01_8	0.858	3.37
0.198	0.010	1.015	5671	1.01_8	0.858	3.37
0.198	0.010	1.053	5329	1.02_2	0.858	3.36
0.208	0.009	1.035	5497	1.02_2	0.865	3.38
0.320	0.011	1.018	5678	1.02_5	0.956	3.73
0.397	0.010	0.963	5246	1.01_9	1.027	4.03
0.560	0.011	1.035	5570	1.03_6	1.188	4.59
0.740	0.011	1.032	5625	1.04_2	1.373	5.27

Table 7.3 (cont.)

0.842	0.011	1.049	5506	1.05_2	1.510	5.74
0.975	0.010	1.069	5285	1.04_4	1.713	6.56
1.079	0.011	1.061	5329	1.03_8	1.850	7.13
1.185	0.011	1.032	5583	1.03_4	2.006	7.76
1.499	0.009	1.040	5341	0.99_9	2.444	9.78
1.685	0.010	1.045	5111	0.95_9	2.711	11.3
1.983	0.012	1.043	4647	0.85_5	3.093	14.5
2.303	0.010	1.044	4032	0.72_4	3.437	19.0
2.491	0.010	1.070	3481	0.64_0	3.581	22.4
2.784	0.010	1.063	2928	0.50_7	3.758	29.6

[a]Units: C and ΔC in mol dm^{-3}; ω in mHz; τ in s; D in 10^{-5} cm^2 s^{-1}; φ/RT in 10^5 s cm^{-2}.

[b]Limiting value calculated from ionic conductivities.

Fig. 7.7 Binary mutual diffusion coefficients of aqueous $LaCl_3$ and $NiCl_2$ plotted against the square root of the concentration. $LaCl_3$: ●, this work; Δ, conductimetric data of Harned and Blake;[23] ▲, limiting value;[24] $NiCl_2$: --------, interferometric data of Rard *et al.*[40]

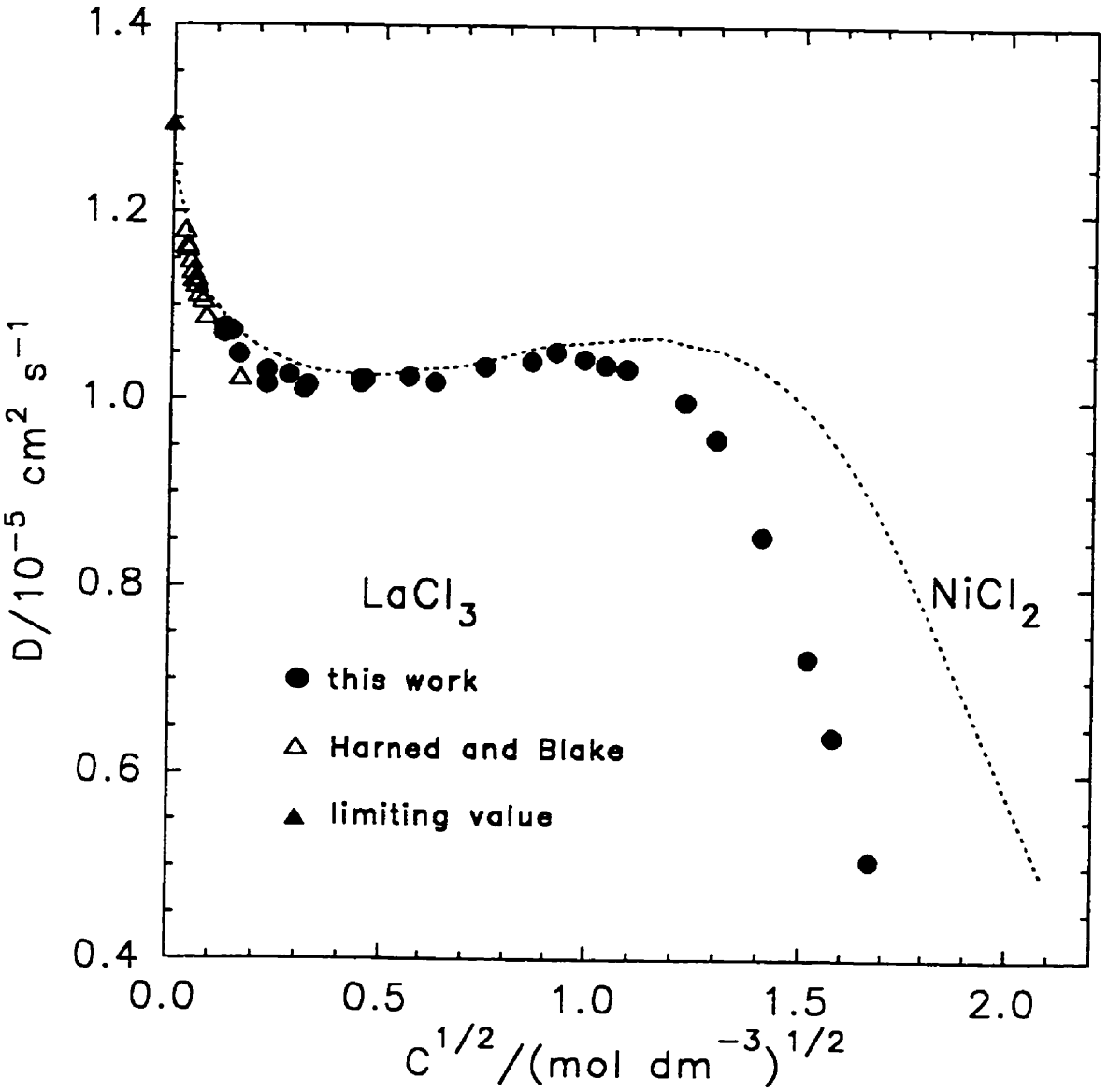
1.4
1.2
1.0
0.8
0.6
0.4
0.0
0.5
1.0
1.5
2.0
D/10^-5 cm^2 s^-1
c^1/2/(mol dm^-3)^1/2
LaCl3
NiCl2
this work
Harned and Blake
limiting value

The resistance coefficient[1] φ defined by eqn. (7.17) gives the driving force per mole of $LaCl_3$ ($-\nabla\mu_1$) required to maintain unit diffusion speed of the salt(1) relative to the solvent(0)

$$\varphi = \frac{-\nabla\mu_1}{U_1 - U_0} \tag{7.18}$$

where μ_1, m, and γ are the chemical potential, molality, and mean ionic activity coefficient of $LaCl_3$. R is the gas constant and T is the temperature.

Published activity coefficients[36-38] were used to evaluate the thermodynamic factors listed in Table 7.3. The resistance coefficients were calculated from the measured diffusion coefficients by using eqn. (7.17). The diffusion coefficient, resistance coefficient and thermodynamic factor for aqueous $LaCl_3$, all normalized to unity at infinite dilution, are plotted in Fig. 7.8.

Strong hydration of the La^{3+} ion leaves relatively little "free" solvent in concentrated $LaCl_3$ solutions. This leads to a sharp increase in the mean ionic activity coefficient with increasing concentration of the salt. For example, γ is about 2.5 for the most concentrated solution studied here (2.784 mol dm^{-3}). The non-ideal behaviour increases the driving force per unit concentration gradient, producing the four-fold increase in the thermodynamic factor shown in Fig. 7.8. Over the same concentration range, however, there is a ten-fold increase in the resistance coefficient. The net result is a 60% drop in the diffusion coefficient.

The relative viscosity curve plotted in Fig. 7.8 closely resembles the curve for the

Fig. 7.8 Normalized diffusion coefficient (●, this work), resistance coefficient (▲, this work), thermodynamic factor (refs. 36 and 37), and viscosity (■, this work; □, ref. 39) of aqueous $LaCl_3$ plotted against the square root of the concentration.

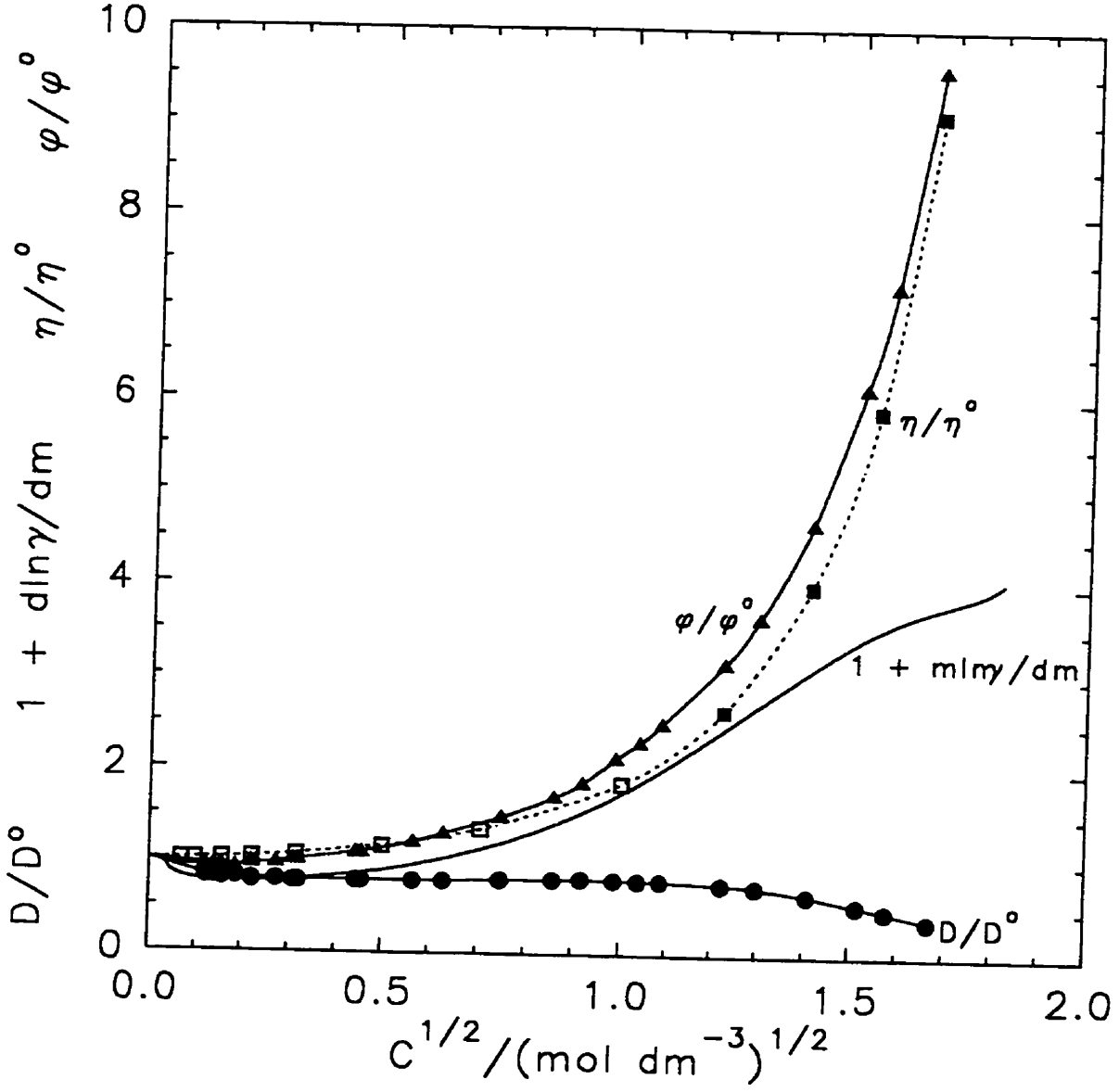
10
8
6
4
2
0
0.0
0.5
1.0
1.5
2.0
D/D°
1 + dlnγ/dm
η/η°
φ/φ°
φ/φ°
η/η°
1 + mlmγ/dm
D/D°
C^1/2/(mol dm^-3)^1/2

relative resistance coefficient. It is tempting, therefore, to attribute the increase in the resistance coefficient to the higher viscosity[39] of concentrated $LaCl_3$ solutions. For most systems, however, relative resistance coefficients for mutual diffusion[1,38] increase more rapidly than relative viscosities.

In a review of the diffusion behaviour of aqueous divalent-metal salts, Rard *et al.*[40] concluded that $NiCl_2$ is a typical strong electrolyte of this class. It is therefore of interest to compare the mutual diffusion coefficients of aqueous $NiCl_2$ and $LaCl_3$. The limiting diffusion coefficient of the aqueous Ni^{2+} ion (0.705×10^{-5} cm^2 s^{-1})[40] is larger than that of the more strongly hydrated and therefore effectively larger La^{3+} ion (0.619×10^{-5} cm^2 s^{-1}).[38] Each La^{3+} ion, however, is constrained by electroneutrality to diffuse with an extra mole of relatively mobile Cl^- ions (limiting diffusion coefficient 2.033×10^{-5} cm^2 s^{-1}).[38] As a result, the limiting diffusion coefficient of $LaCl_3$ (1.292×10^{-5} cm^2 s^{-1}) is actually slightly larger than that of $NiCl_2$ (1.248×10^{-5} cm^2 s^{-1}). In Fig. 7.7 the diffusion coefficients of aqueous $NiCl_2$ and $LaCl_3$ are plotted against the square root of the concentration. Up to about 1 mol dm^{-3} the diffusion coefficients of the two salts differ by no more than a few percent, and both systems show a shallow minimum in D near 0.2 mol dm^{-3}. Above 1.0 mol dm^{-3} the diffusion coefficient of the lanthanum salt falls significantly below that of the nickel salt.

7.5. Conclusions

The work reported here shows that Taylor dispersion experiments can be modified to measure diffusion in closed circuits. Instead of injecting small solution samples into a large excess of carrier solution, two solutions of equal volume are interdispersed in a closed

loop. The average solute concentration remains constant during each run. Consequently, differential diffusion coefficients can be measured by using larger concentration differences, and baseline drift is negligible because of the stronger detector signals. This feature may be useful in studies of slowly diffusing substances, such as polymers, which generate broad dispersion profiles. The closed-circuit modification may also be of value in cases where limited amounts of solution are available. Each of the diffusion measurements for aqueous $LaCl_3$, for example, was made with about 10 cm^3 of solution, 30 to 50 times less than that required for conventional dispersion experiments. The main disadvantage of closed-circuit dispersion measurements is that each circuit must be calibrated.

7.6. References

1 H. J. V. Tyrrell and K. R. Harris, *Diffusion in Liquids*, Butterworths, London, 1984.

2 P. J. Dunlop, K. R. Harris and D. J. Young, *Experimental Methods for Studying Diffusion in Liquids*, in *Physical Methods of Chemistry*, ed. B. Rossiter and R. C. Baetzold, Wiley, New York, 2nd edn., 1992; Vol. 6.

3 C. Erkey and A. Akgerman, in *Measurement of the Transport Properties of Fluids*, ed. W. A. Wakeham, A. Nagashima and J. V. Sengers, Blackwell, London, 1991.

4 K. C. Pratt and W. A. Wakeham, *Proc. R. Soc. London Ser. A*, 1975, **342**, 401.

5 A. Alizadeh, C. A. Nieto de Castro and W. A. Wakeham, *Int. J. Thermophys.*, 1988, **1**, 243.

6 K. R. Harris, T. Goscinska and H. N. Lam, *J. Chem. Soc., Faraday Trans.*, 1993,

89, 1969.

7 J. B. Rodden, C. Erkey and A. Akgerman, *J. Chem. Eng. Data*, 1988, **33**, 450.

8 T. Tominaga, S. Matsumoto, T. Koshiba and Y. Yamamoto, *J. Chem. Soc., Faraday Trans. 1*, 1988, **84**, 4261.

9 R. M. Weinheimer, D. F. Evans, and E. L. Cussler, *J. Colloid Interface Sci.*, 1981, **80**, 357.

10 S. Chen, H. T. Davis and D. F. Evans, *J. Chem. Phys.*, 1982, 77, 2540.

11 D. G. Leaist and L. Hao, *J. Chem. Soc., Faraday Trans.*, 1994, **90**, 133.

12 D. G. Leaist, *J. Chem. Soc., Faraday Trans.*, 1991, **76**, 597.

13 Z. Deng and D. G. Leaist, *Can J. Chem.*, 1991, **69**, 1548.

14 D. G. Leaist and L. Hao, *J. Phys. Chem.*, 1993, **87**, 7763.

15 D. G. Leaist and L. Hao, *J. Chem. Soc., Faraday Trans.*, 1995, **91**, 2837.

16 L. Hao and D. G. Leaist, *J. Solution Chem.*, 1995, **24**, 523.

17 D. G. Leaist and L. Hao, *J. Phys. Chem.*, 1995, **99**, 12896.

18 W. A. Wakeham and K. C. Pratt, *J. Phys. Chem.*, 1975, **79**, 2198.

19 K. C. Pratt and W. A. Wakeham, *J. Chem. Soc., Faraday Trans. 2*, 1997, **73**, 997.

20 D. G. Leaist and L. Hao, *J. Phys. Chem.*, 1994, **98**, 4703.

21 D. G. Leaist and L. Hao, *J. Phys. Chem.*, 1993, **97**, 1464.

22 D. G. Miller and V. Vitagliano, *J. Phys. Chem.*, 1986, **90**, 1706.

23 H. S. Harned and C. A. Blake, *J. Amer. Chem. Soc.*, 1951, **73**, 4255.

24 D. G. Miller, *J. Phys. Chem.*, 1966, **70**, 2639.

25 J. B. J. Fourier, *Theorie Analytique de la Chaleur*, Gauthier-Villars, Paris, 1822.

26 G. Taylor, *Proc. R. Soc. London Ser. A*, 1954, **225**, 473.

27 R. Aris, *Proc. R. Soc. London Ser. A*, 1956, **235**, 67.

28 H. S. Carslaw and J. C. Jaeger, *Conduction of Heat in Solids*, Clarendon, Oxford, 2nd edn., 1959, p. 96, 160.

29 G. Jones and C. F. Bickford, *J. Am. Chem. Soc.*, 1934, **56**, 602.

30 E. Berecz, I. Báder and T. Török, *Acta Chim. Acad. Hung.*, 1976, **91**, 119.

31 L. G. Gosting and M. S. Morris, *J. Am. Chem. Soc.*, 1949, **71**, 1998.

32 H. D. Ellerton, G. Reinfelds, D. Mulcahy and P. J. Dunlop, *J. Phys. Chem.*, 1964, **68**, 403.

33 L. J. Gosting and D. F. Akeley, *J. Am. Chem. Soc.*, 1952, **74**, 2058.

34 J. A. Rard and D. G. Miller, *J. Solution Chem.*, 1979, **8**, 701.

35 J. A. Rard and D. G. Miller, *J. Chem. Eng. Data*, 1980, **25**, 211.

36 T. Shedlovsky, *J. Am. Chem. Soc.*, 1950, **72**, 3680.

37 F. H. Spedding and P. E. Porter, *J. Am. Chem. Soc.*, 1952, **74**, 278.

38 R. A. Robinson and R. H. Stokes, *Electrolyte Solutions*, Academic Press, New York, 2nd edn., 1959.

39 G. Jones and R. E. Stauffer, *J. Am. Chem. Soc.*, 1940, **62**, 335.

40 J. A. Rard, D. G. Miller and C. M. Lee, *J. Chem. Soc., Faraday Trans. 1*, 1989, **85**, 3343.

CONCLUSIONS

The work reported in this thesis shows that Taylor dispersion is a reliable and convenient technique for measuring diffusion coefficients in difficult cases where the diffusion coefficients change very rapidly with the concentration of the diffusing substance.

The technique has been used to study binary diffusion of a number of aqueous strong and weak electrolytes at 25 °C. Equations developed previously for weak-acid diffusion are used to describe the concentration dependence of the diffusion coefficients of aqueous amines which undergo partial hydrolysis. The results illustrate the complexity of the diffusion of weak electrolytes relative to that of strong electrolytes. Also, the measured diffusion coefficients are analyzed to determine the mobilities of molecular amines and the corresponding substituted ammonium ions. These equations are extended to predict diffusion behavior of more complicated systems, such as aqueous aminobenzoic acids which undergo both proton dissociation and association reactions.

Finally, the present work shows that the conventional Taylor dispersion experiment can be modified to measure diffusion in closed circuits. Recirculation drastically reduces the volume of solution required relative to that used in traditional once-through Taylor dispersion measurements, from liters to milliliters. This advantage will be important for measuring the diffusion coefficients of substances that are not available in large amounts, such as certain biochemicals or chemicals that are highly toxic or expensive to purify. Since the average solute concentration remains constant, diffusion coefficients can be measured by using larger concentration differences and less-sensitive detectors.

IMAGE EVALUATION
TEST TARGET (QA-3)

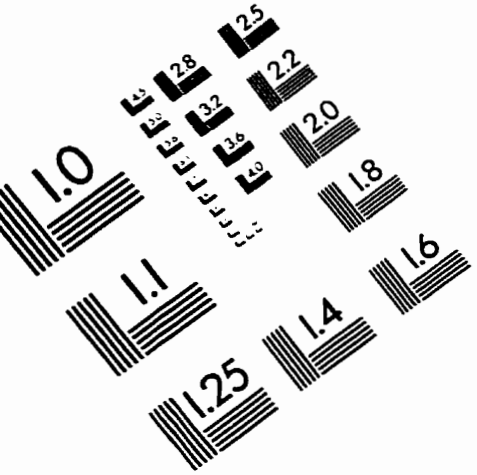

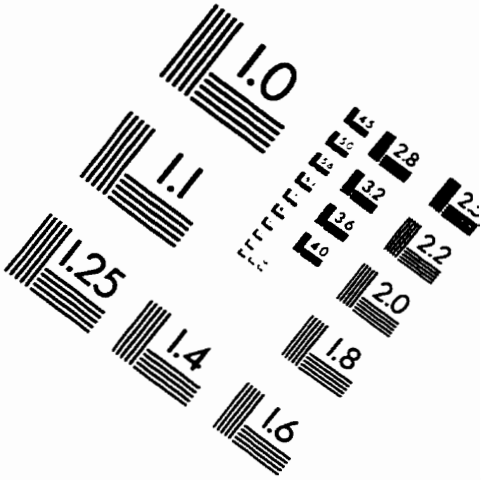

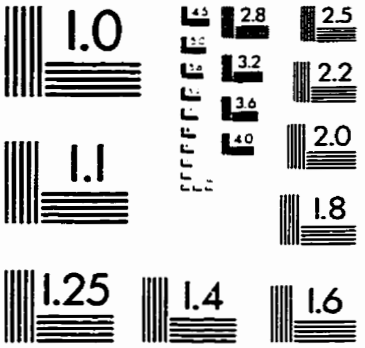

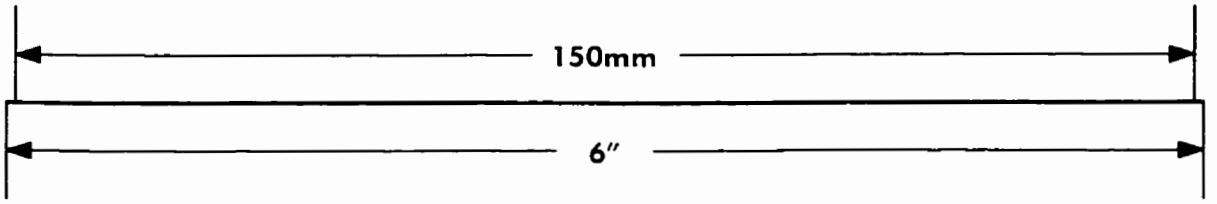

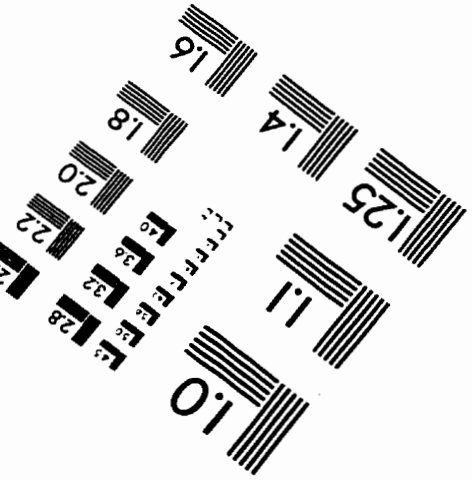

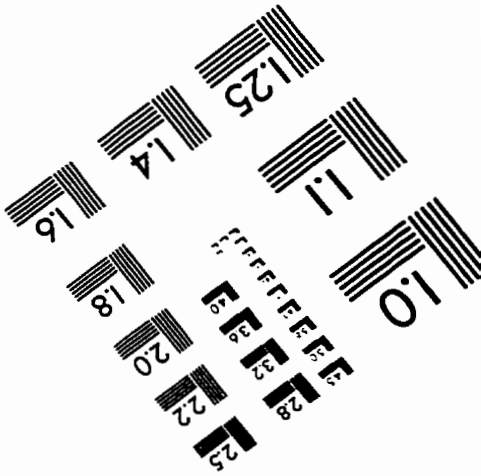

APPLIED IMAGE . Inc
1653 East Main Street
Rochester, NY 14609 USA
Phone: 716/482-0300
Fax: 716/288-5989